

Universiteit
Leiden
The Netherlands

Innate immune signalling of the zebrafish embryo

Stockhammer, O.W.

Citation
Stockhammer, O. W. (2010, May 19). *Innate immune signalling of the zebrafish embryo*. Retrieved from https://hdl.handle.net/1887/15512

Version:	Corrected Publisher's Version
License:	Licence agreement concerning inclusion of doctoral thesis in the Institutional Repository of the University of Leiden
Downloaded from:	https://hdl.handle.net/1887/15512

Note: To cite this publication please use the final published version (if applicable).

Innate immune signalling of the zebrafish embryo

Oliver W. Stockhammer

ISBN: 9789-08-5705-19-2

Printed by Wöhrmann Print Service, Zutphen

Innate immune signalling of the zebrafish embryo

Proefschrift
ter verkrijging van
de graad van Doctor aan de Universiteit Leiden,
op gezag van Rector Magnificus prof. mr. P.F. van der Heijden,
volgens besluit van het College voor Promoties
te verdedigen op woensdag 19 mei 2010
klokke 13.45 uur

door

Oliver W. Stockhammer

geboren te Stuttgart, Duitsland
in 1974

Promotiecommissie:

Promotor:	Prof. dr. H.P. Spaink
Co-Promotor:	Dr. A.H. Meijer
Overige leden:	Prof. dr. P.J.J. Hooykaas
	Prof. dr. J. den Hertog
	Prof. dr. A.J. Durston
	Dr. S.A. Renshaw (University of Sheffield)

The publication of this thesis was sponsored by ZF-screens B.V.

“A day without laughter is a day wasted”
Charlie Chaplin

Für Linda, Noah & Senne

Contents

Chapter 1 Introduction to the vertebrate innate immune system *9*

Chapter 2 MyD88 innate immune function in a zebrafish embryo infection model *27*

Chapter 3 Transcriptome profiling and functional analyses of the zebrafish embryonic innate immune response to Salmonella infection *41*

Chapter 4 Transcriptome analysis of Traf6 function in the innate immune response of zebrafish embryos *75*

Chapter 5 Transcriptome analysis of Traf6 function in early zebrafish embryogenesis *99*

Chapter 6 Summary and discussion *121*

Samenvatting *129*

List of publications *135*

Curriculum vitae *137*

1 Introduction to the vertebrate innate immune system

The immune system of animals is a complex composition of cellular and humoral components that protects the host against infectious diseases and cancer by identifying and killing pathogens and detrimental cells. To successfully protect the host, the immune system must be able to distinguish self from non-self and recognize danger signals. The concept of protecting self from non-self is already present in unicellular organisms, demonstrated by a repertoire of mechanisms ranging from the production of antimicrobial peptides to the employment of specific molecular systems protecting against foreign nucleic acids. With the appearance of multicellular organisms an increasingly complex immune system evolved. Distinct cells of the organism adopted specialized immune functions showing the ability to detect invading pathogens, migrate to sites of infection and eventually engulf and eliminate the encountered microorganisms. At the same time, soluble factors such as antimicrobial peptides and acute-phase proteins are used to combat the infection. To be able to recognize a wide variety of pathogens and detrimental cells various classes of receptors have evolved and diversified in different organisms. The most sophisticated immune system today exists in all higher vertebrates and combines a wide range of receptors with the development of immunological memory. This thesis focuses on the use of the zebrafish (*Danio rerio*) as a model to study the vertebrate immune system.

The vertebrate immune system

Traditionally, the complex defence mechanisms of vertebrates are categorized into the evolutionary ancient innate immune system, that is present in all multicellular organisms, and the relatively young adaptive (acquired) immune system that arose with the appearance of jawed fish (*Chondrichthyes*) (1, 2). Both systems comprise humoral as well as cellular components that synergistically act upon infection. The innate immune system forms the first line of defence against pathogens. The elicited immune responses are rapid, occurring usually within minutes to hours. However, the innate immune mechanisms are considered relatively nonspecific and are mediated by a fixed set of germline-encoded receptors. These receptors are referred to as pattern recognition receptors (PRRs), showing a broad specificity against microbial-derived molecules such as lipopolysaccharide (LPS), flagellin or viral RNA. PRRs are mainly expressed by the cells from the myeloid lineage such as macrophages and dendritic cells (DCs). Activation of PRRs initiates signal transduction pathways that culminate in the production of inflammatory mediators to attract and communicate with other cells of the immune system (T-helper cells, for instance). In contrast, the adaptive immune system takes days to weeks to mount a response mediated by cytotoxic T-lymphocytes, which can recognize and kill infected cells or cancer cells, and B-lymphocytes (plasma cells), producing highly specific antibodies. T- and B-cells, presenting a diverse array of receptors on their surface, are generated by recombi-

nation of gene segments and clonal selection (3). The high affinity of antibodies to specific antigens is further achieved by somatic hypermutation in the gene segments encoding the variable regions of the antibody (4). Subsets of the activated B- and T-lymphocytes will be retained in lymphoid organs as memory cells. These cells can be reactivated by a recurring infection of a particular pathogen leading to a faster and highly specific immune response, thereby generating a long-lasting immunity against previously encountered pathogens. Although the two systems show obvious differences in the molecular tools used to battle infections, one should keep in mind that the innate and the adaptive immune systems in vertebrates are closely linked in their response to infectious microbes and that the innate immune system is pivotal for an accurate adaptive response. Given that the major focus of this thesis is on innate immunity, the components (both humoral and cellular) and the functions of the vertebrate innate immune system will be described in more detail in the following sections.

Humoral components of the vertebrate innate immune system

Acute-phase proteins

Sensing and killing of microbes can be achieved by several molecules of the innate immune system. A group of proteins, collectively termed acute-phase proteins (APPs), are greatly increased or decreased in the blood upon infection. Production and secretion of such proteins occurs in hepatocytes activated by cytokines such as TNFα, IL-6 and IL-1 (5). Acute phase proteins are a heterogenic group of proteins with either pro- or anti-inflammatory functions. A well known factor of the acute-phase response is the C-reactive protein (CRP), a member of the pentraxin family. CRP was shown to bind, among others, phosphocholine and phosphoethanolamine, which can be found on the cell surface of bacteria. CRP bound to macromolecules can lead either to opsonisation of bacteria (or apoptotic cells) or to the activation of the classical complement pathway described below (6).

Complement system

Although some of the proteins of the complement pathway are also considered acute phase proteins, the complement system is a complex humoral mechanism on its own. Core proteins of the complement system are present as inactive enzyme precursors in the blood. Initial activation of the proteolytic complement cascade can be achieved via three independent pathways: the classical, the lectin and the alternative. The classical pathway is activated through C1q, a member of the collectin family, which can bind directly to the surface of a pathogen. In addition, activation of this pathway can also occur through binding of C1q to an antibody-antigen complex, linking this pathway to the adaptive immune system. A similar mode of complement activation is followed by the lectin pathway, where recognition of infectious microorganisms is mediated by the mannan-binding lectin protein. Conversely, the alternative pathway

is mediated by the spontaneous hydrolysis of complement component 3 (C_3) and the subsequent formation of the C_3bBb complex without participation of a specific pathogen-recognizing protein. Activation by any one of these pathways will lead to cleavage of C_3 to C_3a and C_3b by a C_3 convertase. The C_3 convertase has distinct compositions: a C_4bC_2b complex in the classical and lectin pathways, and a complex of C_3b and activated factor B (Bb) in the alternative pathway (3).

The C_3a fragment is a potent inflammatory mediator triggering vasodilatation and increasing permeability of small blood vessels. In addition C_3a can induce oxidative burst in macrophages, neutrophils and eosinophils and leads to degranulation of mast cells and basophils, thereby sustaining the inflammation. The second product of C_3 cleavage, C_3b, can bind to the cell surface of pathogens and either form additional C_3bBb complexes that amplify the complement signal in the close proximity of the pathogen, or function as opsonin, enhancing phagocytosis. The latter is mediated by complement receptors on the surface of phagocytes (3).

Subsequent to C_3 cleavage ,C_3b can complex with C_4bC_2b to form a C_5 convertase leading to the release of C_5a and C_5b. The C_5a fragment functions as a pro-inflammatory mediator in the same fashion as C_3a. On the other hand, C_5b leads to the assembly of the membrane attack complex. Essentially, this complex is composed of C_9 molecules that form a pore in the cell membrane of the pathogen, resulting in a loss of cellular homeostasis and free passage of host enzymes such as lysozyme, ultimately causing cell lysis (3).

Antimicrobial peptides

The diverse group of small molecules (<100 amino acids) that are involved in the elimination of pathogenic microbes and enveloped viruses are collectively named antimicrobial peptides (AMPs) (7-9). In vertebrates AMPs can be classified into three groups: defensins, histatins and cathelicidins (10, 11). They are produced in various tissues and cells types such as Paneth cells of the intestine, lung epithelial cells and leukocytes (12-14). The precise mode of action of antimicrobial peptides is not fully understood, but involves membrane permeabilization and/or inhibition of protein and RNA synthesis (15).

Cell-mediated vertebrate innate immunity

Various cell types of the myeloid lineage are responsible for the detection and clearance of infectious microorganisms, apoptotic cells and tumour cells. Furthermore, they possess an instructive role towards the adaptive immune system. In addition to the various myeloid cells, the natural killer (NK) cells, derived from a lymphoid precursor, are also considered part of the cellular innate immune system. In the following paragraphs, the function of individual cell-types, predominantly studied in rodents, will be discussed in more detail.

Neutrophils, also named neutrophil granulocytes, are the most abundant myeloid

cells in mammals and are major effectors of innate immunity. Together with basophil and eosinophil granulocytes they form the polymorphonuclear cell family. Neutrophils can efficiently phagocytose and kill internalized microbes in phagosomes through reactive oxygen species (ROS) and proteolytic enzymes. In addition, by exocytosis of their granules (degranulation), neutrophils can release a multitude of antimicrobial proteins and proteases that destroy pathogens extracellularly. Another (phagocytosis-independent) mechanism that is used by neutrophils to kill pathogens is the activation of neutrophil extracellular traps (NETs) (16). NETs are web-like structures composed of DNA, histone proteins and neutrophil elastase (a serine protease) that can trap and kill microbes. Both anti-bacterial and anti-fungal properties of NETs have been described (16, 17).

Macrophages are the predominant phagocytic cells of mammals. Immature macrophages derived from bone marrow circulate as monocytes through the blood. A subpopulation of these monocytes leave blood-circulation and migrate into the surrounding tissue were they can develop into resident macrophages such as osteoclasts (bone), microglia (CNS) or Kupffer cells (liver) depending on the tissue they inhabit. Monocytes and macrophages express various types of pattern recognition receptors on their cell surface and intracellularly, that allow these cells to respond effectively to diverse classes of pathogens. Cytokines produced by NK cells or tissue macrophages upon infection or tissue damage can trigger migration of additional monocytes from the blood to the site of the infection, where they differentiate into mature macrophages. Depending on the mode of activation triggered by diverse combinations of cytokines, macrophages can promote inflammation or even participate in wound healing (18). During the adaptive immune response macrophages are activated by T-cells, leading to increased production of ROS and activation of the autophagy pathway. Macroautophagy is a major defence mechanism against intracellular pathogens (19). Beside their function during inflammation, macrophages also contribute to maintaining homeostasis by removal of cell debris, apoptotic cells and erythrocytes (18).

Dendritic cells form, together with macrophages, the major antigen presenting cells (APC) of the mammalian immune system. Immature DCs are constantly patrolling the tissue, taking up pathogens and apoptotic cell fragments by macropinocytosis, eventually leading to antigen presentation on the cell surface. Encounter of pathogen-derived molecules by immature DCs leads to DC activation, maturation and pro-inflammatory cytokine secretion. Mature DCs migrate subsequently to nearby lymph nodes where antigen presentation takes place, inducing primary T-cell mediated immune responses (20).

Mast cells are predominantly found in mucosal and connective tissues of skin, gut and airways. Present as immature progenitors in the blood, they undergo final matu-

ration after tissue migration (21). Several pattern-recognition receptors are expressed on the cell surface of mast cells allowing direct sensing of invading pathogens (22). In addition to this direct activation, mast cells can also be activated indirectly via the complement system, leading to cytokine release and degranulation (22). Mast cell activation leads to a variety of effects, such as degradation of endogenous toxins, bactericidal activity, vasodilatation, T-cell activation and recruitment of neutrophils and DCs to the site of infection (23, 24). On top of their function in innate immune responses, mast cells have been extensively studied in the context of allergies (25).

Natural Killer cells, unlike the aforementioned cell types, derive from a common lymphoid precursor that also generates B- and T- lymphocytes of the cellular adaptive immune system (26). NK cells are able to target both virally infected and tumor cells, and destroy them by releasing cytotoxic molecules such as perforin and granzymes (27). NK cell function is orchestrated by various cell surface receptors that, upon activation, can either lead to inhibition or activation of exocytosis of the cytotoxic granules and lysis of the targeted cell. Inhibitory signals can be mediated via the CD94/NKG2A and CD94/NKG2B receptors that recognize specific major histocompatibility complex (MHC) class I surface proteins (28, 29). Abnormal or virally infected cells tend to down-regulate MHC class I proteins on the cell surface and hence lack an inhibitory signal (30, 31). At the same time these cells present activating signals such as MHC class I chain-related (MIC) molecule MICA that facilitate NK cell activation via NKG2D, a C-type lectin receptor (32, 33). Intercalation of the various signals eventually leads to the formation of the lytic immunological synapse between NK and target cells, cytotoxin release and lysis of the infected cell (34).

Pathogen monitoring by pattern-recognition receptors

Recognizing potentially harmful microorganisms is an essential first step in the initiation of an immune response. The innate immune system relies on the recognition of highly conserved structural components of microbes, often referred to as pathogen-associated molecular patterns (PAMPs) or microbial-associated molecular patterns (MAMPs). PAMPs or MAMPs are usually essential for microbial survival, hence a constant factor for the host to detect. Examples are bacterial cell-wall components such as LPS and peptidoglycan, flagellin from bacterial flagella or viral RNAs. The receptors involved in PAMP recognition, PRRs, are widely expressed on the cells of the innate immune system such as macrophages and DCs, and on non-immune cells that are likely to encounter pathogens, such as epithelial cells. Several families of PRRs have been described in vertebrates, including the Toll-like receptor (TLRs), NOD-like receptor (NLR) and RIG-I-like (RLRs) receptor families (35-37).

The TLRs are the best studied and probably most essential receptors of the vertebrate innate immune system. The TLRs are named after the *Toll* receptor from *Drosophila melanogaster*, which in 1985 was described as having an essential role in

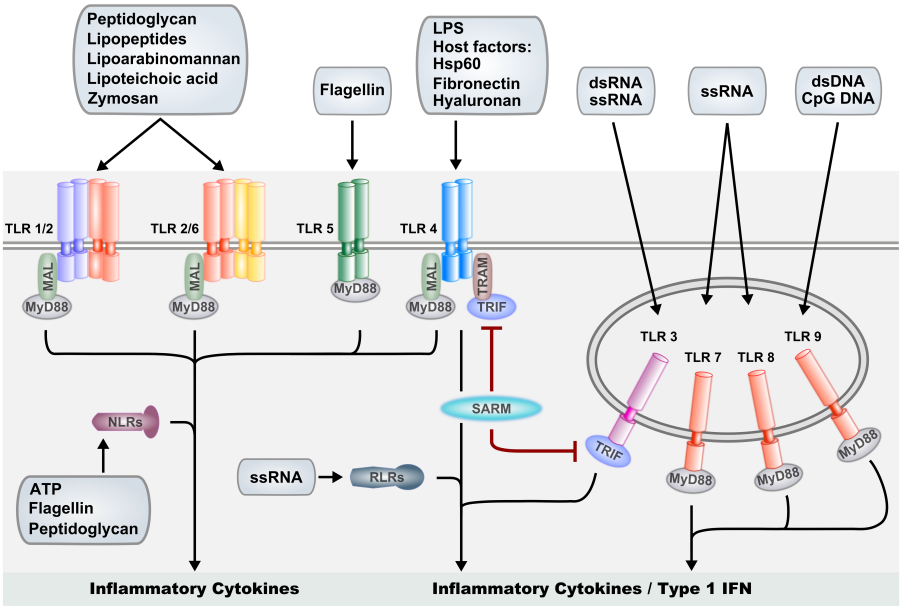


FIGURE 1. Schematic overview of mammalian PRRs and their associated ligands. TLRs are expressed on the cell surface and on endosomal membranes and act cooperatively with cytoplasmic receptors of the NLR and RLR families to induce expression of inflammatory cytokines and type I interferons. Differential use of adaptor proteins (Myd88, Mal, TRIF, TRAM and SARM) is indicated for the TLR family members. Figure adapted from T. Mogensen (54).

dorsal-ventral polarity determination (38). More than a decade later Lemaiter *et al.* unravelled a function of *Toll* in the antifungal immune response of *D. melanogaster* and shortly afterwards mammalian TLR4 was identified as the receptor that mediates LPS signalling (39, 40).

Today, a lot is known about TLR activation and downstream signalling events in mammals. All TLRs are germline-encoded type I transmembrane receptors characterized by a highly variable extracellular leucine-rich repeat (LRR) domain, involved in ligand recognition, and an intracellular tail, containing the conserved Toll/Interleukin-1 receptor (TIR) domain, mediating association of TLRs with downstream signalling intermediates. A set of 10 TLRs have been described in human so far, showing distinct specificity to various PAMPs. For instance, TLR3, -7, and -8 recognize double- and/or single-stranded RNA, whereas TLR-9 recognizes bacterial DNA. TLR4 has been shown to recognize LPS and TLR5 is specific for bacterial flagellin. Heterodimers of TLR2 with TLR1 or TLR6 are able to recognize various lipoproteins and glycolipids from gram-positive bacteria (Fig.1) (41-45). In accordance with their ligand specificity TLR3, -7, -8 and - 9 are located in the endolysosomal

compartments, whereas the TLR1, -2, -4, -5 and -6 are located on the cell surface (46). Activation of the TLRs initiates distinct signalling pathways that result in the accumulation of pro-inflammatory cytokines and type I interferons (IFNs). A group of 5 adaptor proteins (MyD88, MAL, TRIF, TRAM and SARM), binding to the various TLRs upon activation, are differentially used by TLRs to mediate a tailored response. MyD88 is the most commonly used adaptor, and signalling through MyD88 has been reported for all human TLRs with the exception of TLR3, that instead shows a TRIF-dependent signalling route (47, 48). While TLR5, 7, 8 and 9 signal through MyD88 alone, TLR2/TLR1 and TLR2/TLR6 heterodimers require MAL as an additional adaptor to link MyD88 to the receptor complex. TLR4 signalling can lead to activation of pro-inflammatory cytokine genes via a MyD88/MAL-dependent pathway, and can result in type I INF production via a MyD88-independent pathway that utilizes the adaptors TRAM and TRIF (49). The fifth TIR-domain adaptor, SARM, has been proposed to function as a negative regulator of TRIF, but was also shown to positively regulate the response to viral infection in brain cells (50, 51). Downstream of the TLR-adaptors, signals are relayed via TNF-receptor associated factors TRAF6 and TRAF3, activating downstream kinases which eventually lead to gene induction through the nuclear factor kappaB (NF-κB) and interferon response factor (IRF) families of transcription factors, and to MAP kinase (MAPK) signalling pathways activating the AP-1 (JUN/FOS) transcription factor complex (Fig.1) (52, 53).

Whereas the TLRs are located on the cell surface and endolysosomal membranes, the members of the NLR family are predominantly distributed in the cytosol of the cell, where they are primarily involved in bacterial recognition (35). The NLR proteins consist of an N-terminal effector domain, a central nucleotide-binding oligomerization domain (NOD) and a C-terminal LRR domain. The N-terminal domain facilitates signalling through downstream partners, whereas the LRR domain is necessary for PAMP detection. Similarly to the TLRs, NLRs can be activated by microbial compounds such as flagellin and peptidoglycan. In addition, NLRs are responsive to bacterial toxins and crystals as well as to endogenous danger signals. By analogy with PAMPs, these danger signals, of which extracellular ATP is a good example, are referred to as DAMPs (danger associated molecular patterns). As is the case of TLRs, triggering of NLRs can lead to NF-κB and MAPK pathway activation that in turn leads to production of cytokines and anti-microbial proteins. Furthermore, NLR signalling can lead to activation of the inflammasome that is required for secretion of active IL-1β and IL-18. These potent pro-inflammatory cytokines are produced as inactive precursors through TLR pathway activation, and caspase-1 mediated processing in the inflammasome is required for their activation (35). Thus, a robust inflammatory response is dependent on the cooperative action of TLRs and NLRs (Fig.1).

Similarly to NLRs, RLRs are also located in the cytoplasm. Together with TLR3, -7 and -8 the RLRs provide viral recognition and mount a robust induction of type I INF. Activation of RLRs initiates the activation of NF-κB and IRF3 (36).

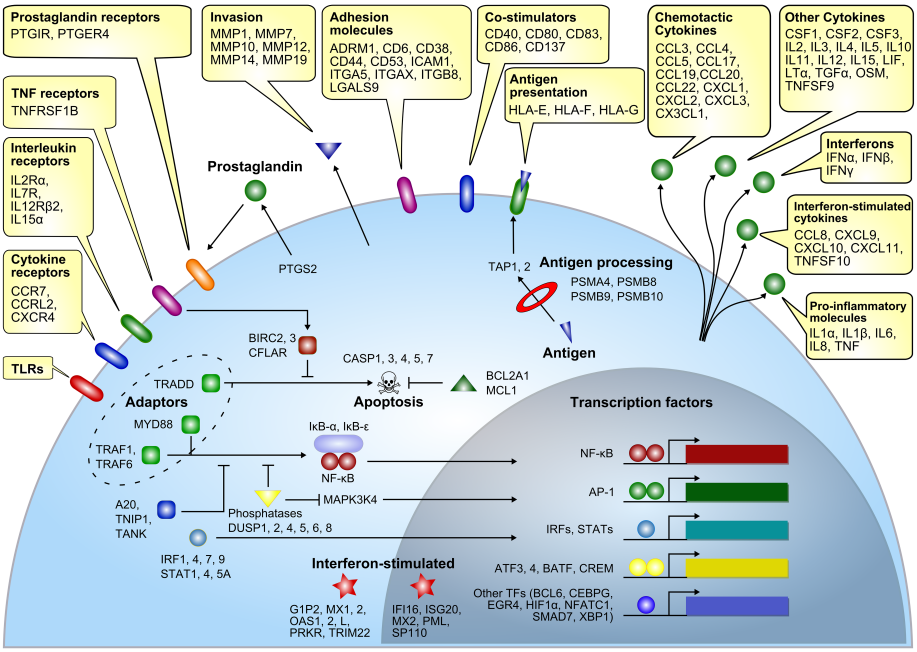


FIGURE 2. The common host immune response. Expression of genes indicated in the figure is induced by a variety of pathogens in human cell cultures. Figure adapted from Jenner and Young (57).

In addition to the above mentioned PRRs, a role in the innate immune defence is also played by the C-type lectin receptor (CLRs) family and the scavenger receptor family. C-type lectin receptors are expressed on such cells as DCs, where they can detect fungi, bacteria and viruses through the recognition of mannose, fucose and glucan carbohydrates. Several CLRs, such as DC-specific ICAM3-grabbing non integrin (DC-SIGN), have been shown to modulate TLR signalling. Dependent on the pathogen involved, both cooperative and antagonizing interactions between CLR and TLR signalling have been found. CLR signalling has furthermore been implicated in the tailored activation of T-cell subsets (55). Finally, scavenger receptors have been shown to participate in TLR signalling as TLR co-receptors; these mediate, in addition, non-opsonic phagocytosis of pathogenic microbes (56).

Common factors of the host response to infection

Activation of PRRs leads to the induction of a transcriptional response, priming the host to adequately respond to the encountered pathogen. In a comprehensive review study, Jenner and Young performed a meta-analysis on transcriptome data from various infection studies of different cells types with different pathogens, leading to the identification of a gene set that is commonly regulated upon infection. Among

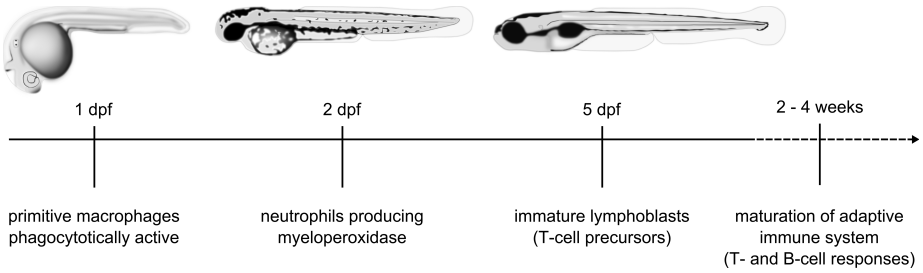


FIGURE 3. Schematic overview of the appearance of myeloid and lymphoid cells along zebrafish embryogenesis.

the identified genes were pro-inflammatory mediators (TNF, IL1β, IL6 and IL8), chemotactic and interferon stimulated cytokines (CCL3, CXCL1, CCL8), tissue invasion proteins (MMP1, MMP14), cell adhesion proteins (CD6, ICAM1), signalling adaptors (MyD88, TRAF6) and various transcription factors (NF-κB, AP1, STATs and IRFs), as shown in figure 2 (57).

Zebrafish embryos as a model to study vertebrate immunity

In recent years the zebrafish (*Danio rerio*) embryo system has emerged as a new model to study vertebrate innate immunity, offering several advantages that complement mammalian model systems. The transparent character of the externally fertilized zebrafish embryo in combination with fluorescently-labelled immune cells and bacteria facilitate the study of host-microbe interaction and inflammation processes in the living organism (58-64). The efficiency at which infections and chemical treatments in zebrafish can be performed at a large-scale allows identification of novel microbial virulence factors and high-throughput compound screens to investigate disease mechanisms (65, 66). Moreover, the zebrafish system is particularly suitable for large-scale forward and reverse genetic screens aimed at the identification of genes with novel functions in the development of the immune system or in the immune response (67-69).

Like other vertebrates the zebrafish has a primitive and definitive wave of hematopoiesis giving rise to various cell types of the erythroid, lymphoid and myeloid lineage. During development, hematopoiesis occurs at several temporal locations in the embryos, finally shifting to the kidney marrow, which is equivalent to the mammalian bone marrow. Similarly to other vertebrates, adult zebrafish possess T- and B-cells, macrophages, neutrophils, eosinophils, basophils, mast cells and probably NK cells (70). Cells of the innate immune system are detectable as early as the first day of zebrafish development (71). These primitive macrophages are able to phagocytose bacteria and foreign material (72, 73). Functional neutrophils, producing the myeloperoxidase enzyme, are present from the second day of embryogenesis. By contrast, a functionally mature adaptive immune system is not active during the first

three weeks of zebrafish development (58, 74, 75). This clear temporal separation in zebrafish embryos provides a convenient system for *in vivo* study of the vertebrate innate immune response to infection, independently from the adaptive immune response (Fig.3). In recent years, numerous bacterial and viral infection models have been established for the zebrafish to study host-pathogen interaction, chemotactic responses and inflammation processes (62, 76-78).

Zebrafish pattern-recognition receptors and innate immune response activation

Genome analysis revealed one or more homologs of the human *TLR* genes (*TLR1,-2, -3,-4,-5-7,-8* and -9) to be present in zebrafish, as well as a group of fish-specific TLRs (79, 80). The zebrafish genome is also known to contain four of the downstream adaptor protein genes (*MyD88*, *TRIF*, *MAL* and *SARM*), while the fifth TLR adaptor TRAM remains to be identified (79, 80). Several other genes of the TLR signalling cascade have been identified in the zebrafish genome, as well as members of the NLR family and the downstream adaptor of the RLR family IPS-1 (81-83). TLR and adaptor genes are broadly expressed during zebrafish embryogenesis, even prior to the appearance of the first innate immune cells (84). Challenge of zebrafish embryos with different pathogens activates the expression of a wide range of innate immune response genes strongly conserved with those in mammals (85). In addition to the cell-mediated innate immune response, zebrafish have a well developed complement system and produce acute-phase response proteins such as hepcidin and fibrinogen (78).

A conserved TLR ligand specificity was demonstrated between human and zebrafish for TLR5 (Chapter 3). Stimulation of zebrafish embryos with purified flagellin led to transcriptional activation of distinct host defence genes such as interleukin-1β (*il1b*), matrix metalloproteinase 9 (*mmp9*) and cxc chemokine ligand C1c (*cxcl-C1c*) *in vivo* that were significantly impaired after knock-down of the *tlr5a* and *tlr5b* genes (85). In contrast, the zebrafish counterparts of TLR4 (Tlr4a and Tlr4b) were reported to be non-responsive to LPS, suggesting a rendered ligand specificity or function in zebrafish (86, 87). While the alternative ligand specificities of zebrafish Tlr4a and b remain unknown, Sullivan *et al.* demonstrated that the intracellular portions of Tlr4a and b have the capacity to activate NF-κB signalling. This is in contrast with data from Sepulcre *et al*, who reported negative regulation of NF-κB by Tlr4b (87).

One of the best studied TLR adaptors in mammals is MyD88. Myd88 transcript was detected in cells of the myeloid lineage in the head, on the yolk sac, the trunk and the posterior blood island of zebrafish embryos. Myd88-positive leukocytes contribute to inflammatory responses and were able to phagocytose bacteria (88). Knock-down studies in zebrafish embryos revealed an essential function of Myd88 during *Salmonella* infection, showing a strongly impaired response to an otherwise non-pathogenic *Salmonella* strain (Chapter 2, 84). Furthermore, challenge of *myd88* morphants by a pathogenic *Salmonella* wild-type strain revealed activation

of Myd88-dependent and -independent signalling pathways, as are also present in mammals (Chapter 3, 85). In addition, like in mammals the zebrafish homolog of TRIF has been shown to play an essential role in antiviral immunity (89). However, the precise mechanisms of NFκB and IFN activation upon viral infection appear to have diverged between fish and mammals. Therefore, while there is a large similarity of TLR receptors and downstream mediators between fish and mammals, further studies should clarify to what extend the TLR ligand specificities and downstream signal transduction mechanisms are conserved.

Outline of this thesis

In the work described in this thesis we make use of the zebrafish embryo to study vertebrate innate immune responses to systemic bacterial infections in general, and to assess the role of the TLR signalling pathway in the innate immune response in particular. To model systemic infections we use the Gram-negative enterobacteria *Salmonella enterica* Serovar Typhimurium (*S. typhimurium*), the cause of human salmonellosis.

In **Chapter 2** the fundamental and conserved role of Myd88 in the zebrafish embryonic innate immune response is demonstrated. Using a morpholino-based knock-down approach we show that Myd88-mediated signalling events are crucial in mounting a sufficiently strong immune response to clear an infection with a non-pathogenic *S. typhimurium* strain.

Chapter 3 presents a time-resolved transcriptome analysis of the inflammatory and innate immune responses elicited by zebrafish embryos to a systemic infection with a pathogenic and non-pathogenic *S. typhimurium* strain. The transcriptional response to infection with both strains shows clear conservation with host responses detected in other vertebrate models and human cells, including induction of genes encoding cell surface receptors, signalling intermediates, transcription factors and inflammatory mediators. Extending the work of chapter 2 we show that *Salmonella* infection is mediated by Myd88-dependent and -independent signalling events. Additionally, we demonstrate that gene induction by flagellin is mediated by Tlr5 in zebrafish embryos, indicating that ligand specificity for this member of the TLR family is conserved between human and zebrafish.

Chapter 4 is focused on the immune function of the zebrafish homolog of mammalian TRAF6, an important downstream mediator of the TLR pathway, demonstrating that *traf6* knock-down leads to a strongly decreased transcriptional immune response upon systemic *Salmonella* infection. Among the Traf6-dependent genes is not only a large set of well known anti-microbial and inflammatory genes but also several genes whose role in the immune system was not previously expected to be Traf6-dependent. One such example is the fertility hormone gene *GnRH*.

Finally, in **Chapter 5** an effort is made to define the role of Traf6 in the early zebrafish development using a microarray-based approach. Comparison of the genes

that were dependent on Traf6 during early development with the Traf6-dependent immune genes from chapter 4 revealed only a minor overlap, indicating the diverse functions of Traf6 during infection and development.

References

1. Kasahara, M., T. Suzuki, and L. D. Pasquier. 2004. On the origins of the adaptive immune system: novel insights from invertebrates and cold-blooded vertebrates. *Trends Immunol* 25:105-111.
2. Kimbrell, D. A., and B. Beutler. 2001. The evolution and genetics of innate immunity. *Nat Rev Genet* 2:256-267.
3. Janeway, C. A. 2001. *Immunobiology: the immune system in health and disease*. Garland Publishing.
4. Li, Z., C. J. Woo, M. D. Iglesias-Ussel, D. Ronai, and M. D. Scharff. 2004. The generation of antibody diversity through somatic hypermutation and class switch recombination. *Genes Dev* 18:1-11.
5. Gabay, C., and I. Kushner. 1999. Acute-phase proteins and other systemic responses to inflammation. *N Engl J Med* 340:448-454.
6. Black, S., I. Kushner, and D. Samols. 2004. C-reactive Protein. *J Biol Chem* 279:48487-48490.
7. Salzman, N. H., D. Ghosh, K. M. Huttner, Y. Paterson, and C. L. Bevins. 2003. Protection against enteric salmonellosis in transgenic mice expressing a human intestinal defensin. *Nature* 422:522-526.
8. Nizet, V., T. Ohtake, X. Lauth, J. Trowbridge, J. Rudisill, R. A. Dorschner, V. Pestonjamasp, J. Piraino, K. Huttner, and R. L. Gallo. 2001. Innate antimicrobial peptide protects the skin from invasive bacterial infection. *Nature* 414:454-457.
9. Daher, K. A., M. E. Selsted, and R. I. Lehrer. 1986. Direct inactivation of viruses by human granulocyte defensins. *J Virol* 60:1068-1074.
10. Yang, D., A. Biragyn, D. M. Hoover, J. Lubkowski, and J. J. Oppenheim. 2004. Multiple roles of antimicrobial defensins, cathelicidins, and eosinophil-derived neurotoxin in host defense. *Annu Rev Immunol* 22:181-215.
11. De Smet, K., and R. Contreras. 2005. Human antimicrobial peptides: defensins, cathelicidins and histatins. *Biotechnol Lett* 27:1337-1347.
12. Ayabe, T., D. P. Satchell, C. L. Wilson, W. C. Parks, M. E. Selsted, and A. J. Ouellette. 2000. Secretion of microbicidal alpha-defensins by intestinal Paneth cells in response to bacteria. *Nat Immunol* 1:113-118.
13. Bals, R., X. Wang, M. Zasloff, and J. M. Wilson. 1998. The peptide antibiotic LL-37/hCAP-18 is expressed in epithelia of the human lung where it has broad antimicrobial activity at the airway surface. *Proc Natl Acad Sci U S A* 95:9541-9546.
14. Ganz, T. 1987. Extracellular release of antimicrobial defensins by human polymorphonuclear leukocytes. *Infect Immun* 55:568-571.
15. Brogden, K. A. 2005. Antimicrobial peptides: pore formers or metabolic inhibitors in bacteria? *Nat Rev Microbiol* 3:238-250.
16. Brinkmann, V., U. Reichard, C. Goosmann, B. Fauler, Y. Uhlemann, D. S. Weiss, Y. Weinrauch, and A. Zychlinsky. 2004. Neutrophil extracellular traps kill bacteria. *Science* 303:1532-1535.
17. Urban, C. F., U. Reichard, V. Brinkmann, and A. Zychlinsky. 2006. Neutrophil extracellular traps capture and kill Candida albicans yeast and hyphal forms. *Cell Microbiol* 8:668-676.
18. Mosser, D. M., and J. P. Edwards. 2008. Exploring the full spectrum of macrophage activation. *Nat Rev Immunol* 8:958-969.
19. Levine, B., and V. Deretic. 2007. Unveiling the roles of autophagy in innate and adaptive immunity. *Nat Rev Immunol* 7:767-777.
20. Liu, Y. J. 2001. Dendritic cell subsets and lineages, and their functions in innate and adaptive immunity. *Cell* 106:259-262.
21. Nakano, T., T. Sonoda, C. Hayashi, A. Yamatodani, Y. Kanayama, T. Yamamura, H. Asai, T. Yonezawa, Y. Kitamura, and S. J. Galli. 1985. Fate of bone marrow-derived cultured mast cells after intracutaneous, intraperitoneal, and intravenous transfer into genetically mast cell-deficient W/Wv mice. Evidence that cultured mast cells can give rise to both connective tissue type and mucosal mast cells. *J Exp Med* 162:1025-1043.
22. Marshall, J. S. 2004. Mast-cell responses to pathogens. *Nat Rev Immunol* 4:787-799.
23. Shelburne, C. P., H. Nakano, A. L. St John, C. Chan, J. B. McLachlan, M. D. Gunn, H. F. Staats, and S. N. Abraham. 2009. Mast cells augment adaptive immunity by orchestrating dendritic cell trafficking through infected tissues. *Cell Host Microbe* 6:331-342.
24. Metz, M., and M. Maurer. 2007. Mast cells--key effector cells in immune responses. *Trends Immunol* 28:234-241.
25. Gilfillan, A. M., and C. Tkaczyk. 2006. Integrated signalling pathways for mast-cell activation. *Nat Rev Immunol* 6:218-230.
26. Vosshenrich, C. A., S. I. Samson-Villeger, and J. P. Di Santo. 2005. Distinguishing features of developing natural killer cells. *Curr Opin Immunol* 17:151-158.
27. Topham, N. J., and E. W. Hewitt. 2009. Natural killer cell cytotoxicity: how do they pull the trigger? *Immunology* 128:7-15.
28. Braud, V. M., D. S. Allan, C. A. O'Callaghan, K. Soderstrom, A. D'Andrea, G. S. Ogg, S. Lazetic, N. T. Young, J. I. Bell, J. H. Phillips, L. L. Lanier, and A. J. McMichael. 1998. HLA-E binds to natural killer cell receptors CD94/NKG2A, B and C. *Nature* 391:795-799.
29. O'Callaghan, C. A. 2000. Molecular basis of human natural killer cell recognition of HLA-E (human leucocyte antigen-E) and its relevance to clearance of pathogen-infected and tumour cells. *Clin Sci (Lond)* 99:9-17.

30. Hewitt, E. W. 2003. The MHC class I antigen presentation pathway: strategies for viral immune evasion. *Immunology* 110:163-169.
31. Waldhauer, I., and A. Steinle. 2008. NK cells and cancer immunosurveillance. *Oncogene* 27:5932-5943.
32. Bahram, S., H. Inoko, T. Shiina, and M. Radosavljevic. 2005. MIC and other NKG2D ligands: from none to too many. *Curr Opin Immunol* 17:505-509.
33. Mistry, A. R., and C. A. O'Callaghan. 2007. Regulation of ligands for the activating receptor NKG2D. *Immunology* 121:439-447.
34. Lanier, L. L. 2005. NK cell recognition. *Annu Rev Immunol* 23:225-274.
35. Franchi, L., N. Warner, K. Viani, and G. Nunez. 2009. Function of Nod-like receptors in microbial recognition and host defense. *Immunol Rev* 227:106-128.
36. Kawai, T., and S. Akira. 2008. Toll-like receptor and RIG-I-like receptor signaling. *Ann N Y Acad Sci* 1143:1-20.
37. Medzhitov, R. 2001. Toll-like receptors and innate immunity. *Nat Rev Immunol* 1:135-145.
38. Anderson, K. V., G. Jurgens, and C. Nusslein-Volhard. 1985. Establishment of dorsal-ventral polarity in the Drosophila embryo: genetic studies on the role of the Toll gene product. *Cell* 42:779-789.
39. Lemaitre, B., E. Nicolas, L. Michaut, J. M. Reichhart, and J. A. Hoffmann. 1996. The dorsoventral regulatory gene cassette spatzle/Toll/cactus controls the potent antifungal response in Drosophila adults. *Cell* 86:973-983.
40. Poltorak, A., X. He, I. Smirnova, M. Y. Liu, C. Van Huffel, X. Du, D. Birdwell, E. Alejos, M. Silva, C. Galanos, M. Freudenberg, P. Ricciardi-Castagnoli, B. Layton, and B. Beutler. 1998. Defective LPS signaling in C3H/HeJ and C57BL/10ScCr mice: mutations in Tlr4 gene. *Science* 282:2085-2088.
41. Alexopoulou, L., A. C. Holt, R. Medzhitov, and R. A. Flavell. 2001. Recognition of double-stranded RNA and activation of NF-kappaB by Toll-like receptor 3. *Nature* 413:732-738.
42. Diebold, S. S., T. Kaisho, H. Hemmi, S. Akira, and C. Reis e Sousa. 2004. Innate antiviral responses by means of TLR7-mediated recognition of single-stranded RNA. *Science* 303:1529-1531.
43. Hayashi, F., K. D. Smith, A. Ozinsky, T. R. Hawn, E. C. Yi, D. R. Goodlett, J. K. Eng, S. Akira, D. M. Underhill, and A. Aderem. 2001. The innate immune response to bacterial flagellin is mediated by Toll-like receptor 5. *Nature* 410:1099-1103.
44. Heil, F., H. Hemmi, H. Hochrein, F. Ampenberger, C. Kirschning, S. Akira, G. Lipford, H. Wagner, and S. Bauer. 2004. Species-specific recognition of single-stranded RNA via toll-like receptor 7 and 8. *Science* 303:1526-1529.
45. Hemmi, H., O. Takeuchi, T. Kawai, T. Kaisho, S. Sato, H. Sanjo, M. Matsumoto, K. Hoshino, H. Wagner, K. Takeda, and S. Akira. 2000. A Toll-like receptor recognizes bacterial DNA. *Nature* 408:740-745.
46. Barton, G. M., and J. C. Kagan. 2009. A cell biological view of Toll-like receptor function: regulation through compartmentalization. *Nat Rev Immunol* 9:535-542.
47. O'Neill, L. A., and A. G. Bowie. 2007. The family of five: TIR-domain-containing adaptors in Toll-like receptor signalling. *Nat Rev Immunol* 7:353-364.
48. Oshiumi, H., M. Matsumoto, K. Funami, T. Akazawa, and T. Seya. 2003. TICAM-1, an adaptor molecule that participates in Toll-like receptor 3-mediated interferon-beta induction. *Nat Immunol* 4:161-167.
49. Yamamoto, M., K. Takeda, and S. Akira. 2004. TIR domain-containing adaptors define the specificity of TLR signaling. *Mol Immunol* 40:861-868.
50. Carty, M., R. Goodbody, M. Schroder, J. Stack, P. N. Moynagh, and A. G. Bowie. 2006. The human adaptor SARM negatively regulates adaptor protein TRIF-dependent Toll-like receptor signaling. *Nat Immunol* 7:1074-1081.
51. Szretter, K. J., M. A. Samuel, S. Gilfillan, A. Fuchs, M. Colonna, and M. S. Diamond. 2009. The immune adaptor molecule SARM modulates tumor necrosis factor alpha production and microglia activation in the brainstem and restricts West Nile Virus pathogenesis. *J Virol* 83:9329-9338.
52. Kawai, T., and S. Akira. 2007. Signaling to NF-kappaB by Toll-like receptors. *Trends Mol Med* 13:460-469.
53. Oganesyan, G., S. K. Saha, B. Guo, J. Q. He, A. Shahangian, B. Zarnegar, A. Perry, and G. Cheng. 2006. Critical role of TRAF3 in the Toll-like receptor-dependent and -independent antiviral response. *Nature* 439:208-211.
54. Mogensen, T. H. 2009. Pathogen recognition and inflammatory signaling in innate immune defenses. *Clin Microbiol Rev* 22:240-273, Table of Contents.
55. Geijtenbeek, T. B., and S. I. Gringhuis. 2009. Signalling through C-type lectin receptors: shaping immune responses. *Nat Rev Immunol* 9:465-479.
56. Areschoug, T., and S. Gordon. 2009. Scavenger receptors: role in innate immunity and microbial pathogenesis. *Cell Microbiol* 11:1160-1169.
57. Jenner, R. G., and R. A. Young. 2005. Insights into host responses against pathogens from transcriptional profiling. *Nat Rev Microbiol* 3:281-294.
58. Davis, J. M., H. Clay, J. L. Lewis, N. Ghori, P. Herbomel, and L. Ramakrishnan. 2002. Real-time visualization of mycobacterium-macrophage interactions leading to initiation of granuloma formation in zebrafish embryos. *Immunity* 17:693-702.
59. Mathias, J. R., B. J. Perrin, T. X. Liu, J. Kanki, A. T. Look, and A. Huttenlocher. 2006. Resolution of inflammation by retrograde chemotaxis of neutrophils in transgenic zebrafish. *J Leukoc Biol* 80:1281-1288.
60. Meijer, A. H., A. M. van der Sar, C. Cunha, G. E. Lamers, M. A. Laplante, H. Kikuta, W. Bitter, T. S. Becker, and H. P. Spaink. 2008. Identification and real-time imaging of a myc-expressing neutrophil population involved in

inflammation and mycobacterial granuloma formation in zebrafish. *Dev Comp Immunol* 32:36-49.
61. Redd, M. J., G. Kelly, G. Dunn, M. Way, and P. Martin. 2006. Imaging macrophage chemotaxis in vivo: studies of microtubule function in zebrafish wound inflammation. *Cell Motil Cytoskeleton* 63:415-422.
62. Renshaw, S. A., C. A. Loynes, D. M. Trushell, S. Elworthy, P. W. Ingham, and M. K. Whyte. 2006. A transgenic zebrafish model of neutrophilic inflammation. *Blood* 108:3976-3978.
63. van der Sar, A. M., R. J. Musters, F. J. van Eeden, B. J. Appelmelk, C. M. Vandenbroucke-Grauls, and W. Bitter. 2003. Zebrafish embryos as a model host for the real time analysis of Salmonella typhimurium infections. *Cell Microbiol* 5:601-611.
64. Ward, A. C., D. O. McPhee, M. M. Condron, S. Varma, S. H. Cody, S. M. Onnebo, B. H. Paw, L. I. Zon, and G. J. Lieschke. 2003. The zebrafish spi1 promoter drives myeloid-specific expression in stable transgenic fish. *Blood* 102:3238-3240.
65. Miller, J. D., and M. N. Neely. 2005. Large-scale screen highlights the importance of capsule for virulence in the zoonotic pathogen Streptococcus iniae. *Infect Immun* 73:921-934.
66. Lieschke, G. J., and P. D. Currie. 2007. Animal models of human disease: zebrafish swim into view. *Nat Rev Genet* 8:353-367.
67. Trede, N. S., T. Ota, H. Kawasaki, B. H. Paw, T. Katz, B. Demarest, S. Hutchinson, Y. Zhou, C. Hersey, A. Zapata, C. T. Amemiya, and L. I. Zon. 2008. Zebrafish mutants with disrupted early T-cell and thymus development identified in early pressure screen. *Dev Dyn* 237:2575-2584.
68. Schorpp, M., M. Bialecki, D. Diekhoff, B. Walderich, J. Odenthal, H. M. Maischein, A. G. Zapata, and T. Boehm. 2006. Conserved functions of Ikaros in vertebrate lymphocyte development: genetic evidence for distinct larval and adult phases of T cell development and two lineages of B cells in zebrafish. *J Immunol* 177:2463-2476.
69. Pase, L., J. E. Layton, W. P. Kloosterman, D. Carradice, P. M. Waterhouse, and G. J. Lieschke. 2009. miR-451 regulates zebrafish erythroid maturation in vivo via its target gata2. *Blood* 113:1794-1804.
70. Wang, Y., H. Zong, Y. Chi, Y. Hong, Y. Yang, W. Zou, X. Yun, and J. Gu. 2009. Repression of estrogen receptor alpha by CDK11p58 through promoting its ubiquitin-proteasome degradation. *J Biochem* 145:331-343.
71. Herbomel, P., B. Thisse, and C. Thisse. 1999. Ontogeny and behaviour of early macrophages in the zebrafish embryo. *Development* 126:3735-3745.
72. Herbomel, P., B. Thisse, and C. Thisse. 2001. Zebrafish early macrophages colonize cephalic mesenchyme and developing brain, retina, and epidermis through a M-CSF receptor-dependent invasive process. *Dev Biol* 238:274-288.
73. Lieschke, G. J., A. C. Oates, M. O. Crowhurst, A. C. Ward, and J. E. Layton. 2001. Morphologic and functional characterization of granulocytes and macrophages in embryonic and adult zebrafish. *Blood* 98:3087-3096.
74. Lam, S. H., H. L. Chua, Z. Gong, T. J. Lam, and Y. M. Sin. 2004. Development and maturation of the immune system in zebrafish, Danio rerio: a gene expression profiling, in situ hybridization and immunological study. *Dev Comp Immunol* 28:9-28.
75. Willett, C. E., A. Cortes, A. Zuasti, and A. G. Zapata. 1999. Early hematopoiesis and developing lymphoid organs in the zebrafish. *Dev Dyn* 214:323-336.
76. Kizy, A. E., and M. N. Neely. 2009. First Streptococcus pyogenes signature-tagged mutagenesis screen identifies novel virulence determinants. *Infect Immun* 77:1854-1865.
77. Lesley, R., and L. Ramakrishnan. 2008. Insights into early mycobacterial pathogenesis from the zebrafish. *Curr Opin Microbiol* 11:277-283.
78. Meeker, N. D., and N. S. Trede. 2008. Immunology and zebrafish: spawning new models of human disease. *Dev Comp Immunol* 32:745-757.
79. Meijer, A. H., S. F. Gabby Krens, I. A. Medina Rodriguez, S. He, W. Bitter, B. Ewa Snaar-Jagalska, and H. P. Spaink. 2004. Expression analysis of the Toll-like receptor and TIR domain adaptor families of zebrafish. *Mol Immunol* 40:773-783.
80. Jault, C., L. Pichon, and J. Chluba. 2004. Toll-like receptor gene family and TIR-domain adapters in Danio rerio. *Mol Immunol* 40:759-771.
81. Stein, C., M. Caccamo, G. Laird, and M. Leptin. 2007. Conservation and divergence of gene families encoding components of innate immune response systems in zebrafish. *Genome Biol* 8:R251.
82. Laing, K. J., M. K. Purcell, J. R. Winton, and J. D. Hansen. 2008. A genomic view of the NOD-like receptor family in teleost fish: identification of a novel NLR subfamily in zebrafish. *BMC Evol Biol* 8:42.
83. Biacchesi, S., M. LeBerre, A. Lamoureux, Y. Louise, E. Lauret, P. Boudinot, and M. Bremont. 2009. Mitochondrial antiviral signaling protein plays a major role in induction of the fish innate immune response against RNA and DNA viruses. *J Virol* 83:7815-7827.
84. van der Sar, A. M., O. W. Stockhammer, C. van der Laan, H. P. Spaink, W. Bitter, and A. H. Meijer. 2006. MyD88 innate immune function in a zebrafish embryo infection model. *Infect Immun* 74:2436-2441.
85. Stockhammer, O. W., A. Zakrzewska, Z. Hegedus, H. P. Spaink, and A. H. Meijer. 2009. Transcriptome profiling and functional analyses of the zebrafish embryonic innate immune response to Salmonella infection. *J Immunol* 182:5641-5653.
86. Sullivan, C., J. Charette, J. Catchen, C. R. Lage, G. Giasson, J. H. Postlethwait, P. J. Millard, and C. H. Kim. 2009. The gene history of zebrafish tlr4a and tlr4b is predictive of their divergent functions. *J Immunol* 183:5896-

5908.
87. Sepulcre, M. P., F. Alcaraz-Perez, A. Lopez-Munoz, F. J. Roca, J. Meseguer, M. L. Cayuela, and V. Mulero. 2009. Evolution of lipopolysaccharide (LPS) recognition and signaling: fish TLR4 does not recognize LPS and negatively regulates NF-kappaB activation. *J Immunol* 182:1836-1845.
88. Hall, C., M. V. Flores, A. Chien, A. Davidson, K. Crosier, and P. Crosier. 2009. Transgenic zebrafish reporter lines reveal conserved Toll-like receptor signaling potential in embryonic myeloid leukocytes and adult immune cell lineages. *J Leukoc Biol* 85:751-765.
89. Sullivan, C., J. H. Postlethwait, C. R. Lage, P. J. Millard, and C. H. Kim. 2007. Evidence for evolving Toll-IL-1 receptor-containing adaptor molecule function in vertebrates. *J Immunol* 178:4517-4527.

2 MyD88 innate immune function in a zebrafish embryo infection model

Astrid M. van der Sar[1], Oliver W. Stockhammer[2], Carina van der Laan[1], Herman P. Spaink[2], Wilbert Bitter[1] and Annemarie H. Meijer[2]

1 Department of Medical Microbiology, VU Medical Centre, Amsterdam, The Netherlands 2 Institute of Biology, Leiden University, Leiden, The Netherlands

Abstract

Innate immunity signalling mechanisms during vertebrate embryogenesis are largely unknown. To study Toll-like receptor (TLR) signalling function in the zebrafish embryo model, we designed an experimental setup for antisense morpholino knockdown under conditions of bacterial infection. Clearance of *Salmonella typhimurium* Ra bacteria was significantly impaired after knockdown of myeloid differentiation factor 88 (MyD88), a common adaptor protein in TLR and interleukin-1 receptor signalling. Thereby, we demonstrate for the first time that the innate immune response of the developing embryo involves MyD88-dependent signalling, which further establishes the zebrafish embryo as a model to study vertebrate innate immunity.

Introduction

Innate immunity relies heavily on signalling by members of the Toll-like receptor (TLR) family (25). TLRs and associated adaptor molecules are highly conserved between zebrafish (*Danio rerio*) and other vertebrates (13, 18). Bacterial and viral infections were found to induce expression levels of different zebrafish *TLR* genes (18, 20). However, direct functional evidence to confirm the role of TLR signalling in the innate immune response of zebrafish has not yet been reported.

The exploitation of zebrafish as an animal model to study immunity and infectious diseases is attractive for three main reasons (34, 28, 29, 30). First, high-throughput forward genetic screens in zebrafish are a powerful means to uncover novel immune functions. Second, the optical transparency of the free-living zebrafish embryos makes it possible to examine the early development of the immune system and the progression of microbial infections in real-time (11, 32, 12, 6, 31). Third, the zebrafish embryo is easily accessible to experimental manipulations and efficient inactivation of gene functions can be achieved by injection of antisense morpholino oligonucleotides (19). However, a major obstacle is that many of the immunological details and research tools that are available for more established animal models have not yet been resolved and developed for zebrafish.

The innate immune system of the zebrafish embryo starts developing during the first day post fertilization (dpf). Myeloid precursors originate from the anterior lateral plate mesoderm and migrate to the yolk sac, where they differentiate before the onset of blood circulation (11). Differentiated myeloid cells invade the head mesenchyme tissue or join the blood circulation (11, 32, 12). It has been shown that they are able to phagocytose apoptotic cell corpses (11). Furthermore, myeloid cells show specific adherence to bacteria injected into the blood and phagocytose them rapidly (11, 6, 31). They are also able to sense the presence of bacteria injected into one of the closed body cavities and to respond by migration to the infection site (11). All cells of

the myeloid lineage initially express the transcription factor gene Pu.1 (Spi1), which is essential for their differentiation (21). After 1 dpf Pu.1 expression decreases and two distinct populations of myeloid cells can be distinguished by the expression of two marker genes, *L-plastin*, which encodes a macrophage-specific actin-bundling protein, and *mpx*, which encodes a member of the myeloperoxidase family (11, 3, 17). At 2 dpf, the mpx-positive cells show the morphological characteristics of neutrophil granulocytes and are able to migrate to sites of trauma (17, 4). Immature lymphoblasts can first be detected by 3 dpf, but T and B lymphocytes do not mature until 4 to 6 weeks after hatching (5, 16). Therefore, the zebrafish embryo model is useful to determine the role of innate immunity in responses to different infectious agents, as it is uncoupled from adaptive immunity. With this approach, Davis et al. (6) showed that, during the first days of development, innate immunity determinants are sufficient for granuloma formation resulting from a mycobacterial infection.

Results and discussion

To investigate the potential of the zebrafish embryo as a model to study vertebrate innate immune signalling, we first set out to determine the expression of *TLRs* and associated adaptor genes during embryo development. Semi-quantitative RT-PCR analysis, using the Superscript II one-step system (Invitrogen) with previously described conditions and primers (18), showed that at least 15 zebrafish *TLR* genes are expressed at 1 dpf, when the first functional macrophages and neutrophils enter blood circulation (Fig.1). Most of these *TLRs* are also maternally present, since expression was already detected at the 4-cell stage, which is prior to the onset of zygotic gene expression. Several *TLRs* display distinct differential expression patterns during early stages of embryogenesis. For example, *zTLR1* expression peaks during blastula and gastrula stages (dome to 80% epiboly) and is high during embryogenesis compared to the adult stage. Expression of *zTLR3* peaks during gastrulation and segmentation (80% epiboly to 5-somite stage), is reduced between 1 to 5 dpf, but returns to higher levels in the adult stage. Diffuse *zTLR3* expression in the developing brain of zebrafish embryos was previously reported (20). A peak in the expression of *zTLR5a*, *zTLR5b*, *zTLR7*, *zTLR8a*, *zTLR8b* and *zTLR18* coincides with the appearance of embryonic macrophages at 1 dpf. Expression of the *zMyD88* adaptor gene is highest in adults. In the embryo, maternal *zMyD88* transcript levels are reduced during blastula and gastrula stages and return to higher levels during segmentation and later stages (Fig.1). The other MyD88-like adaptor genes *zMAL*, *zTRIF* and *zSARM* are also maternally present and expressed throughout embryogenesis (Fig.1).

To study innate immunity signalling function in the zebrafish embryo, we targeted MyD88, which is known to function as a common adaptor protein in the downstream signalling pathways of all mammalian TLRs, except TLR3, and as an adaptor of the interleukin-1/-18 receptors that are activated through TLR signalling (1, 7, 2). A

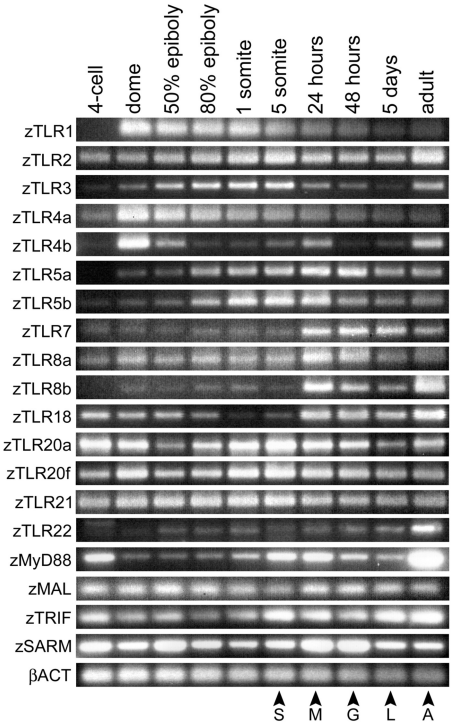


FIGURE 1. RT-PCR analysis of zebrafish TLR and adaptor genes at different developmental stages. β-Actin (βACT) expression was determined for reference. 100 ng of total RNA was used in the RT-PCR reactions, except for *zTRIF* and *βACT* where 50 ng was used. 40 cycles of amplification were used in all cases. The timing of development of the zebrafish immune system is indicated with marked arrow heads: S, haematopoietic stem cells can be distinguished in the ventro-lateral mesoderm; M, embryonic macrophages migrate over the yolk sac, enter blood circulation and are able to phagocytose injected bacteria; G, cells with typical granulocyte morphology can be distinguished that are able to localize to sites of acute inflammation; L, immature lymphoblasts can be detected and myelopoiesis is taken over by the anterior kidney; A, adaptive immunity is matured after 4-6 weeks of development.

morpholino knockdown approach (19) was used to interfere with MyD88 function by inhibition of its mRNA translation. An antisense morpholino (GeneTools) (5'-TAGCAAAACCTCTGTTATCCAGCGA-3') was designed, which targets the leader sequence of the *zMyD88* mRNA (DQ100359) at positions -30 to -7 with respect to the ATG. A 5-basepair mismatch control morpholino was used with the sequence 5'-TAcCAtAACCTgTGTTATCgAGgGA-3' (mismatches in lower case). For microinjection morpholinos were diluted to different concentrations in Danieu's buffer (19) and approximately 1 nl was injected into the blastomere of the 1-2 cell stage embryo. To test the specificity of the MyD88 morpholino and its 5-mismatch control sequence, each of these morpholinos was first coinjected with a *zMyD88-EGFP* fusion mRNA including the 5' leader sequence. Embryos coinjected with the 5-mismatch control morpholino and *zMyD88-GFP* mRNA showed clear fluorescence at the 70-90% epiboly stage (Fig.2B,D). In contrast, embryos coinjected with the MyD88 morpholino and *zMyD88-GFP* mRNA showed only autofluorescence of the yolk (Fig.2A,C), similar as in embryos injected with morpholinos only (Fig.2E,F). Therefore, the MyD88 morpholino effectively blocks translation of *zMyD88-GFP* mRNA. Coinjection of each of the morpholinos with *GFP* mRNA (Fig.2G,H) or with a modified *zMyD88-GFP* mRNA lacking the 5' leader sequence (Fig.2I,J), resulted in similar fluorescence levels in embryo tissues, confirming that the MyD88 morpholino specifically targets the *zMyD88* leader sequence.

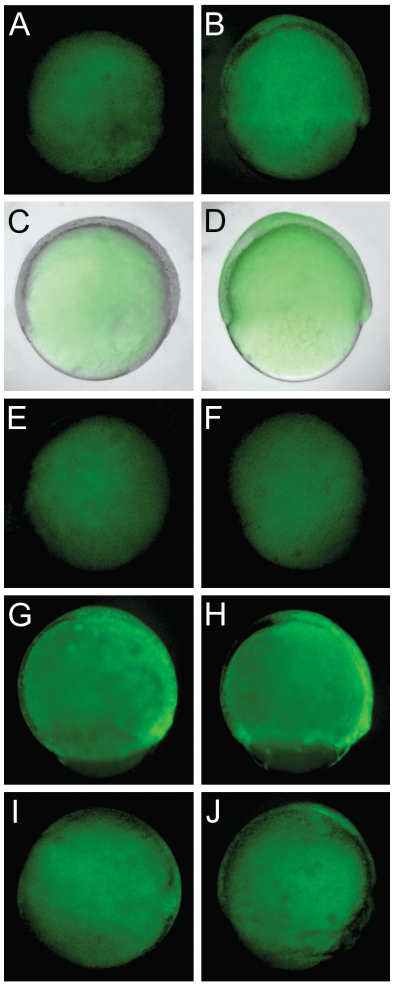


FIGURE 2. Specificity of the MyD88 and 5-basepair mismatch control morpholino. Embryos were injected with 2 ng of MyD88 morpholino (A,C,E,G,I) or with 2 ng of 5-basepair mismatch control morpholino (B,D,F,H,J). (A,B) Coinjection of MyD88 (A) or mismatch (B) morpholino with 2 pg of zMyD88-GFP mRNA, which includes the 5′ leader sequence at which the morpholino is targeted. (C,D) Overlay of the fluorescence images from A and B with bright field images of the same embryos. Note the absence of GFP signal in the embryonic tissues of the embryo co-injected with the MyD88 morpholino (A,C) and the presence of GFP signal in the embryonic tissues of the embryo co-injected with the mismatch control morpholino (B,D). The yolk shows autofuorescence independent of injection of the GFP construct. (E,F) Control embryos injected with MyD88 (E) or mismatch (F) morpholinos only, showing similar yolk autofluorescence as the embryo in A. (G,H) Coinjection of MyD88 (G) or mismatch (H) morpholino with 2 pg of GFP mRNA. (I,J) Coinjection of MyD88 (I) or mismatch (J) morpholino with 2 pg of a modified zMyD88-GFP mRNA lacking the morpholino target site. Note that fluorescence in the embryonic tissues of the embryos shown in G-J is unaffected by injection of the different morpholinos. Fluorescence images were acquired with a Leica DC500 camera and MZ Fluo 3 stereomicroscope. Fluorescence recordings were made with a fixed exposure time of 10.4 s and with the gain set at 1. Contrast was enhanced by 70% during image processing with Adobe Photoshop 6.0.

Embryos injected with 1.7 to 4 ng of MyD88 or control morpholinos showed no apparent morphological differences with wild type embryos. To determine if myelopoiesis was affected in MyD88 morphants, we analysed the expression of myeloid cell markers. From 1 dpf onwards all myeloid cells of zebrafish embryos express either one of the two markers, *L-plastin* or *mpx* (11, 3, 17, 4). Expression of the macrophage marker gene, *L-plastin*, was examined at 1 dpf, after the onset of blood circulation. To this extent a digoxigenin-labeled antisense riboprobe was synthesized with T7 RNA polymerase from an EcoRI-linearized *l-plastin* cDNA clone (AF157110) and whole-mount in situ hybridization was carried out according to the protocol of Thisse et al. (27). In MyD88 morphants, *L-plastin*-positive macrophages were dispersed over the yolk sac and some had accumulated in the ventral venous plexus (Fig.3A). This pat-

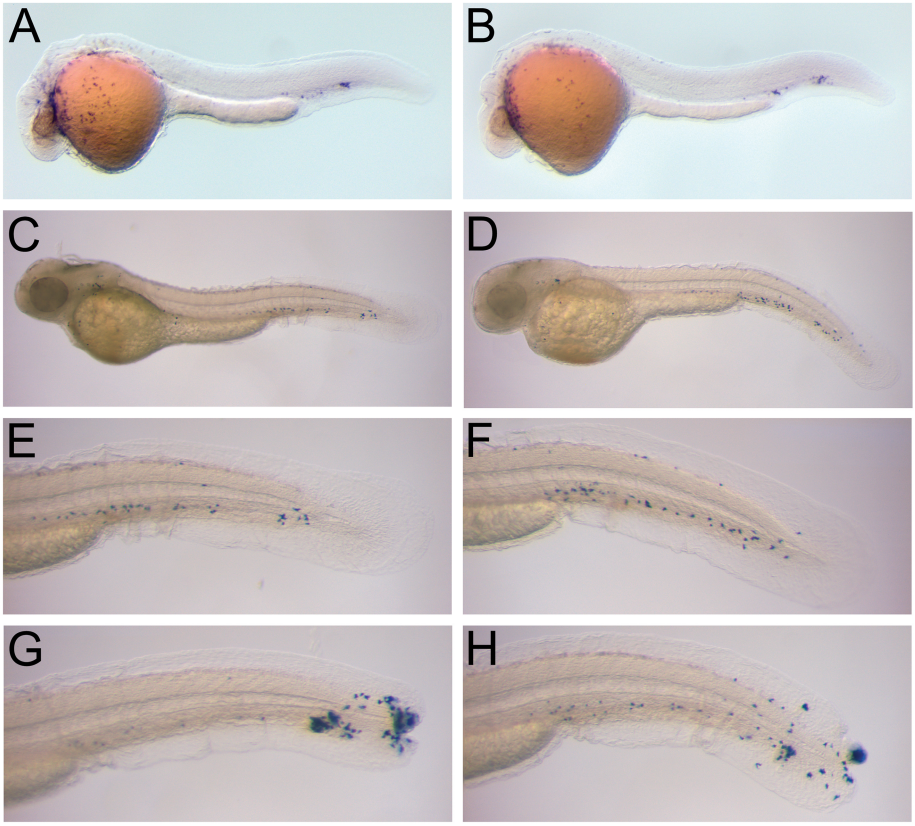


FIGURE 3. Development and properties of myeloid cells in MyD88 morphants. Embryos injected with 1.7 ng of MyD88 morpholino (A,C,E,G) or with 1.7 ng of 5-mismatch control morpholino (B,D,F,H) were analysed for l-plastin expression in macrophages (A,B) and for myeloperoxidase activity in granulocytes (C-H). (A,B), 1 dpf embryos; (C,D), 2 dpf embryos; (E,F) tails of the embryos shown in C and D; (G,H) tails of 2 dpf embryos analysed 6 hours after wounding of the tail fin. Embryos were grown in 0.003% 1-phenyl-2-thiourea (Sigma) to prevent melanization. Composite images were made of different focal planes.

tern was similar to that observed in mismatch control morphants (Fig.3B) and to the reported *L-plastin* expression pattern of wild type zebrafish embryos (11).

A histochemical staining for myeloperoxidase (MPX) activity (17) was performed to check for the presence of granulocytes in embryos at 2 dpf. Peroxidase-positive cells in both the MyD88 and control morphants were abundantly present in the ventral venous plexus and some were scattered over the yolk surface or had invaded the head region (Fig.3C-F). The same distribution pattern of granulocytes was observed in non-injected control embryos (data not shown) and has been previously reported, based on both peroxidase staining and *mpx* gene expression (3, 17). Next, we took ad-

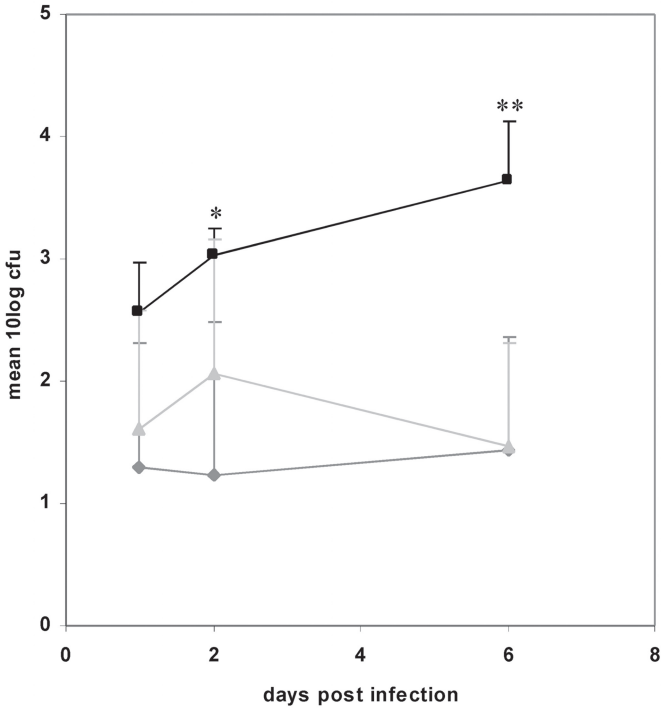


FIGURE 4. Number of colony forming units (cfu) of *S. typhimurium* Ra isolated from infected wild type (◆), mismatch (▲) and MyD88 (■) morphant embryos at different time points (dpi). Groups of 5 embryos were analysed at each time point and the mean $\log_{10}$ cfu is presented in the graph. The numbers are the average of four independent experiments. Statistical analyses were performed with single factor ANOVA tests and indicated that the difference between total cfu in wild type and morphant embryos was significant at $p<0.05$ (*) at 2 dpi and $p<0.01$ (**) at 6 dpi. The difference between total cfu in mismatch and morphant embryos was also significant at $p<0.01$ (**) at 6 dpi.

vantage of an acute inflammation assay devised by Lieschke et al. (17) to determine if the granulocytes of MyD88 morphants were functional. After wounding of the caudal fin with a sharp forceps, peroxidase-positive granulocytes of both MyD88 and control morphants accumulated at the site of trauma within 6 hours, indicating their functional involvement in acute inflammation (Fig.3G,H). In conclusion, based on *L-plastin* and MPX marker analyses, MyD88 morphants showed no apparent myelopoietic defects.

To demonstrate a function for MyD88 in the innate immune response of the zebrafish embryo, we made use of a *Salmonella typhimurium* infection model that was previously established (31). In this infection model, a low dose of DsRed-labeled bacteria is injected into the embryo's bloodstream just after the onset of circula-

tion at 1 dpf. While injection of the wild type *S. typhimurium* strain SL1027 resulted in a rapid lethal infection, its isogenic lipopolysaccharide (LPS) derivative SF1592 (Ra-type LPS mutant) proved to be non-pathogenic (31). In the present study, wild-type embryos, embryos injected with 1.7 ng of MyD88 morpholino, and embryos injected with the control morpholino were challenged in an infection experiment with *S. typhimurium* Ra mutant bacteria containing the DsRED plasmid pGMDs3 (31). Embryos were staged at 28 hpf (15) and individually infected by microinjection of approximately 100 colony forming units (cfu) into the axial vein near the blood island and the urogenital opening as previously described (31). As a control, a similar dose as used in the infection experiment was spotted onto LB agar plates for cfu counting.

Embryos were monitored daily until 6 days after infection with *S. typhimurium* Ra. No differences in survival rate were found between the infected wild-type embryos and MyD88 morphants. However, when embryos were examined for the presence of fluorescent bacteria, the MyD88 morphants showed more red spots, representing bacteria, than the wild-type embryos (data not shown). Therefore, total cfu counts were analysed from groups of five embryos that were sampled at 1 day post infection (dpi), 2 and 6 dpi. The pooled embryos were disintegrated (31) and the mixture was plated on LB agar plates. Four independent infection experiments were performed. At 1 dpi the average number of total cfu was approximately 5-fold higher in the MyD88 morphants as compared to wild type and mismatch control embryos (Fig.4). At 2 dpi, the difference between MyD88 morphants and wild type embryos was 10-fold and significant at $p<0.05$. Although it is not likely that morpholino knockdown is completely penetrant after 3 days of embryo development (19), a further increase of total cfu was still observed in MyD88 morphants at 6 dpi. At this stage the difference with total cfu in wild type and mismatch control embryos was significant at $p<0.01$. Between different experiments MyD88 morphant embryos harboured 100- to 1000- fold more bacteria than wild-type and mismatch control embryos, which had either completely cleared the infection or contained only low amounts of bacteria not higher than the inoculum size (Fig.4). Therefore we conclude that MyD88 morphants are not able to clear an infection with *S. typhimurium* Ra effectively.

Although there was a clear increase in cfu counts, it is interesting that infection with the normally non-pathogenic LPS Ra mutant of *S. typhimurium* was not lethal for MyD88 morphant embryos, indicating that multiplication of *S. typhimurium* Ra is not completely uncontrolled in MyD88 morphant embryos. Future analysis of a stable MyD88 knockout line should clarify if this was due to incomplete loss of MyD88 function in morphant embryos or due to MyD88-independent innate immunity mechanisms.

To investigate if the inability of MyD88 morphants to clear *S. typhimurium* Ra bacteria could be due to a defect in phagocytosis, embryos were examined at 1 h post infection with a Leica MZ 16 FA microscope. Ds-red labeled bacteria were observed

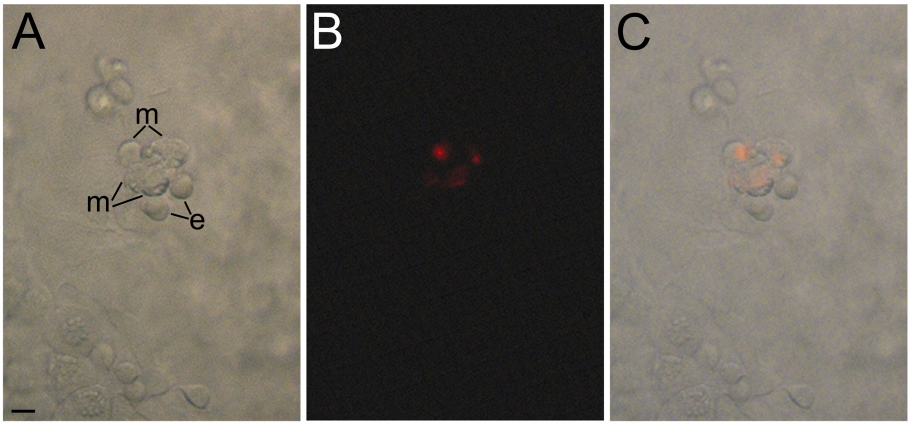


FIGURE 5. Presence of *S. typhimurium* Ra bacteria inside macrophages of a MyD88 morphant embryo. MyD88 morphant embryos were infected at 28 hpf by injection of DsRed-expressing *S. typhimurium* Ra bacteria into the axial vein and images of infected macrophages in the yolk sac circulation valley were taken after 1 h using a Leica DC500 camera and MZ 16 FA microscope. (A) Brightfield image showing a group of macrophages (m) and erythrocytes (e). (B) Fluorescence image of *S. typhimurium* Ra in the same location as the macrophages. (C) Overlay image of A and B, indicating the ability of macrophages of MyD88 morphants to phagocytose bacteria. Scale bar: 10 µm.

inside macrophages of MyD88 morphants (Fig.5), similar as in wild type embryos or in embryos injected with the mismatch control morpholino. Although we cannot yet exclude differences in phagocytosis efficiency or phagosome maturation, our present observations suggest that MyD88 morphants are primarily affected in activation of the bacterial killing mechanisms.

In conclusion, we have shown that TLRs are broadly expressed during zebrafish embryo development and that MyD88 is required for a wild-type response of zebrafish embryos to *S. typhimurium* Ra infection. These results indicate that MyD88-dependent signalling functions and is important in the early innate immune responses of embryonic zebrafish, independent from coupling to adaptive signalling responses. Furthermore, we have shown that zebrafish embryos express other MyD88-like adaptor molecules, such as Mal, TRIF and SARM, suggesting that MyD88-independent signalling pathways also exist in zebrafish, similar as in other vertebrates (14, 33, 8). The critical role of zebrafish MyD88 is consistent with many infection studies in MyD88-/- adult mice, which showed increased susceptibility to a variety of pathogens (26, 9, 23, 10, 22, 24). Therefore, the present study validates the zebrafish embryo as a useful model for analysis of the vertebrate innate immune system, which creates exciting possibilities for future studies in zebrafish embryo infection models.

Acknowledgments

The authors thank Ben Appelmelk and Ewa Snaar-Jagalska for valuable discussions, Indira Medina Rodriguez for initial testing of morpholinos and Wim Schouten, Teun Tak and Davy de Witt for fish care. Research at the VU Medical Centre was supported by a Horizon Breakthrough grant from the Netherlands Organisation for Scientific Research (NWO) and research at Leiden University was supported by a European Commission 6th Framework Programme grant (contract LSHG-CT-2003-503496, ZF-MODELS).

References

1. Adachi, O., T. Kawai, K. Takeda, M. Matsumoto, H. Tsutsui, M. Sakagami, K. Nakanishi, and S. Akira. 1998. Targeted disruption of the *MyD88* gene results in loss of IL-1- and IL-18-mediated function. Immunity 9: 143–150.
2. Akira, S., and K. Takeda. 2004. Toll-like receptor signalling. Nat. Rev. Immunol. 4:499-511.
3. Bennett, C. M., J. P. Kanki, J. Rhodes, T. X. Liu, B. H. Paw, M. W. Kieran, D. M. Langenau, A. Delahaye-Brown, L. I. Zon, M. D. Fleming, and A. T. Look. 2001. Myelopoiesis in the zebrafish, *Danio rerio*. Blood 98:643-651.
4. Crowhurst, M. O., J. E. Layton, and G. J. Lieschke. 2002. Developmental biology of zebrafish myeloid cells. Int. J. Dev. Biol. 46:483-492.
5. Davidson, A. J., and L. I. Zon. 2004. The 'definitive' (and 'primitive') guide to zebrafish hematopoiesis. Oncogene 23:7233-7246.
6. Davis, J. M., H. Clay, J. L. Lewis, N. Ghori, P. Herbomel, and L. Ramakrishnan. 2002. Real-time visualization of mycobacterium-macrophage interactions leading to initiation of granuloma formation in zebrafish embryos. Immunity 17:693-702.
7. Dunne, A., and L. A. O'Neill. 2003. The interleukin-1 receptor/Toll-like receptor superfamily: signal transduction during inflammation and host defense. Sci. STKE. 2003:re3.
8. Dunne, A., and L. A. O'Neill. 2005. Adaptor usage and Toll-like receptor signaling specificity. FEBS Lett. 579:3330-3335.
9. Edelson, B. T., and E. R. Unanue. 2002. MyD88-dependent but Toll-like receptor 2-independent innate immunity to *Listeria*: no role for either in macrophage listericidal activity. J. Immunol. 169:3869-3875.
10. Feng, C. G., C. A. Scanga, C. M. Collazo-Custodio, A. W. Cheever, S. Hieny, P. Caspar, and A. Sher. 2003. Mice lacking myeloid differentiation factor 88 display profound defects in host resistance and immune responses to *Mycobacterium avium* infection not exhibited by Toll-like receptor 2 (TLR2)- and TLR4-deficient animals. J. Immunol. 171:4758-4764.
11. Herbomel, P., B. Thisse, and C. Thisse. 1999. Ontogeny and behaviour of early macrophages in the zebrafish embryo. Development 126:3735-3745.
12. Herbomel, P., B. Thisse, and C. Thisse. 2001. Zebrafish early macrophages colonize cephalic mesenchyme and developing brain, retina, and epidermis through a M-CSF receptor-dependent invasive process. Dev. Biol. 238:274-288.
13. Jault, C., L. Pichon, and J. Chluba. 2004. Toll-like receptor gene family and TIR-domain adapters in *Danio rerio*. Mol. Immunol. 40:759-771.
14. Kaisho, T., O. Takeuchi, T. Kawai, K. Hoshino, and S. Akira. 2001. Endotoxin-induced maturation of MyD88-deficient dendritic cells. J. Immunol. 166:5688-5694.
15. Kimmel, C. B., W. W. Ballard, S. R. Kimmel, B. Ullmann, and T. F. Schilling. 1995. Stages of embryonic development of the zebrafish. Dev. Dyn. 203:253-310.
16. Lam, S. H., H. L. Chua, Z. Gong, T. J. Lam, and Y. M. Sin. 2004. Development and maturation of the immune system in zebrafish, *Danio rerio*: a gene expression profiling, in situ hybridization and immunological study. Dev. Comp. Immunol. 28:9-28.
17. Lieschke, G. J., A. C. Oates, M. O. Crowhurst, A. C. Ward, and J. E. Layton. 2001. Morphologic and functional characterization of granulocytes and macrophages in embryonic and adult zebrafish. Blood 98:3087-3096.
18. Meijer, A. H., S. F. G. Krens, I. A. Medina Rodriguez, S. He, W. Bitter, B. E. Snaar-Jagalska, and H. P. Spaink. 2004. Expression analysis of the Toll-like receptor and TIR domain adaptor families of zebrafish. Mol. Immunol. 40:773-783.
19. Nasevicius, A., and S. C. Ekker. 2000. Effective targeted gene 'knockdown' in zebrafish. Nat. Genet. 26:216-220.
20. Phelan, P. E., M. T. Mellon, and C. H. Kim. 2005. Functional characterization of full-length TLR3, IRAK-4, and TRAF6 in zebrafish (*Danio rerio*). Mol. Immunol. 42:1057-1071.
21. Rhodes, J., A. Hagen, K. Hsu, M. Deng, T.X. Liu, A.T. Look, and J. P. Kanki. 2005. Interplay of Pu.1 and Gata1 determines myelo-erythroid progenitor cell fate in zebrafish. Dev. Cell, 8:97–108.
22. Scanga, C. A., A. Bafica, C. G. Feng, A. W. Cheever, S. Hieny, and A. Sher. 2004. MyD88-deficient mice display a profound loss in resistance to *Mycobacterium tuberculosis* associated with partially impaired Th1 cytokine and nitric oxide synthase 2 expression. Infect. Immun. 72:2400-2404.
23. Seki, E., H. Tsutsui, N. M. Tsuji, N. Hayashi, K. Adachi, H. Nakano, S. Futatsugi-Yumikura, O. Takeuchi, K. Hoshino, S. Akira, J. Fujimoto, and K. Nakanishi. 2002. Critical roles of myeloid differentiation factor 88-dependent proinflammatory cytokine release in early phase clearance of *Listeria monocytogenes* in mice. J. Immunol. 169:3863-3868.
24. Skerrett, S. J., H. D. Liggitt, A. M. Hajjar, and C. B. Wilson. 2004. Cutting edge: myeloid differentiation factor 88 is essential for pulmonary host defense against *Pseudomonas aeruginosa* but not *Staphylococcus aureus*. J. Immunol. 172:3377-3381.
25. Takeda, K., T. Kaisho, and S. Akira. 2003. Toll-like receptors. Annu. Rev. Immunol. 21:335-376.
26. Takeuchi, O., K. Hoshino, and S. Akira. 2000. Cutting edge: TLR2-deficient and MyD88-deficient mice are

highly susceptible to *Staphylococcus aureus* infection. J. Immunol. 165:5392-5396.
27. Thisse, C., B. Thisse, T. F. Schilling, and J. H. Postlethwait. 1993. Structure of the zebrafish snail1 gene and its expression in wild-type, *spadetail* and *no tail* mutant embryos. Development 119:1203-1215.
28. Traver, D., P. Herbomel, E. E. Patton, R. D. Murphey, J. A. Yoder, G. W. Litman, A. Catic, C. T. Amemiya, L. I. Zon, and N. S. Trede. 2003. The zebrafish as a model organism to study development of the immune system. Adv. Immunol. 81:253-330.
29. Trede, N. S., D. M. Langenau, D. Traver, A. T. Look, and L. I. Zon. 2004. The use of zebrafish to understand immunity. Immunity 20:367-379.
30. Van der Sar, A. M., B. J. Appelmelk, C. M. J. E. Vandenbroucke-Grauls, and W. Bitter. 2004. A star with stripes: zebrafish as an infection model. Trends Microbiol. 12:451-457.
31. Van der Sar, A. M., R. J. P. Musters, F. J. M. Van Eeden, B. J. Appelmelk, C. M. J. E. Vandenbroucke-Grauls, and W. Bitter. 2003. Zebrafish embryos as a model host for the real time analysis of *Salmonella typhimurium* infections. Cell. Microbiol. 5:601-611.
32. Willett, C. E., A. Cortes, A. Zuasti, and A. G. Zapata. 1999. Early hematopoiesis and developing lymphoid organs in the zebrafish. Dev. Dyn. 214:323-336.
33. Yamamoto, M., K. Takeda, and S. Akira. 2004. TIR domain-containing adaptors define the specificity of TLR signaling. Mol. Immunol. 40:861-868.
34. Yoder, J. A., M. E. Nielsen, C. T. Amemiya, and G. W. Litman. 2002. Zebrafish as an immunological model system. Microbes Infect. 4:1469-1478.

3 Transcriptome profiling and functional analyses of the zebrafish embryonic innate immune response to *Salmonella* infection

Oliver W. Stockhammer[1], Anna Zakrzewska[1], Zoltán Hegedûs[2, 3], Herman P. Spaink[1] and Annemarie H. Meijer[1]

1 Institute of Biology, Leiden University, Leiden, The Netherlands 2 ZenonBio Ltd., Szeged, Hungary 3 Bioinformatics Laboratory, Biological Research Center, Hungarian Academy of Sciences, Szeged, Hungary

published in The Journal of Immunology, 2009, 182, 5641 -5653
Copyright © 2009 by The American Association of Immunologists, Inc.

Abstract

Due to the clear separation of innate immunity from adaptive responses, the externally developing zebrafish embryo represents a useful *in vivo* model for identification of innate host determinants of the response to bacterial infection. Here we performed a time-course transcriptome profiling study and gene ontology analysis of the embryonic innate immune response to infection with two model *Salmonella* strains that elicit either a lethal infection or an attenuated response. The transcriptional response to infection with both the lethal strain and the avirulent LPS O-antigen mutant strain showed clear conservation with host responses detected in other vertebrate models and human cells, including induction of genes encoding cell surface receptors, signalling intermediates, transcription factors and inflammatory mediators. Furthermore, our study led to the identification of a large set of novel immune response genes and infection markers, the future functional characterization of which will support vertebrate genome annotation. From the time series and bacterial strain comparisons, matrix metalloproteinase genes, including *mmp9*, were among the most consistent infection-responsive genes. Purified *Salmonella* flagellin also strongly induced *mmp9* expression. Using knockdown analysis we showed that this gene was downstream of the zebrafish homologs of the flagellin receptor TLR5 and the adaptor MyD88. In addition, flagellin-mediated induction of other inflammation markers, including *il1b, il8* and *cxcl-C1c*, was reduced upon TLR5 knockdown as well as expression of *irak3*, a putative negative TLR pathway regulator. Finally, we showed that induction of *il1b*, *mmp9* and *irak3* requires MyD88-dependent signalling, while *ifn1* and *il8* were induced MyD88-independently during *Salmonella* infection.

Introduction

The innate immune system represents the evolutionary ancient part of vertebrate immunity and relies on germline encoded receptors, commonly referred to as pattern recognition receptors (PRRs), to mediate immune responses to pathogenic microorganisms. Triggering of these receptors activates a variety of signal transduction pathways ultimately resulting in large alterations of the host transcriptome profile, of which the dynamic complexity and underlying mechanisms are still poorly understood, especially at the whole organism level.

An essential class among the investigated PRRs are the Toll-like receptors. Detection of microorganisms by TLRs is facilitated through specific interaction of the members of this family with evolutionary conserved microbial molecules that are not found in higher eukaryotes, e.g. lipopolisaccharide (LPS) from the outer membrane of gram-negative bacteria (TLR4), flagellin from bacterial flagella (TLR5) or unmethylated CpG dinucleotides commonly found in bacterial DNA (TLR9) (1-3). Stimulation of TLRs by their ligands leads to the recruitment of adaptor pro-

teins to the receptors. Differential utilization of the adaptor molecules by the TLRs causes specific activation of a range of transcription factors such as nuclear factor-κB (NF-κB), activator protein 1 (AP-1) and interferon regulatory factor (IRF) 3, 5 and 7 through distinct signalling pathways eventually leading to the downstream activation of pro-inflammatory cytokines (4). To date five adaptor proteins involved in TLR signalling have been described in human: myeloid differentiation factor-88 (MyD88), MyD88 adaptor-like protein (Mal/TIRAP), Toll/IL1 receptor (TIR) domain- containing adaptor protein inducing IFNβ (TRIF/TICAM1), TRIF-related adaptor molecule (TRAM/TICAM2) and sterile α- and armadillo motif-containing protein (SARM) (4). Among all adaptors, MyD88 is the most commonly used adaptor and signalling through MyD88 has been implicated for all human TLRs with the exception of TLR3 that was shown to signal in a TRIF-dependent and MyD88-independent fashion (4, 5). Furthermore, MyD88 is involved in signal transduction of the interleukin 1 receptor (IL-1R) and is associated with interferon-γ receptor signalling (IFN-γR) leading to p38 activation (6, 7).

In recent years the zebrafish (*Danio rerio*) embryo system has emerged as a new model to study vertebrate innate immunity, offering several advantages that complement mammalian model systems. The transparent character of the externally fertilized zebrafish embryo in combination with fluorescently labelled immune cells and bacteria facilitate the study of host microbe interaction and inflammation processes in the living organism (8-14). The efficiency at which infections and chemical treatments in zebrafish can be performed at a large-scale allows identification of novel microbial virulence factors and high throughput compound screens to investigate disease mechanisms (15, 16). Moreover, the zebrafish system is particularly suitable for large-scale forward and reverse genetic screens aimed at the identification of genes with novel functions in development of the immune system or in the immune response (17-19).

Analysis of the immune system of the zebrafish revealed a fully developed adaptive and innate immune system showing notable similarities to the mammalian equivalent (20-25). An active innate immune system is detectable already at day one of zebrafish embryogenesis demonstrated by the appearance of macrophages originating from the lateral plate mesoderm (26). Phagocytic activity of these cells was demonstrated upon bacterial encounter (8, 26, 27). By contrast, a functionally mature adaptive immune system is not active during the first three weeks of zebrafish development (28-30). This clear temporal separation in zebrafish embryos provides a convenient system for in vivo study of the vertebrate innate immune response to infection independently from the adaptive immune response. To validate this model, we previously demonstrated that zebrafish embryos express a broad range of TLRs and adaptors. Furthermore, we demonstrated a conserved immune function for the TLR adaptor Myd88 by showing elevated susceptibility of the zebrafish embryo to an avirulent strain of Salmonella enterica serovar Typhimurium (hereafter referred to as S. typhimurium) upon morpholino mediated knockdown (31). Zebrafish embryos

also release conserved cytokines and chemokines, such as TNFα, IL-1β and IL-8, in response to bacterial infections (32, 33). In addition, zebrafish embryos express a virus-induced interferon system ancestral to that of other vertebrates (34). However, knowledge of infection markers is still limited and the global transcriptional response to an infection has not been previously investigated in zebrafish embryos.

In recent years many infection systems for zebrafish have been developed (35-37). In this paper we used *S. typhimurium* as a case study for gram-negative infections. An infection model for this well studied human pathogen in zebrafish embryos has previously been established and it was demonstrated that an LPS-mutant that shows an attenuated pathogenesis in mouse studies shows also attenuated infection in zebrafish embryos (9). Here we report on a time resolved transcriptome profiling study of the zebrafish embryonic host immune response to *S. typhimurium* wild type and LPS-mutant infection. Gene ontology comparisons of expression signatures in infections of zebrafish embryos and human and other vertebrate systems revealed a substantial overlap, further underscoring the validity of the zebrafish model. Furthermore, we identified a large set of novel immune response genes and infection markers, providing a strong basis for future research. Finally, we used infection markers resulting from this study to investigate the functions of Tlr5 and MyD88 by knockdown analysis using morpholino antisense oligonucleotides.

Results

Global changes in gene expression upon *Salmonella typhimurium* infection

To characterize the host response of zebrafish embryos to bacterial infection we performed a time-resolved transcriptome analysis of zebrafish embryos infected with either the *Salmonella typhimurium* wild type strain TL2 (wt) or an isogenic LPS mutant (Ra) (9). Zebrafish embryos were systemically infected at the onset of blood circulation (27 hpf) by microinjection of 250 cfu of DsRed-labelled bacteria into the caudal vein or were mock injected with PBS. Injected embryos were sacrificed after incubation periods of 2, 5, 8 and 24 h and microarray experiments were performed using a custom designed 4x44k Agilent zebrafish platform. Datasets of three independent experiments revealed a strong response of the embryo to systemic infection with *S. typhimurium* compared to the mock injected control group (Fig. 1, Supplementary table II). The response to *S. typhimurium* wt was characterized by a gradually increasing number of responsive genes over the time course of the experiment, peaking at 24 hours post infection (hpi). A similar but attenuated response was visible for the Ra infection over the first 8 h. Furthermore, in contrast to the wt infection, a clear decline of responsive genes was observed at 24 hpi (Fig. 1). The temporal expression profiles correspond well to the course of *S. typhimurium* wt and Ra mutant infections in the zebrafish embryo as observed by fluorescence imaging.

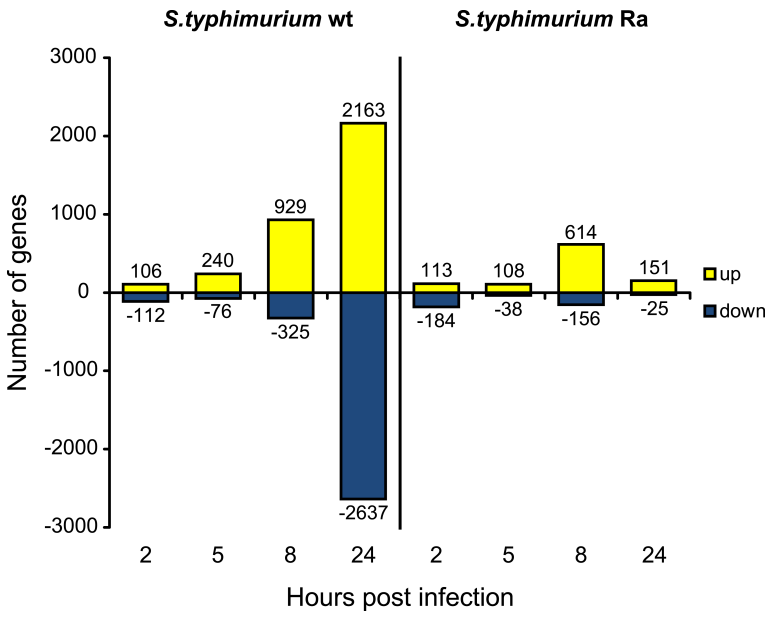


FIGURE 1. Temporal expression profiles of genes responsive to *S. typhimurium* wt and Ra infection. Total numbers of UniGene clusters that were significantly ($p \leq 10^{-4}$) up- or down-regulated (fold change ≥1.5 or ≤-1.5) compared to the mock-injected control group at 2, 5, 8 and 24 hpi.

As shown in supplementary figure 1, the transient infection caused by the Ra mutant was nearly eliminated at 24 hpi, while a strong accumulation of DsRed-labelled wt bacteria was observed at 24 hpi resulting in lethality around 30 hpi.

To further analyse the response to the wt and Ra strain over the first 8 h of the infection we performed two dimensional hierarchical cluster analysis. In the first dimension, the *S. typhimurium* wt and Ra infection profiles clustered together according to the experimental time points (Fig. 2A), indicating that zebrafish embryos respond similarly to infections with both strains. In the second dimension, we could distinguish three major clusters of genes showing different trends in expression over the time course (Fig. 2A-C, Supplementary table V). Genes in cluster 1 exhibited a successive down-regulation over the first 8 h of the infection whereas genes grouped in cluster 2 were generally induced over time. This cluster was further partitioned into four sub-clusters termed 2a-2d (Fig 2A and 2D-E). Genes in cluster 2a showed induction over all time points. However, induction at 5 and 8 hpi was more pronounced after *S. typhimurium* wt infection. In contrast genes in cluster 2b exhibited a broad down-regulation at 2 hpi followed by a successive up-regulation peaking at 8 hpi. In general down-regulation of genes in cluster 2b was stronger for the Ra infection. A transient response was observed for genes in cluster 2c, showing an induction peak at 5 hpi followed by a declined at 8 hpi. Genes in cluster 2d showed a

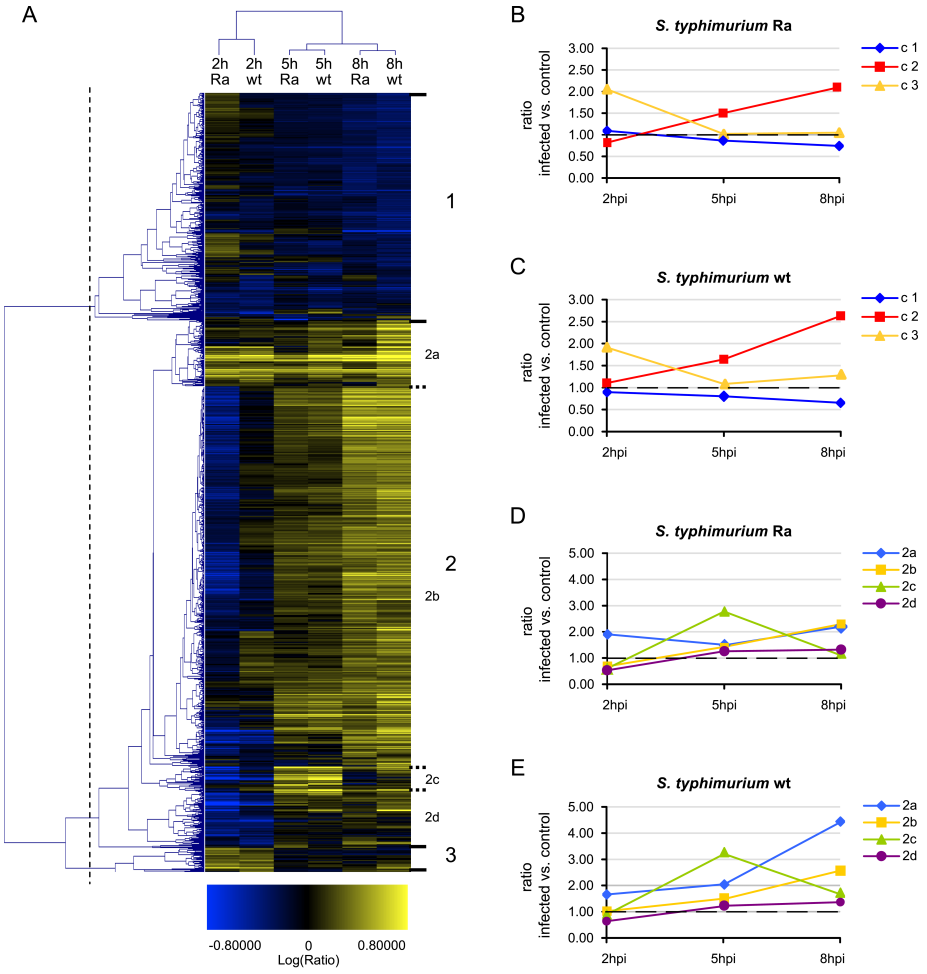
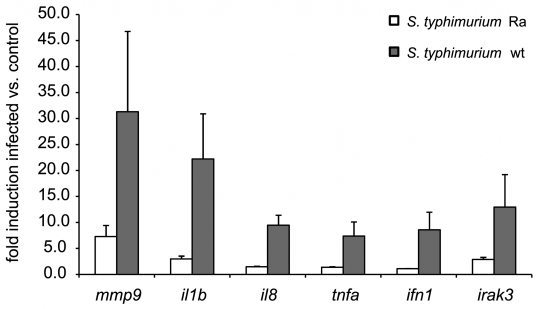


FIGURE 2. Trend analysis of gene expression patterns. (A) Two dimensional hierarchical clustering (average link, cosine correlation) performed on the UniGene clusters that were significantly up- or down-regulated over the first 8h by wt and/or Ra infection. Induced genes are indicated by increasingly brighter shades of yellow and down-regulated genes are indicated by increasingly brighter shades of blue. The three main clusters are named 1 – 3, and the four sub-clusters of cluster 2 are named 2a – 2d. (B-E) Trend graphs indicating the representative temporal expression profiles of the identified clusters. Average gene expression ratios at each time point upon *S. typhimurium* wt and Ra mutant infection are displayed for the three main clusters (B-C) and the four sub clusters (D-E).

significant down-regulation at 2 hpi, followed by relatively low induction at 5 and/or 8 hpi. Finally, genes in cluster 3 showed a strong induction at 2 hpi with a subsequent decrease at 5 and 8 hpi.

A



B

gene	treatment	qRT-PCR	microarray
mmp9	*S. typhimurium* wt	**+31.3**	**+22.5**
	S. typhimurium Ra	**+7.3**	**+6.5**
il1b	*S. typhimurium* wt	**+22.2**	**+10.1**
	S. typhimurium Ra	**+3.0**	**+2.6**
il8	*S. typhimurium* wt	**+9.5**	**+4.2**
	S. typhimurium Ra	**+1.5**	**+1.7**
tnfa	*S. typhimurium* wt	+7.4	**+7.3**
	S. typhimurium Ra	+1.4	+1.9
ifn1	*S. typhimurium* wt	**+8.6**	**+7.6**
	S. typhimurium Ra	+1.1	+1.3
irak3	*S. typhimurium* wt	**+12.9**	**+4.0**
	S. typhimurium Ra	**+2.9**	**+2.5**

FIGURE 3. Validation of microarray data by qRT-PCR. Selected genes were analysed on RNA samples from the 8 hpi time point previously used for the microarray experiment. qRT-PCR results were normalized to peptidylprolyl isomerase A like (*ppial*) and data are presented as relative induction of the infected groups compared to the relevant mock injected control groups. Values are the mean ± s.e.m. of three independent experiments. Fold changes determined by qRT-PCR and microarray experiment are listed in the table below the graph. Fold changes indicated in bold are significant with $p<0.0001$ for the microarray data and $p<0.05$ in a unpaired t-test for the qRT-PCR data.

In conclusion, we observed a strong response to *S. typhimurium* infection in the zebrafish embryo with largely similar temporal expression profiles upon wt or Ra infection during the first 8 h after inoculation. Even though the Ra strain elicits only a transient infection and the wt infection becomes lethal, no gene groups with clearly anti-correlated behaviour were revealed by hierarchical cluster analysis. Instead, differences in the host response to wt and Ra infection appeared to be limited to differences in trend at a single time point and to quantitative differences in up- or down-regulation.

Validation of microarray data by qRT-PCR and in situ hybridisation

To validate the microarray data quantitative real time PCR (qRT-PCR) was performed on six genes that were significantly induced upon *S. typhimurium* infection (Fig. 3). The expression levels for *mmp9* (matrix metalloproteinase 9, NM_213123), *il1b* (interleukin 1, beta, NM_212844), *LOC100002946* (similar to interleukin 8, XM_001342570) hereafter referred to as *il8*, *tnfa* (tumor necrosis factor a, NM_212859), *ifn1* (interferon 1, NM_207640) and *irak3* (interleukin-1 receptor-associated kinase 3, NM_001099421) were evaluated on the RNA samples of the 8 hpi time point previously used for the microarray study. The expression levels were normalized to *ppial* (peptidylprolyl isomerase A like, NM_199957) (44), which showed no changes over the infection time course. Expression levels are presented as the relative induction in the infected group compared to the control group (Fig. 3A). In agreement with the

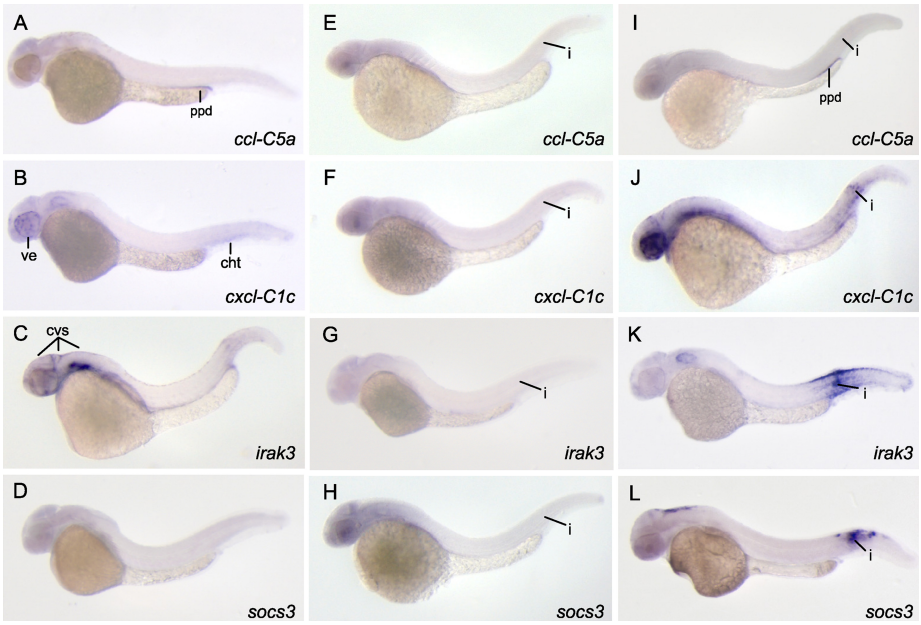


FIGURE 4. Analysis of spatial expression patterns of *S. typhimurium*-induced genes. Expression patterns of the indicated genes were analysed at 8 hpi by whole mount in-situ hybridization. Embryos were injected at 27 hpf with *S. typhimurium* wt bacteria into the caudal vein (A,B,C,D), or injected with *S. typhimurium* wt bacteria into the somite tissue of the tail above the urogenital opening (I,J,K,L), or mock-injected with PBS at the same location (E,F,G,H). All embryos are oriented anterior to the left and dorsal to the top. cht, caudal hematopoietic tissue; cvs, cranial vascular system; i, location of injection into somite tissue; ppd, posterior pronephric duct; ve, vessels of the eye.

microarray data, all genes tested in the qRT-PCR assay showed clear induction upon *S. typhimurium* wt infection and showed a lower response (*mmp9*, *il1b, il8* and *irak3*) or no significant response (*tnfa*, *ifn1*) after infection with the Ra mutant (Fig. 3B).

In addition to the quantitative analysis by qRT-PCR we also tested several genes by whole mount in situ hybridization to further validate the microarray data and to add spatial information to the expression of infection-induced genes. Embryos were challenged with S. typhimurium wt by injection into the caudal vein close to the urogenital opening as in the microarray study. At 8 hpi the expression patterns of chemokine *cxcl-C1c* (LOC795785, AB331773.1), chemokine *ccl-C5a* (CH211-89F7.4, AB331770.1), *irak3* and *socs3a* (suppressor of cytokine signalling 3a, NM_199950.1) were analysed (Fig. 4A-D). The selected genes were chosen on the criteria of a p-value smaller than 10-5 and an induction greater than 3 fold at 5- and 8 hpi. The *ccl-C5a* gene showed a specific expression pattern restricted to a narrow streak along the ventral side of the trunk, most likely representing the posterior region of the prone-

phric duct (Fig. 4A). Expression of *cxcl-C1c* (Fig. 4B) was predominantly visible in single cells located in the vascular system of the embryonic eyes. A second area of elevated expression was observed around the caudal vein, also defined to single cells. Like *cxcl-C1c*, also the zebrafish homolog of *irak3* (Fig. 4C) showed an expression pattern restricted to the cranial vascular system of the embryo. However, a small number of embryos displayed a diverse pattern with a strong expression restricted to an area in the tail that corresponds with the site of the bacterial injection. To further investigate this observation we repeated the assay with a revised infection strategy. Bacteria were now locally injected into the somite tissue of the tail at 27 hpf leading to a confined accumulation of the bacteria at that site. Analysis of the expression pattern at 8 hpi confirmed the observed expression of *irak3* (Fig. 4K) in the tissue closely surrounding the infection site. Similarly, *socs3* also showed locally increased expression upon injection of bacteria into somite tissue (Fig. 4L). Local infection increased *ccl-C5a* (Fig. 4I) in the pronephric duct similar as observed upon blood infection (Fig. 4A), however, *ccl-C5a* expression did not accumulate around the infection site. In contrast, *cxcl-C1c* (Fig. 4J) did exhibit localized expression around the infection site, apparently restricted to single cells. To exclude the possibility that the observed expression patterns were provoked by local damage of the tissue that occurs upon bacterial injection we also investigated the expression of all four genes in mock (PBS) injected embryos (Fig. 4E-H). No signal was detected in the controls (n=5 per gene) validating the specific host response towards the bacterial infection. Furthermore, the in situ hybridization results show that transcriptome profiling at the whole embryo level is highly suited to identify gene expression changes that are restricted to specific tissues or cell types.

Statistical testing for enrichment of gene ontology groups

To perform an unbiased functional annotation of the genes identified by microarray analysis we used *e*GOn, a web-based gene ontology (GO) tool (40). The *e*GOn software classifies user input gene lists by GO criteria for Biological Process (BP), Molecular Function (MF) and Cellular Component (CC), it produces hierarchical trees of GO-terms in these three categories, and it allows statistical testing for enrichment or under representation of specific GO-terms in the input lists.

First we used the *e*GOn software to perform master-target statistical tests on the clusters of genes described above (Fig. 2), comparing the UniGene identifiers of each cluster (targets) versus all UniGene identifiers present on the chip (master). Master-target testing of the three main clusters (clusters 1-3 in Fig. 2) showed that the GO-terms "immune system process" and "response to stimulus", at level 2 in the hierarchical tree for BP, were significantly enriched in cluster 2 that contained the majority of the up-regulated genes. Next we analysed the responses to the wt and Ra strains separately and at each individual time point of the infection. In agreement with the result obtained for cluster 2, master-target tests on the up-regulated UniGene sets showed that the BP GO-terms "immune system process" and "response to stimulus"

Table I. Master-target test of GO analysis of up-regulated genes for Biological Process*

GO-term	Name		*S. typhimurium* Ra mutant target lists				*S. typhimurium* wild type target lists			
		master	2h	5h	8h	24h	2h	5h	8h	24h
zebrafish UniGene identifiers										
GO:0008150	biological_process	6170	39	28	158	56	41	61	249	831
GO:0022610	biological adhesion	74	0	0	0	0	1	0	1	9
GO:0065007	biological regulation	1177	11	9	23	15	13	13	50	179
GO:0009987	cellular process	3177	22	16	74	29	25	32	128	437
GO:0032502	developmental process	653	4	4	8	5	5	4	21	94
GO:0051234	establishment of localization	1138	3	3	29	6	5	7	47	160
GO:0040007	growth	50	1	0	1	2	1	2	3	13
GO:0002376	immune system process	72	**5**	**4**	4	**8**	**5**	**7**	**9**	**19**
GO:0051179	localization	1195	3	3	29	6	6	7	47	167
GO:0040011	locomotion	6	0	0	0	0	0	0	0	1
GO:0051235	maintenance of localization	2	0	0	0	0	0	0	0	0
GO:0008152	metabolic process	2493	19	12	63	24	18	25	100	351
GO:0051704	multi-organism process	1	0	0	0	0	0	0	0	0
GO:0032501	multicellular organismal process	633	3	7	9	6	4	6	18	68
GO:0043473	pigmentation	13	0	0	0	0	0	0	0	0
GO:0000003	reproduction	24	0	0	0	1	0	1	0	7
GO:0022414	reproductive process	7	0	0	0	1	0	0	0	1
GO:0050896	response to stimulus	213	5	**5**	8	**13**	5	**11**	**17**	**44**
GO:0048511	rhythmic process	8	0	0	0	0	0	0	0	1
UniGene identifiers of human homologs										
GO:0008150	biological_process	5974	52	38	243	54	49	79	354	1319
GO:0022610	biological adhesion	282	2	0	11	2	3	3	19	60
GO:0065007	biological regulation	2079	22	13	**110**	25	**27**	30	**154**	**512**
GO:0001906	cell killing	4	0	0	0	0	0	0	1	1
GO:0009987	cellular process	5156	43	28	217	45	42	64	306	1140
GO:0032502	developmental process	1402	16	8	41	15	**22**	18	81	322
GO:0051234	establishment of localization	1132	7	10	45	14	7	19	73	259
GO:0040007	growth	118	2	1	6	4	**5**	4	14	35
GO:0002376	immune system process	230	**9**	**11**	**18**	**12**	**12**	**19**	**31**	**73**
GO:0051179	localization	1290	8	10	51	14	8	20	80	287
GO:0040011	locomotion	31	0	0	0	0	0	0	1	8
GO:0051235	maintenance of localization	17	1	1	1	1	**2**	1	2	3
GO:0008152	metabolic process	3899	29	22	177	34	31	48	244	877
GO:0051704	multi-organism process	35	0	0	0	0	0	1	2	10
GO:0032501	multicellular organismal process	1372	17	11	44	16	18	20	72	289
GO:0043473	pigmentation	12	0	0	0	0	0	0	0	2
GO:0000003	reproduction	178	3	1	3	0	0	3	9	39
GO:0022414	reproductive process	88	1	1	2	0	0	2	4	20
GO:0050896	response to stimulus	817	**15**	**12**	41	**18**	**17**	**23**	**67**	**225**
GO:0048511	rhythmic process	34	0	0	1	0	0	1	1	8
GO:0016032	viral reproduction	21	0	1	0	0	0	0	0	3

*A master-target statistical test using eGOn software was performed with input gene lists of zebrafish UniGene identifiers or the UniGene identifiers of their human homologs. The master input lists contained all UniGene identifiers present on the microarray (19122 zebrafish UniGenes, for 10620 of which the human homologs could be identified). The target lists contained the UniGene identifiers that were ≥ 1.5-fold up-regulated ($p \leq 0.0001$) at different time points of *S. typhimurium* wild type or Ra mutant infection. The table indicates the number of genes in each list that are associated with the indicated GO-terms. Highlighted numbers are significantly enriched in the target list compared to the master ($p < 0.01$). It should be noted that genes can be associated with more than one GO-term. For example, enrichment of the GO-terms "development" and "growth" in the target list of *S. typhimurium* wild type 2h infection is due to the presence of genes such as *socs1* and *3*, *c7*, *il10*, *mmp9*, *fos*, *pim2* and *nfκb2*, which also fall under the GO-terms "immune response" and/or "response to stimulus".

were significantly enriched at multiple time points of both the wt and Ra infections (Table I). In the MF tree, the level 2 GO-term "enzyme regulator activity" was enriched (Supplementary table VI), and in the CC tree there was enrichment of GO-terms associated with extracellular compartments (Supplementary table VII).

Although master-target testing of the up-regulated UniGenes identified several enriched GO-terms with obvious relevance to an infection study, we noted that the number of UniGene identifiers associated with each of these GO-terms was relatively low. We considered that this might be due to poor annotation of the zebrafish genome and that we might strengthen the results by performing a GO analysis of the human homologs of the zebrafish genes, thereby taking advantage of the much better annotated human genome. To this extent we developed a software tool with which the human homologs of the zebrafish UniGene list could be automatically retrieved from the NCBI HomoloGene database. Using this approach we could identify the human homologs of 56 % of the zebrafish UniGene clusters present on the chip. As we had anticipated the total number of associated GO-terms was 1.6 fold higher. Furthermore, the relevant GO-terms "immune system process" and "response to stimulus" were associated with 230 and 817 of all human homologs compared to only 72 and 213 of all zebrafish UniGenes. Repeating the master-target tests at the level of the human homologs showed that a larger number of genes was now associated with each of the enriched GO-terms in the up-regulated signature sets of the infection time course. For example, in the *S. typhimurium* wt infection signature of 24 hpi there were 73 human homologs with the GO-term "immune system process" compared to 19 zebrafish UniGenes, and 225 human homologs with the GO-term "response to stimulus" compared to 44 zebrafish UniGenes (Table I). Additionally, the GO-terms "biological regulation" (BP) and "transporter activity" (MF) were significantly enriched at multiple time points in the analysis of the human homologs, while not in the analysis of the zebrafish UniGenes.

For a more detailed GO analysis of the up- and down-regulated gene groups at the different time points of the infection study, we used the DAVID tools for Functional Classification and Functional Annotation Clustering (41). The results of DAVID analyses are described in the supplementary material 1. In summary, DAVID analyses of the infections with both strains demonstrated rapid induction over the first 8h of the time course of an increasing number of gene groups encoding transcription factors, signalling molecules, complement and acute phase response proteins, proteinases and proteinase inhibitors, and solute carriers. At 24 hpi, the near-lethal wild type infection led to the additional induction of apoptotic and anti-apoptotic genes as well as negative regulators of cell cycle and proliferation, whereas gene groups involved in primary metabolic processes and DNA replication were down-regulated.

Comparison with expression data from infection studies using human cell lines

To compare the *S. typhimurium*-induced gene profiles of zebrafish with gene profiles

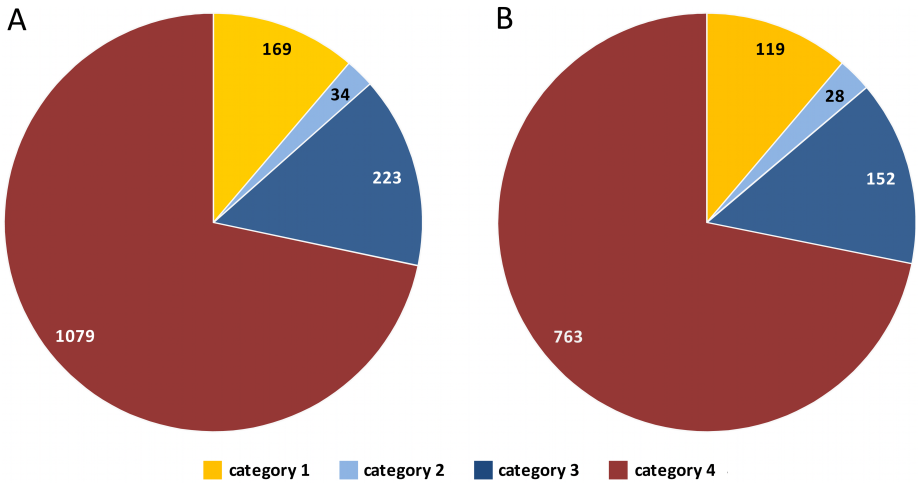


FIGURE 5. Identification of novel infection-responsive genes. All UniGene clusters regulated upon *S. typhimurium* wt (A) and Ra (B) challenge (infected versus control, p≤0.0001 and fold changes ≥1.5 and ≤-1.5) were grouped into four categories. Category 1: immune specific by means of GO-annotation and overlap with the common host response genes in supplementary table III; Category 2: described immune function but missed out on category 1; Category 3: functionally annotated but not associated to an immune function; Category 4: no functional annotation. The numbers of UniGene clusters in each category are indicated in the pie-diagrams.

of infected human cell lines, we took advantage of a study by Jenner and Young (42) who systematically compared transcription profiling data from 32 studies that involved 77 different host-pathogen interactions. By cluster analysis of these data the authors identified an expression signature of 511 genes, which they designated 'the common host response' as most of these genes were induced in many different human cell types upon exposure to several different pathogens. We sought to identify the zebrafish homologs of the genes in this common host response cluster using the ZFIN and NCBI Gene and Homologene databases, and found that 322 out of the 511 genes were represented on our zebrafish microarray. Of these 39% were up-regulated (≥ 1.5-fold, $p < 0.0001$) at one or more time points of *S. typhimurium* wild type and/or Ra infection (Supplementary table III). The overlap included genes encoding matrix metalloproteinases (e.g. *mmp9*, *mmp13*), adhesion molecules (e.g. *itga5*, *lgals9*), co-stimulatory molecules (e.g. CD83), antigen processing molecules (e.g. *tap2*, *psmb* family members), prostaglandin biosynthetic enzymes (e.g. *ptgs2*), signalling intermediates (e.g *tradd*, *myd88*, *traf6*, *dusp* family members), apoptotic and anti-apoptotic molecules (e.g. *casp* family members, *mcl1*, *birc2*, *cflar*), transcription factors (e.g. members of the *NFκB*, *Jun*, *Fos, ATF*, *IRF* and *STAT* families, BCL6, Cebpg, xbp1), interferons and interferon-stimulated genes (e.g. *isg15*(*g1p2*), *mx1/2* homologs) and various chemotactic, proinflammatory and other cytokines (e.g. ho-

mologs of *IL1β*, *IL8*, *IL10*, *TNF*, *TNFSF10*, *ccl* and *cxcl* chemokines). In conclusion, many important immune markers respond in a similar way in human cell cultures and in the early embryonic zebrafish system, thus allowing further functional *in vivo* studies of these genes.

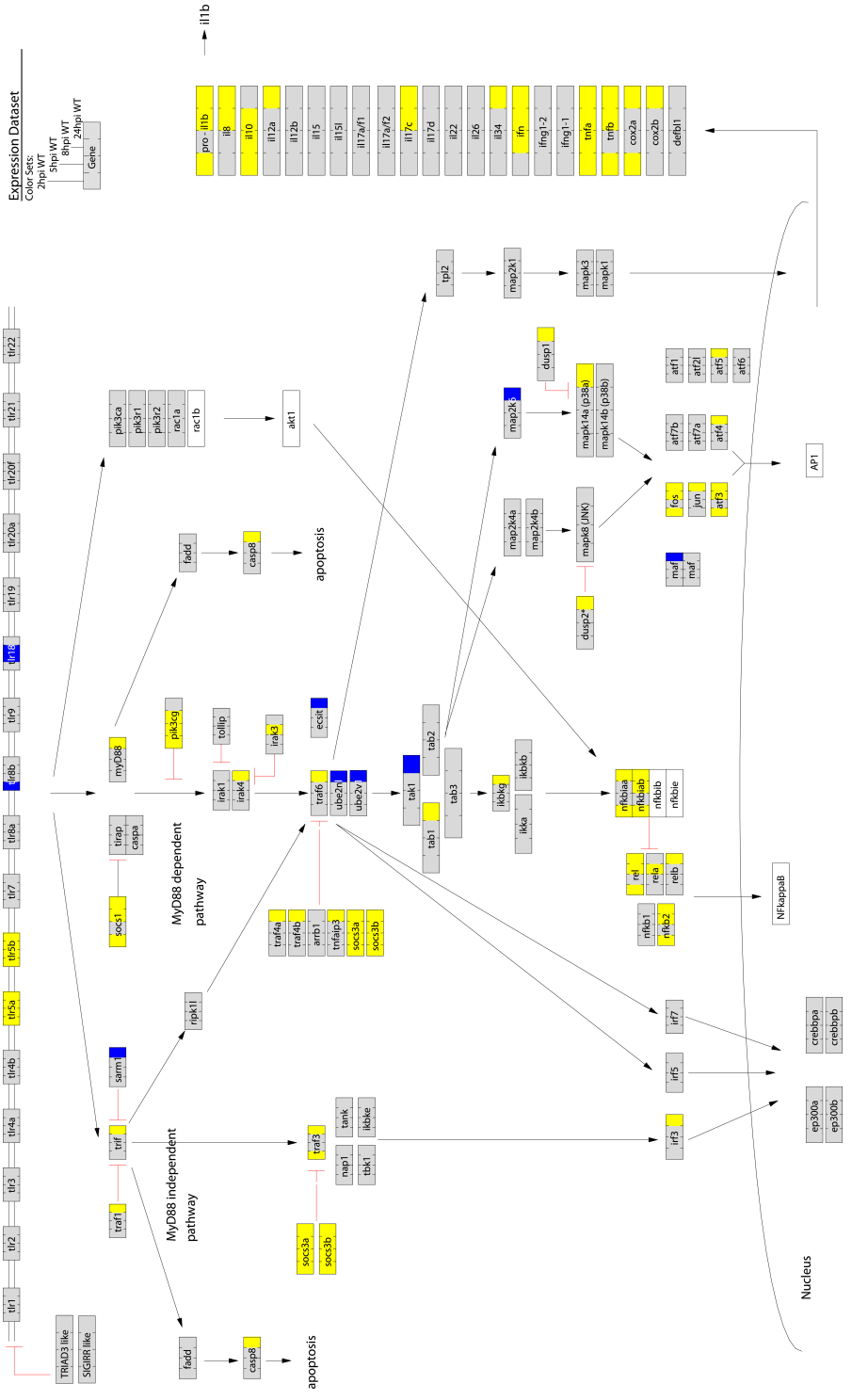
Identification of novel putative immune response genes

As the next step we sought to determine which proportion of the genes regulated by *S. typhimurium* infection had not been previously linked to a function in the immune response. To this extent we grouped all genes that were differentially expressed over the first 8 h of the infection time course (i.e. all genes included in the cluster analysis of Fig. 2) into four distinct categories (Fig. 5, Supplementary table VIII). The first category contained all genes that were identified as immune specific by means of GO annotation and by overlap with the common host response gene set as described above (wt 169 genes, Ra 119 genes). In the second category we gathered those genes that have a described immune function in vertebrates but were missed in category 1, e.g. *cebpb* and *socs3a* (wt 34 genes, Ra 28 genes). The third category consists of genes that were functionally annotated in zebrafish but were not yet linked to immune defence processes (wt 223 genes, Ra 152 genes). The remaining genes, grouped in category 4, still lack any functional annotation (wt 1079 genes and Ra 763 genes). The distribution of genes over the four categories (Fig. 5) shows that a substantial proportion (50%) of all annotated genes that we identified upon *S. typhimurium* wt or Ra infection were correlated to an immune function (categories 1 and 2). Still, considering all genes that were regulated over the first 8 h upon infection, the majority of genes (approximately 70%) have not yet been functionally characterized in the context of immunological processes and therefore represent novel putative immune response genes.

GenMapp-based Toll-like receptor pathway analysis reveals specific regulation of zebrafish TLR5 and downstream signalling components

To further examine the immune response profiles of *S. typhimurium* wt and Ra infection at the level of a single signal transduction pathway we performed a map based

FIGURE 6. GenMapp analysis of gene expression responses in the TLR pathway upon *S. typhimurium* wt infection. Expression profiles of the 2, 5, 8 and 24 hpi time points (infected versus control, $p \leq 0.0001$ and fold changes ≥ 1.5 and ≤ -1.5) were simultaneously mapped on the TLR pathway. Gene boxes are colour coded from left to right with the 2, 5, 8 and 24 hpi expression data. Up-regulation is indicated in yellow, down-regulation in blue and unchanged expression in grey. White denotes genes that were not represented on the array platform. The pathway is based on knowledge of TLR signalling in mammalian species and it should be noted that most interactions remain to be experimentally confirmed in zebrafish. GenMapp analysis of infection with the Ra mutant strain is shown in supplementary Fig. 2.


Expression Dataset
Color Sets:
2hpi WT
5hpi WT
8hpi WT
24hpi WT
Gene
il1b
pro_il1b
il8
il10
il12a
il12b
il15
il15l
il17a/f1
il17a/f2
il17c
il17d
il22
il26
il34
ifn
ifng1-2
ifng1-1
tnfa
tnfb
cox2a
cox2b
defbl1
tlr1
tlr2
tlr3
tlr4a
tlr4b
tlr5a
tlr5b
tlr7
tlr8a
tlr8b
tlr9
tlr18
tlr19
tlr20a
tlr20f
tlr21
tlr22
TRIAD3 like
SIGRR like
myD88
tirap
caspa
socs1
sarm1
trif
traf1
ripk1l
MyD88 dependent pathway
MyD88 independent pathway
pik3cg
tollip
irak1
irak4
irak3
ecsit
traf6
ube2n
ube2v
traf4a
traf4b
arrb1
tnfaip3
socs3a
socs3b
tak1
tab1
tab2
tab3
ikbkg
ikka
ikbkb
nfkbiaa
nfkbiab
nfkbib
nfkbie
rel
rela
relb
nfkb1
nfkb2
NFkappaB
fadd
casp8
apoptosis
traf3
tank
nap1
tbk1
ikbke
irf3
irf5
irf7
crebbpa
crebbpb
ep300a
ep300b
Nucleus
pik3ca
pik3r1
pik3r2
rac1a
rac1b
akt1
tpl2
map2k1
mapk3
mapk1
dusp1
map2k3
mapk14a (p38a)
mapk14b (p38b)
atf1
atf2l
atf5
atf6
atf7b
atf7a
atf4
map2k4a
map2k4b
mapk8 (JNK)
dusp2*
fos
jun
atf3
maf
AP1

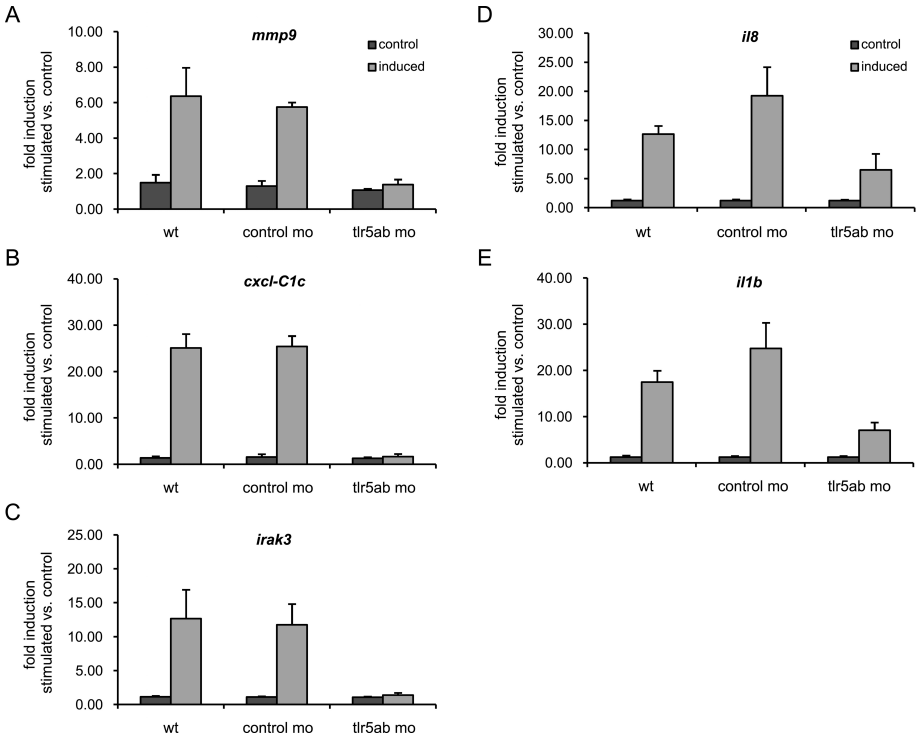


FIGURE 7. Response to *S. typhimurium* flagellin challenge in Tlr5a/b knock down embryos. Embryos were injected at the single cell stage with *tlr5a/b* or control morpholinos (mo) or were untreated (wt). The three groups were challenged at 27 hpf by flagellin injection or injection of toxin-free water as a control. Gene expression levels of *mmp9* (A), *cxcl-C1c* (B), *irak3* (C), *il8* (D), *il1b* (E) at 1 hpi were determined by qRT-PCR and are shown as the fold induction of flagellin stimulation versus the water control. Values are the mean ± S.D. of three independent experiments. The untreated and control mo groups did not behave significantly different. Differences between the tlr5a/b mo and control mo groups were significant by two way ANOVA analysis ($p<0.01$).

pathway analysis using the GenMapp software package (Gene Map Annotator and Pathway Profiler, http://www.genmapp.org) (43). GenMapp provides a platform to visualize gene expression datasets on customised maps of a desired signalling cascade and thereby allows the interpretation of gene expression changes in the context of a biological pathway. We used GenMapp for the analysis of the Toll-like receptor pathway, one of the most important pathways of the innate immune system (Fig. 6 and Supplementary figure 2). Zebrafish homologs of the TLR pathway components used to create the GenMapp were identified by searching the database of ZFIN (http://www.zfin.org) or the Gene and HomoloGene databases at the National Center for Biotechnology Information (NCBI, http://www.ncbi.nlm.nih.gov) (Supplementary

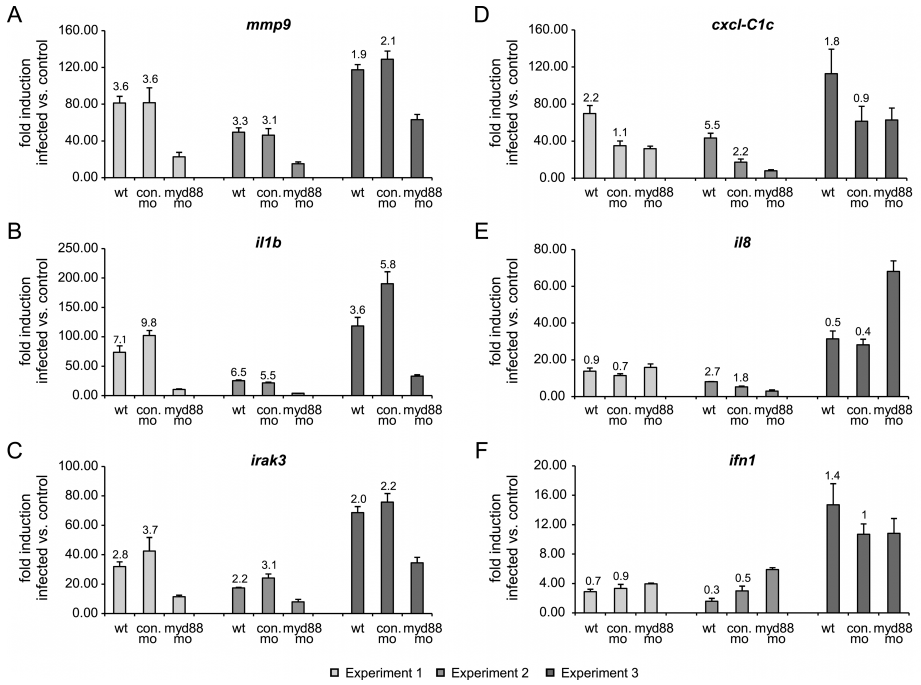


FIGURE 8. Response to *S. typhimurium* wt challenge in MyD88 knock down embryos. Embryos were injected at the single cell stage with MyD88 or control morpholinos (con. mo) or were untreated (wt). The three groups were infected at 27 hpf with *S. typhimurium* wt bacteria or mock-injected with PBS as a control. Gene expression levels of *mmp9* (A), *il1b* (B), *irak3* (C), *cxcl-C1c* (D) *il8* (E) and *ifn1* (F) at 8 hpi were determined by qRT-PCR and are shown as the fold induction of *S. typhimurium* infection versus the PBS control for all three experiments. The ratios of the untreated and the control groups over the MyD88 morpholino group are indicated above the individual bars. The untreated and control mo groups did not behave significantly different with the exception of *cxcl-C1c*. Differences between the MyD88 mo and control mo groups were significant by unpaired student t-test ($p<0.01$) for *mmp9*, *il1b*, and *irak3*.

table IV). The responses upon *S. typhimurium* wt (Fig. 6) and Ra (Supplementary figure 2) infection showed a similar trend between 2 to 8 hpi with a strong initial response at 2 hpi (14 genes wt, 11 genes Ra), a decrease at 5 hpi (6 genes wt, 2 genes Ra) followed by a new increase at 8 hpi (14 genes wt, 8 genes Ra). At 24 hpi the wt infection peaked with 38 regulated genes whereas the Ra infection showed a decline (4 genes), similar to what was observed for the global changes in gene expression described above (Fig. 1). GenMapp analysis of the TLR pathway revealed a conserved pattern between wt and Ra mediated infection. Both bacterial strains likewise induced the expression levels of genes encoding members of the NF-κB protein complex (*rel*, *rela*, *relb*, and *nfkb2*) that plays a key role in the transcriptional activa-

tion of pro-inflammatory cytokines (46). At the same time also *nfkbiaa* and *nfkbiab* genes that encode the zebrafish homologs of the NF-κB transcription factor inhibitor NFKBIA are induced. Other transcription factor genes responsive to both strains include the *fos*, *jun, atf3*, *atf4* and *atf5* genes encoding components of the AP1 transcription factor complex. Genes that have been implicated in the negative regulation of the TLR-pathway in higher vertebrates like *socs1*, s*ocs3a* and *socs3b*, *irak3*, *traf1* and *pik3cg* (phosphatidylinositol 3-kinase gamma) showed a clear activation from the earliest time point on. Finally, among the members of the Toll-like receptors that we previously identified in zebrafish (23), only *tlr5a* and *tlr5b* (the counterparts of the human *tlr5* gene) show a broad up-regulation over the course of the infection.

TLR5a/b is required for the activation of distinct host defence genes upon flagellin stimulation

Zebrafish *tlr5a* and *tlr5b* are two highly homologous genes located in tandem on chromosome 20 (Zv7_scaffold2018.4). To elucidate their role in the embryonic immune response we performed knockdown experiments simultaneously using two morpholinos that specifically target the *tlr5a* and *tlr5b* mRNAs. Preliminary results indicated that Tlr5a/b was not required for the induction of inflammation markers such as *il1b*, *il8* and *mmp9* upon *S. typhimurium* infection, which is not surprising since many other TLRs are involved in sensing of gram-negative bacteria.

To further investigate Tlr5a/b function, we next addressed the question if the presumed ligand flagellin is able to elicit an immune response in the zebrafish embryo. Embryos were challenged by injection of 4nl (100µg/ml) purified *S. typhimurium* flagellin (Invivogen) or solvent (toxin-free water) into the caudal vein at 27 hpf and the effect on expression of infection marker genes was investigated by qRT-PCR. Expression levels of *tlr5a*, *tlr5b*, *ifn1*, *irak3*, *il1b*, *il8*, *cxcl-C1c* and *mmp9* were used as readout for qRT-PCR analyses. In wild type embryos the expression of *il1b*, *il8*, *cxcl-C1c*, *mmp9* and *irak3* was induced within 1 h of flagellin stimulation, while the expression of *tlr5a*, *tlr5b* and *ifn1* was not induced over a time course of 5 h (Fig.7 and Supplementary figure 3). Results of three independent experiments showed that knockdown of Tlr5a/b led to an almost complete block of gene regulation of *mmp9*, *cxc-C1c* and *irak3* upon flagellin stimulation (Fig. 7A-C). Furthermore *il8* and *il1b* showed a reduced response to the flagellin challenge after *tlr5a/b* knockdown (Fig. 7D-E). These data demonstrate that flagellin is a bona fide ligand of the zebrafish Tlr5a/b receptor and that Tlr5a/b plays a pivotal role in the activation of specific host defence genes upon stimulation.

Myd88 knockdown reveals Myd88-dependent and -independent gene activation upon bacterial infection

Signal transduction upon TLR stimulation is dependent on a group of five TIR domain containing adaptor molecules. Among these MyD88 is the most commonly used adaptor participating in signal transduction processes with all TLRs except

TLR3 in mammals (4). To further investigate the role of the TLR pathway during bacterial infection we performed *myd88* knockdown studies followed by *S. typhimurium* wt challenge and analyzed expression of the same infection marker set as used in the *tlr5* knockdown analysis. Due to the stochastic nature of bacterial infections, the absolute levels of gene induction that were observed upon *S. typhimurium* challenge varied considerably between different experiments. However, in three independent experiments, the induction levels of *mmp9*, *il1b* and *irak3* expression were significantly reduced in the *myd88* morphants compared to non treated embryos and embryos injected with the control morpholino (Fig. 8A-C). Induction of *cxcl-C1c* was reduced in both mismatch control and *myd88* morphants, suggesting a currently unexplainable aspecific morpholino effect on the expression of this gene under infection conditions (Fig. 6F). Notably no changes were observed for *ifn1* and *il8* expression, indicating a MyD88-independent activation of these genes (Fig. 6D-E). Therefore, we conclude that the innate immune response of zebrafish embryos to *S. typhimurium* infection involves both MyD88-dependent and MyD88-independent signalling pathways.

Discussion

Here we report the first time-resolved characterization of the immune response of a vertebrate embryo to a systemic bacterial infection at the transcriptome level. Aiming specifically at the analysis of innate host determinants, we took advantage of the clear temporal separation of the innate from the adaptive immune system in the externally developing zebrafish embryos (22, 28-30). In addition to the identification of a large set of genes that had not been previously linked to the immune response, we found a substantial overlap between the embryonic host response and immune responses measured in human and other vertebrate systems, indicating that the embryo model has a good predictive value for the vertebrate immunity. Furthermore, we present here the first demonstration of a conserved Toll-like receptor ligand specificity and the presence of MyD88-dependent and -independent signalling pathways in the zebrafish embryo.

The bacterial infection model used in this study is a previously described *Salmonella typhimurium* system where a wild type (wt) and an attenuated LPS O-antigen mutant strain (Ra) are utilized (9). Our transcriptome analysis of *S. typhimurium* wt and Ra mutant challenge demonstrated that both strains elicit a distinct temporal expression profile, correlated to the symptoms of disease progression. Comparison of the host response over the first 8 hours revealed similar expression trends for both strains in spite of the fact that the wt strain elicits a fatal infection, and the Ra mutant infection is cleared within a day. The main difference between the strains was observed at 24 hpi, when the transcriptome response to the wt strain further increased and the response to the attenuated Ra mutant strain was on its

return. The pathological differences are most likely due to a higher susceptibility of the Ra mutant to the embryonic immune response. As previously suggested, the complement system might be responsible for extracellular lysis of *S. typhimurium* LPS mutants observed in infected zebrafish embryos (9). In agreement, *S. typhimurium* O-antigen mutants showed higher susceptibility to complement lysis in *in vitro* studies (47, 48). The rapid induction of complement components like *c3b*, *c3c*, *c6* and *cfb* (Supplementary table II) upon *S. typhimurium* challenge that we observed in our microarray study further supports the role of the complement system. Although there was a large overlap in the expression signatures of *S. typhimurium* wt and Ra infection during the first 8h of the infection, the majority of the affected genes showed quantitative differences in expression levels, the functional implications of which are not yet understood. The transcriptome study reported here provides a useful reference for future studies aimed to advance the understanding of host-pathogen interactions.

Unbiased analysis of the infection datasets by two complementary annotation tools, eGOn and DAVID, clearly demonstrated an immune specific host response of the zebrafish embryo to the *S. typhimurium* wt and Ra infections. Master-target testing performed by eGOn revealed the GO-terms "immune system process" and "response to stimulus" as significantly enriched in the infection-upregulated signature sets over the microarray background. However, fairly low numbers of genes were associated with these GO-terms, which could be attributed to the still poor annotation of the zebrafish genome. We found that use of the NCBI HomoloGene database to convert the zebrafish UniGene identifiers to their predicted human homologs was a powerful tool to overcome this problem. Through their human homologs, over 3-fold more zebrafish genes could be associated with the immune-specific GO-terms. In addition, gene groups with a clear correlation to immune processes (i.e. "complement pathway" and "acute phase response") were identified by DAVID analysis taking advantage of the human homolog conversion dataset. It remains to be experimentally confirmed if there is functional conservation between these unannotated zebrafish genes and their predicted human homologs, however their up-regulation in response to *S. typhimurium* infection supports that they play a role in the host immune response.

The relevance of the zebrafish embryo model to study vertebrate immunity was further investigated by comparison of our transcriptome data to a meta analysis of microarray data of various human cell lines challenged by different pathogens (42). We found a substantial overlap between the zebrafish host response to *S. typhimurium* and a set of genes that was commonly induced in all cell lines upon pathogen challenge referred to as "the common host response". The overlap included genes for well known immune responsive transcription factors, cell surface receptors, signal transduction intermediates, adhesion factors and proteins involved in tissue remodelling. Even though adaptive immunity is not yet developed in the zebrafish embryo, we also observed induction of genes encoding predicted zebrafish homologs of

molecules involved in antigen processing and co-stimulation. Furthermore, various interferon, chemokine, proinflammatory cytokine and anti-inflammatory cytokine genes were shared between the gene sets of the zebrafish embryonic host response and the human common host response. Taken together, these observations further underscore the predictive value of the zebrafish embryo model.

Toll-like receptors are key players in the recognition of pathogens during host defence. We previously analysed the zebrafish genome for genes encoding members of TLR signalling pathway leading to the identification of the zebrafish counterparts of the human TLRs and adapter proteins (23). GenMapp based analysis of the TLR pathway in this study demonstrated that various TLR signalling intermediates at different levels in the pathway are induced upon *S. typhimurium* wt and Ra infection in vivo. Genes implicated in the negative regulation of the pathway, e.g. *socs1*, *socs3* and *pik3cg,* were among the earliest regulated genes (49-51). In addition, we observed induction of genes encoding NF-κB inhibitors and the *irak3* gene, whose human homolog functions as a negative regulator of the TLR pathway (52). These observations suggest a tight regulation of the TLR pathway most likely to limit the potential negative consequences of excessive cytokine production. Furthermore the zebrafish homologs of the human TLR5, Tlr5a and Tlr5b, were specifically up-regulated upon *S. typhimurium* wt and Ra challenge. It has previously been demonstrated that the mammalian TLR5 is mediating the immune response to bacterial flagellin (53) specifically recognizing conserved domains of monomeric flagellin crucial for bacterial motility and protofilament assembly (54). Our results showed that challenge of the zebrafish embryo with purified *S. typhimurium* flagellin elicited a strong activation of zebrafish homologs of the pro-inflammatory cytokines *il1b*, *il8* and *tnfa*. Flagellin challenge also induced expression of the chemokine gene *cxcl-C1c,* the matrix metalloproteinase gene *mmp9*, and the putative negative regulator *irak3* discussed above. Functional assessment of *tlr5a* and *tlr5b* by morpholino-mediated knockdown followed by flagellin stimulation clearly demonstrated tlr5-dependent gene activation of *mmp9*, *cxcl-C1c* and *irak3* in the zebrafish embryo. Therefore, Tlr5 pathway activation appears to induce the expression of inflammatory mediators as well as feedback control of the innate immune response.

Although we found that flagellin induction of immune response genes was mediated by Tlr5, the *tlr5a* and *tlr5b* genes themselves were not induced upon flagellin stimulation. Furthermore, induction of *tlr5a* and *tlr5b* was still observed upon challenge with a non-flagellated derivative of the *S. typhimurium* wt strain (data not shown), demonstrating a flagellin-independent transcriptional activation of *tlr5a* and *tlr5b* during infection in the zebrafish embryo. Furthermore, preliminary results of knockdown experiments suggest that Tlr5 expression is not required for the induction of inflammatory mediators during *S. typhimurium* infection. This is consistent with observations in mice showing that TLR4 is able to compensate for the function of TLR5 upon *Salmonella* infection (55).

MyD88 functions as adaptor protein of TLR5 in mammalian systems and is also

an important adaptor of other TLRs, including TLR4. In previous work we demonstrated the significance of MyD88 in the zebrafish embryo host defence by showing that accumulation of *S. typhimurium* Ra bacteria was increased upon MyD88 morpholino knockdown (31). Here, we extended this work and assessed transcriptional effects of MyD88 on downstream target genes of innate immunity signalling. Our results demonstrated a clear dependency of *mmp9*, *il1b* and *irak3* on MyD88 for transcriptional activation upon *S. typhimurium* wt challenge. In contrast, *ifn1* and *il8* did not show changes in their induction upon bacterial challenge, demonstrating MyD88-independent activation of these genes. Differential use of the MyD88 adaptor in the TLR-pathway is well documented in mammalian systems with *IL1b* as the primary example of a MyD88-dependent target gene and *IFN* as a target of both MyD88-dependent and independent routes (3, 4, 56). Our observations suggest a conserved mechanism in the zebrafish embryo. Furthermore, we have identified *mmp9* and *irak3* as novel MyD88-dependent immune response genes. MyD88-dependent as well as MyD88-independent induction of *il8* has been observed in mammalian systems (57, 58). However, regarding the MyD88-independent *il8* induction that we observed in zebrafish embryos it should be noted that the orthology of this gene with mammalian *il8* is ambiguous and that zebrafish express other closely related putative *il8* homologs.

In this study we found that the matrix metalloproteinase genes *mmp9* and *mmp13* were among the strongest infection responsive genes, with induction levels around 10 to 20-fold at 8 hpi for the *S. typhimurium* Ra and wt strains and over 100-fold at 24 hpi for the *S. typhimurium* wt strain. Proteins of the mammalian MMP family degrade extracellular matrices thereby facilitating cell migration. Additionally, they are thought to affect the activity of inflammatory molecules (59). *S. typhimurium* and other bacterial species have been reported to secrete proteases that activate inactive proenzyme forms of MMPs, which may promote bacterial spreading through the host tissues (60). Here we have shown that *mmp9* expression is a target of the TLR5 pathway that is induced by *Salmonella* flagellin. Therefore, it appears that *Salmonella*-derived molecules can stimulate MMP activity both at the transcriptional and the post-translational level. We have observed that induction of *mmp* genes is a common characteristic also of other types of bacterial infections in zebrafish, including *Edwardsiella*, *Pseudomonas* and *Mycobacterium* infections (unpublished results). Likewise, these genes are induced during pulmonary *Mycobacterium* infection in mice (61). Another metalloproteinase gene that we found induced upon *S. typhimurium* infection is *adam8* (a disintegrin and metalloproteinase domain 8), which belongs to a family of membrane-anchored glycoproteins that have been implicated in a variety of biological processes involving cell-cell and cell-matrix interactions. Recently, up-regulation of ADAM8 surface expression in human neutrophils was correlated with joint inflammation (62) and increased ADAM8 mRNA expression was also associated with allergic inflammation (63). The transparency of zebrafish embryos offers good possibilities to further investigate how gene expression of met-

alloproteinases such as the MMPs and ADAM8 contribute to tissue remodelling, inflammation and bacterial dissemination.

Providing a case study for future immunity research in the zebrafish embryo model, our transcriptome analysis of the host response to *S. typhimurium* has linked a large set of zebrafish genes to the process of bacterial infection. Among these are a number of chemokine genes that have previously been annotated in the zebrafish genome, but that have not been functionally studied (64). Infection responsive chemokine genes that were more than 3-fold induced over multiple time points of our in vivo infection study include *cxcl-C1c*, *cxcl-C5c*, *ccl-C5a*, *ccl-C24a*, and *similar to ccl-CUb* (Dr.125570). Another example of a putative immune response gene that we found to be strongly induced by S. typhimurium infection is the *zgc:65788* gene that encodes a homolog of the mammalian acidic chitinase family (5-10 fold at 8 hpi by the wt and Ra strains, and over 30-fold at 24 hpi by the wt strain). Increased chitinase gene expression was also observed in our previous *Mycobacterium*-infection study of adult zebrafish (65). There is increasing evidence for a role of acidic mammalian chitinases in Th2 inflammation and asthma (66, 67). The strong induction of *zgc:65788* expression during infection of zebrafish embryos suggests that chitinases may also play a role in the innate immune response. Finally, we found that approximately 70% of all genes that were specifically regulated during the first hours of *S. typhimurium* infection had not been previously linked to immunological processes. Many of these genes include transcribed loci that have unknown functions and for which the functions of their predicted human homologs are also unknown. With the possibility of performing rapid gene knockdown studies, the zebrafish embryo provides a useful model for the future functional characterization of these genes that will also support the further annotation of the human genome.

Materials and Methods

Bacterial Strains and Growth Conditions

S. typhimurium wild type (wt) strain SL1027 and its isogenic LPS derivative SF1592 (*Ra*), both containing the DsRed expression vector pGMDs3, were used for the infection of zebrafish embryos (9). A non-flagellated derivative of this strain (*flhC*$^-$) contained an flhC::Mu*dJ* insertion generously provided by K. Hughes (University of Utah) (38). Bacteria were freshly grown overnight on LB agar plates supplemented with 100µg/ml carbenicillin (wt and Ra mutant strain) and 50µg/ml kanamycin (*flhC*$^-$) and resuspended in phosphate-buffered saline (PBS) prior to injection.

Zebrafish husbandry

Zebrafish were handled in compliance with the local animal welfare regulations and maintained according to standard protocols (http://ZFIN.org). Embryos were grown at 28,5 -30 °C in egg water (60µg/ml Instant Ocean sea salts). For the duration of bac-

terial injections embryos were kept under anaesthesia in egg water containing 0.02% buffered 3-aminobenzoic acid ethyl ester (tricaine, Sigma). Embryos used for whole mount in situ staining were kept in egg water containing 0.003% 1-phenyl-2-thiourea (Sigma) to prevent melanization.

Morpholino knock-down experiments

For morpholino knockdown experiments, morpholino oligonucleotides (Gene Tools) were diluted to desired concentrations in 1x Danieu's buffer [58 mM NaCl, 0.7 mM KCl, 0.4 mM $MgSO_4$, 0.6 mM $Ca(NO_3)_2$, 5.0 mM HEPES; pH 7.6] containing 1% Phenol red (Sigma). To block translation of the *tlr5a*, *tlr5b* or *myd88* mRNA we injected 0.85ng (0.1mM), 4.2ng (0.5mM) and 8.4ng (1mM) per embryo, respectively. To control for aspecific morpholino effects we used the standard control morpholino (0.6mM) for the Tlr5 knockdown experiments and a previously described 5 bp mismatch morpholino (1mM) (31) for the MyD88 knockdown studies. Morpholinos used target the 5' UTR region of the respective gene. Morpholino sequences are shown in supplementary table I.

Experimental design of infection study

All infection experiments were performed using mixed egg clutches from three tanks of AB strain zebrafish. Embryos were staged at 27 hours post fertilization (hpf) by morphological criteria (39) and approximately 250 cfu of DsRed expressing *S. typhimurium* wt and *Ra* mutant bacteria were injected into the caudal vein close to the urogenital opening. As a control an equal volume of PBS was likewise injected. Injections were controlled using a Leica MZ Fluo 3 stereomicroscope with epifluorescence attachment together with a Femtojet microinjector (Eppendorf) and a micromanipulator with pulled microcapillary pipettes. Pools of 20-40 embryos were collected at 2, 5, 8 and 24 hours post infection (hpi). For the microarray analysis, the whole infection procedure was performed in triplicate on separate days. The order of injecting wt bacteria, *Ra* bacteria and PBS control was randomized in the different experiments. Microarray analysis was performed using custom-designed 44k Agilent chips. All *S. typhimurium* wt, *S. typhimurium Ra* and PBS control RNA samples were labelled with Cy5 and hybridized against a Cy3-labelled common reference, which consisted of a mixture of all samples from the infection study.

Microarray design

The micro-array slides were custom designed by Agilent Technologies. The slides contained in total 43.371 probes of a 60 oligonucleotide length. Of these probes a total of 21.496 probes were identical to the probes present on the Agilent probe set that is commercially available under catalogue number 013223_D. Most of the additional probes were designed using the eArray software from Agilent Technologies (https://earray.chem.agilent.com/earray/). Settings used were based on the following settings: base composition methodology, best probe methodology and design

with 3' bias. The Agilent *D. rerio* transcriptome was used as a reference database. A small number of probes were manually designed based on knowledge of particular polymorphisms for genes encoding protein families such as 14-3-3 proteins, chitinase-like proteins and Toll-like receptors in order to obtain gene-specific probes. The micro-array design has been submitted to the GEO database under accession number GPL7735.

RNA isolation, labelling and hybridization

Embryos for RNA isolation were snap frozen in liquid nitrogen and subsequently stored at -80°C. Embryos were homogenized in 1 ml of TRIZOL® Reagent (Invitrogen) and subsequently total RNA was extracted according to the manufacturer's instructions. The RNA samples were incubated for 20 min at 37° with 10 units of DNaseI (Roche Applied Science) to remove residual genomic DNA prior to purification using the RNeasy MinElute Cleanup kit (Qiagen) according to the RNA clean up protocol. The integrity of the RNA was confirmed by Lab-on-chip analysis using the 2100 Bioanalyzer (Agilent Technologies). Samples used for microarray analysis had an average RIN value of 9 and a minimum RIN value of 8.

Amino Allyl modified amplified RNA (aRNA) was synthesized in one amplification round from 1 μg of total RNA using the Amino Allyl MessageAmp™ II aRNA Amplification Kit (Ambion). Subsequently, 6 μg of Amino Allyl modified aRNA was used for coupling of monoreactive Cy3 and Cy5 dyes (GE Healthcare) and column purified. The dual colour hybridization of the microarray chips was performed at ServiceXS (ServiceXS, Leiden, The Netherlands) according to Agilent protocol G4140-90050 v.5.7 (www.Agilent.com) for Two-Color Microarray-Based Gene Expression Analysis.

Data analysis

Microarray data was processed from raw data image files with Feature Extraction Software 9.5.3 (Agilent Technologies). Processed data were subsequently imported into Rosetta Resolver 7.0 (Rosetta Biosoftware, Seattle, Washington) and subjected to default ratio error modelling. The raw data were submitted to the GEO database under accession number GSE13994. In order to compare *S. typhimurium* wild type and *S. typhimurium Ra* treated samples to the PBS injected control samples a re-ratio experiment was performed using the Rosetta build in re-ratio with common reference application. Data were analyzed at the level of UniGene clusters (UniGene build #105). Significance cut-offs for the ratios of wt versus PBS and Ra versus PBS were set at 1.5 fold change at $P < 10^{-4}$ for UniGene clusters. Two-dimensional hierarchical cluster analyses were performed with Rosetta Resolver settings for agglomerative algorithm (average link) with Cosine correlation.

Gene ontology (GO) analysis was performed using the GeneTools eGOn V2.0 web-based gene ontology analysis software (http://www.genetools.microarray.ntnu.no/) (40) and using DAVID software tools (http://david.abcc.ncifcrf.gov/home.jsp)

(41). GO analysis using *e*GOn was done at the level of the UniGene clusters (*D. rerio* UniGene build #105). GO analyses using DAVID tools were performed at the level of the Entrez Gene codes, because the DAVID database was not updated to a recent *D. rerio* UniGene build. To take advantage of the much better GO annotation of the human genome, we developed a software tool with which the UniGene and Entrez Gene records of the functionally related human homologs of our zebrafish UniGene list could be automatically retrieved from the NCBI HomoloGene database. Subsequently, *e*GOn and DAVID GO analyses were repeated using the UniGene (*H. sapiens* UniGene build #202) and Entrez Gene lists of human orthologs, respectively. UniGene and Entrez Gene lists subjected to *e*GOn and DAVID analyses are included in supplementary table II. In addition, for comparison with human microarray data, the (putative) zebrafish homologs of the set of 511 human common host response genes described by Jenner and Young (42) were manually identified by searching ZFIN (http://zfin.org) and the Gene and HomoloGene databases of the National Center for Biotechnology Information (NCBI) (Supplementary table III). Homologs of human cytokines were identified based on phylogeny reconstructions to be reported elsewhere. Direct or putative homologs could be identified for 397 out of the 511 human common host response genes (78%) and 322 of these (63%) were represented on our zebrafish microarray. Since some genes are duplicated in zebrafish and since sometimes there was more than one putative homolog, there were 473 zebrafish UniGenes corresponding to the 322 human genes represented on the array.

Pathway analysis was performed using the GenMapp software package (www.genmap.org) (43). GenMapp analysis was done at the level of UniGene clusters (*D.rerio* UniGene build #105). Significance cut-off was set at 1.5 fold change at $P < 10^{-4}$. Zebrafish homologs of the genes contributing to the TLR pathway were identified by either searching the ZFIN (http://zfin.org) database or the Gene and HomoloGene database of NCBI (Supplementary table IV).

cDNA synthesis and quantitative Real-time PCR

cDNA synthesis reactions were performed in a 20 µl mixture of 500 ng RNA, 4 µl of 5x iScript Reaction mix (Bio-Rad) and 1 µl of iScript Reverse Transcriptase (Bio-Rad). The reaction mixtures were incubated at 25 °C for 5 min, 42 °C for 30 min, and 85 °C for 5 min.

Real-time PCR was performed using the Chromo4 Real-time PCR detection system (Bio-Rad laboratories, Hercules, CA) according to the manufacturer's instructions. Each reaction was performed in a 25 µl volume comprised of 1 µl cDNA, 12.5 µl of 2x iQ SYBR Green Supermix (Bio-Rad) and 10 pmol of each primer. Cycling parameters were 95 °C for 3 min to activate the polymerase, followed by 40 cycles of 95 °C for 15 sec and 59 °C for 45 sec. Fluorescence measurements were taken at the end of each cycle. Melting curve analysis was performed to verify that no primer dimers were amplified. All reactions were performed as technical duplicates. For normalization peptidylprolyl isomerase A like (*ppial*), which showed no changes over the

infection time course series, was taken as reference (44) . Results were analysed using the ΔΔCt method. Sequences of forward and reverse primers are described in supplementary table I.

Whole-mount in situ hybridization

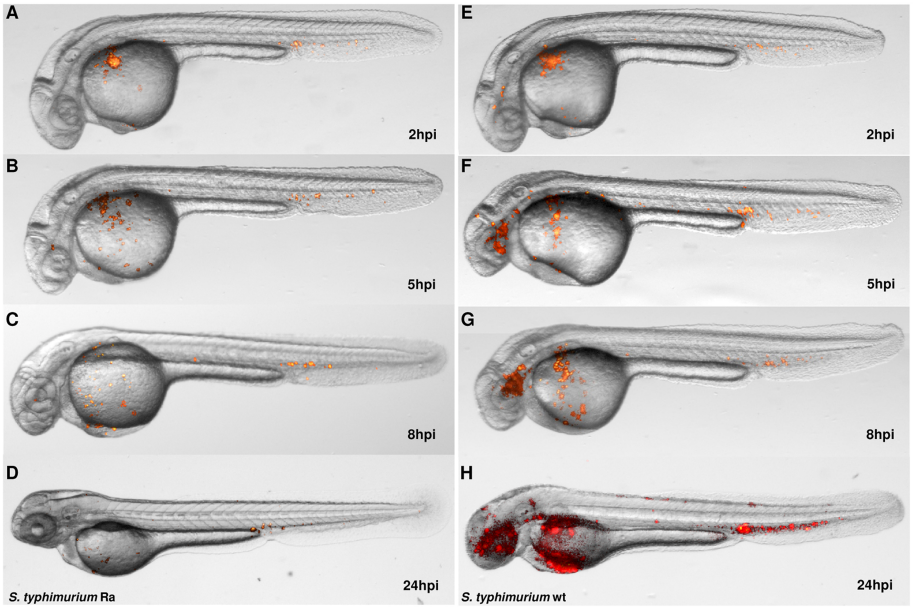
Embryos were fixed overnight in 4% paraformaldehyde in PBS at 4 °C and whole mount in situ hybridization using alkaline phosphatase detection with BM Purple substrate (Roche) was performed according to Thisse et al. (45). Genomic DNA was used to generate templates for riboprobes synthesis by PCR using gene specific primers sets including the binding site for T7 RNA polymerase in the reverse primer. Sequences of forward and reverse primers are described in supplementary table I. Digoxigenin-labeled riboprobes were synthesised using the labelling mixes from Roche and Ambion MEGAscript reagents for in vitro transcription.

Acknowledgments

We are grateful to Astrid van der Sar (VU Medical Centre, the Netherlands) for providing DsRed-labelled S. typhimurium strains and for advise on infection experiments. We thank Wilbert Bitter (VU Medical Centre, the Netherlands) Ben Appelmelk (VU Medical Centre, the Netherlands), Kelly T. Hughes (University of Utah, USA) and Jelle Goeman (LUMC, the Netherlands) for helpful discussions as well as Marcel Schaaf, Ewa Snaar-Jagalska and other members of the Institute of Biology. We are also grateful to Carianne Langerijs for testing in situ probes and to Davy de Witt and Ulrike Nehrdich for fish maintenance. This work was financially supported by the European Commission 6th Framework Programs ZF-MODELS (LSHG-CT-2003-503496) and ZF-TOOLS (LSHG-CT-2006-037220).

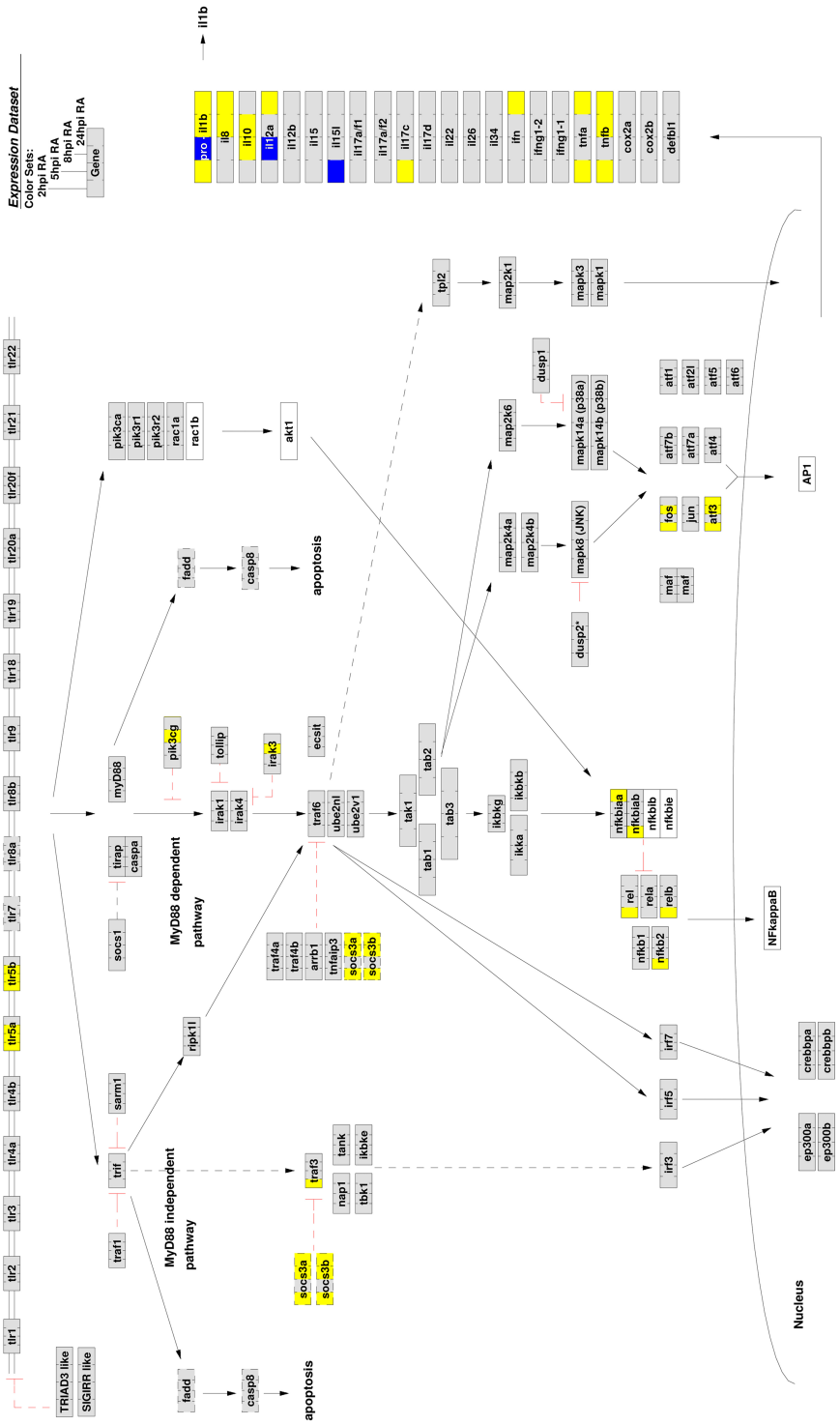
Supplementary data

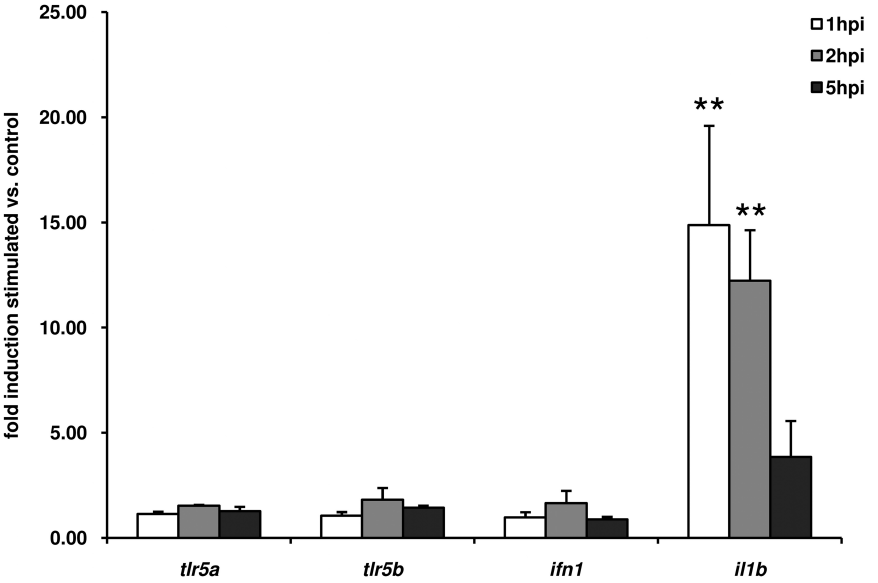
Supplementary tables and supplementary material 1 can be found online at: http://www.jimmunol.org/cgi/content/full/182/9/5641/DC1



SUPPLEMENTARY FIGURE 1. Imaging analysis of *S. typhimurium* wt and Ra infection over the experimental time course. Embryos were injected at 27 hpf with approximately 250 cfu of *S. typhimurium* Ra (A-D) or wt (E-H) into the caudal vein and imaged at 2, 5, 8 and 24 hpi. Overlay pictures of bright field and DsRed fluorescent images are shown. Anterior side is to the left and dorsal is to the top.

SUPPLEMENTARY FIGURE 2. GenMapp analysis of the TLR-pathway upon *S. typhimurium* Ra infection. Expression profiles (infected versus control, $p<0.0001$ and fold changes >1.5 and <-1.5) of the 2, 5, 8 and 24 hpi time points were simultaneously mapped on the TLR pathway. Gene boxes are colour coded from left to right with the 2, 5, 8 and 24 hpi expression data. Up-regulation is indicated in yellow, down-regulation in blue and unchanged expression in grey. White denotes genes that were not represented on the array platform. The pathway is based on knowledge of TLR signalling in mammalian species and it should be noted that most interactions remain to be experimentally confirmed in zebrafish.


Expression Dataset
Color Sets:
2hpi RA
5hpi RA
8hpi RA
24hpi RA
Gene
il1b
pro il1b
il8
il10
il12a
il12b
il15
il15l
il17a/f1
il17a/f2
il17c
il17d
il22
il26
il34
ifn
ifng1-2
ifng1-1
tnfa
tnfb
cox2a
cox2b
defb1
tlr1
tlr2
tlr3
tlr4a
tlr4b
tlr5a
tlr5b
tlr7
tlr8a
tlr6b
tlr9
tlr18
tlr19
tlr20a
tlr20f
tlr21
tlr22
TRIAD3 like
SIGIRR like
trif
trif1
sarm1
myD88
tirap
caspa
socs1
MyD88 dependent pathway
MyD88 independent pathway
ripk1l
pik3cg
tollip
irak3
irak1
irak4
trif6
ecsit
ube2ni
ube2v1
tak1
tab1
tab2
tab3
ikbkg
ikka
ikbkb
nfkbiaa
nfkbiab
nfkbib
nfkbie
rel
rela
relb
nfkb1
nfkb2
NFkappaB
pik3ca
pik3r1
pik3r2
rac1a
rac1b
akt1
fadd
casp8
apoptosis
tpl2
map2k1
mapk3
mapk1
dusp1
map2k6
mapk14a (p38a)
mapk14b (p38b)
map2k4a
map2k4b
mapk8 (JNK)
dusp2*
atf1
atf2l
atf5
atf6
atf7b
atf7a
atf4
fos
jun
atf3
maf
maf
AP1
traf4a
traf4b
arrb1
tnfaip3
socs3a
socs3b
traf3
nap1
tank
tbk1
ikbke
irf3
irf5
irf7
crebbpa
crebbpb
ep300a
ep300b
Nucleus



SUPPLEMENTARY FIGURE 3. Temporal expression profiles of immune response genes upon challenge with purified *S. typhimurium* flagellin. Embryos were challenged with flagellin by injection of 4nl (100ug/ml) into the caudal vein at 27 hpf. Gene induction levels upon stimulation compared to the mock-injected controls were analyzed by qRT-PCR at 1, 2 and 5 hpi for *tlr5a*, *tlr5b*, *ifn1* and *il1b*. Values are the mean ± S.D. of at least 2 independent experiments. **p<0.01 (tested by one way ANOVA).

References

1. Medzhitov, R. 2001. Toll-like receptors and innate immunity. *Nat.Rev.Immunol.* 1:135-145.
2. Beutler, B., and M. Rehli. 2002. Evolution of the TIR, tolls and TLRs: functional inferences from computational biology. *Curr.Top.Microbiol.Immunol.* 270:1-21.
3. Kawai, T., and S. Akira. 2007. TLR signaling. *Seminars in immunology* 19:24-32.
4. O'Neill, L. A., and A. G. Bowie. 2007. The family of five: TIR-domain-containing adaptors in Toll-like receptor signalling. *Nature reviews* 7:353-364.
5. Oshiumi, H., M. Matsumoto, K. Funami, T. Akazawa, and T. Seya. 2003. TICAM-1, an adaptor molecule that participates in Toll-like receptor 3-mediated interferon-beta induction. *Nat.Immunol.* 4:161-167.
6. Adachi, O., T. Kawai, K. Takeda, M. Matsumoto, H. Tsutsui, M. Sakagami, K. Nakanishi, and S. Akira. 1998. Targeted disruption of the MyD88 gene results in loss of IL-1- and IL-18-mediated function. *Immunity.* 9:143-150.
7. Sun, D., and A. Ding. 2006. MyD88-mediated stabilization of interferon-gamma-induced cytokine and chemokine mRNA. *Nature immunology* 7:375-381.
8. Davis, J. M., H. Clay, J. L. Lewis, N. Ghori, P. Herbomel, and L. Ramakrishnan. 2002. Real-time visualization of mycobacterium-macrophage interactions leading to initiation of granuloma formation in zebrafish embryos. *Immunity.* 17:693-702.
9. Van der Sar, A. M., R. J. Musters, F. J. van Eeden, B. J. Appelmelk, C. M. Vandenbroucke-Grauls, and W. Bitter. 2003. Zebrafish embryos as a model host for the real time analysis of Salmonella typhimurium infections. *Cell Microbiol.* 5:601-611.
10. Ward, A. C., D. O. McPhee, M. M. Condron, S. Varma, S. H. Cody, S. M. Onnebo, B. H. Paw, L. I. Zon, and G. J. Lieschke. 2003. The zebrafish spi1 promoter drives myeloid-specific expression in stable transgenic fish. *Blood* 102:3238-3240.
11. Redd, M. J., G. Kelly, G. Dunn, M. Way, and P. Martin. 2006. Imaging macrophage chemotaxis in vivo: studies of microtubule function in zebrafish wound inflammation. *Cell Motil.Cytoskeleton* 63:415-422.
12. Renshaw, S. A., C. A. Loynes, D. M. Trushell, S. Elworthy, P. W. Ingham, and M. K. Whyte. 2006. A transgenic zebrafish model of neutrophilic inflammation. *Blood* 108:3976-3978.
13. Mathias, J. R., B. J. Perrin, T. X. Liu, J. Kanki, A. T. Look, and A. Huttenlocher. 2006. Resolution of inflammation by retrograde chemotaxis of neutrophils in transgenic zebrafish. *J.Leukoc.Biol.* 80:1281-1288.
14. Meijer, A. H., A. M. van der Sar, C. Cunha, G. E. Lamers, M. A. Laplante, H. Kikuta, W. Bitter, T. S. Becker, and H. P. Spaink. 2008. Identification and real-time imaging of a myc-expressing neutrophil population involved in inflammation and mycobacterial granuloma formation in zebrafish. *Developmental and comparative immunology* 32:36-49.
15. Miller, J. D., and M. N. Neely. 2005. Large-scale screen highlights the importance of capsule for virulence in the zoonotic pathogen Streptococcus iniae. *Infect Immun* 73:921-934.
16. Lieschke, G. J., and P. D. Currie. 2007. Animal models of human disease: zebrafish swim into view. *Nat Rev Genet* 8:353-367.
17. Schorpp, M., M. Bialecki, D. Diekhoff, B. Walderich, J. Odenthal, H. M. Maischein, A. G. Zapata, and T. Boehm. 2006. Conserved functions of Ikaros in vertebrate lymphocyte development: genetic evidence for distinct larval and adult phases of T cell development and two lineages of B cells in zebrafish. *J Immunol* 177:2463-2476.
18. Trede, N. S., T. Ota, H. Kawasaki, B. H. Paw, T. Katz, B. Demarest, S. Hutchinson, Y. Zhou, C. Hersey, A. Zapata, C. T. Amemiya, and L. I. Zon. 2008. Zebrafish mutants with disrupted early T-cell and thymus development identified in early pressure screen. *Dev Dyn* 237:2575-2584.
19. Pase, L., J. E. Layton, W. P. Kloosterman, D. Carradice, P. M. Waterhouse, and G. J. Lieschke. 2008. miR-451 regulates zebrafish erythroid maturation in vivo via its target gata2. *Blood*.
20. Yoder, J. A., M. E. Nielsen, C. T. Amemiya, and G. W. Litman. 2002. Zebrafish as an immunological model system. *Microbes.Infect.* 4:1469-1478.
21. Traver, D., P. Herbomel, E. E. Patton, R. D. Murphey, J. A. Yoder, G. W. Litman, A. Catic, C. T. Amemiya, L. I. Zon, and N. S. Trede. 2003. The zebrafish as a model organism to study development of the immune system. *Adv.Immunol.* 81:253-330.
22. Trede, N. S., D. M. Langenau, D. Traver, A. T. Look, and L. I. Zon. 2004. The use of zebrafish to understand immunity. *Immunity.* 20:367-379.
23. Meijer, A. H., S. F. G. Krens, I. A. Medina Rodriguez, S. He, W. Bitter, B. E. Snaar-Jagalska, and H. P. Spaink. 2004. Expression analysis of the Toll-like receptor and TIR domain adaptor families of zebrafish. *Mol Immunol.* 40:773-783.
24. Stein, C., M. Caccamo, G. Laird, and M. Leptin. 2007. Conservation and divergence of gene families encoding components of innate immune response systems in zebrafish. *Genome biology* 8:R251.
25. Murayama, E., K. Kissa, A. Zapata, E. Mordelet, V. Briolat, H. F. Lin, R. I. Handin, and P. Herbomel. 2006. Tracing hematopoietic precursor migration to successive hematopoietic organs during zebrafish development. *Immunity.* 25:963-975.
26. Herbomel, P., B. Thisse, and C. Thisse. 1999. Ontogeny and behaviour of early macrophages in the zebrafish em-

bryo. *Development* 126:3735-3745.
27. Herbomel, P., B. Thisse, and C. Thisse. 2001. Zebrafish early macrophages colonize cephalic mesenchyme and developing brain, retina, and epidermis through a M-CSF receptor-dependent invasive process. *Dev.Biol.* 238:274-288.
28. Willett, C. E., A. Cortes, A. Zuasti, and A. G. Zapata. 1999. Early hematopoiesis and developing lymphoid organs in the zebrafish. *Dev.Dyn.* 214:323-336.
29. Davidson, A. J., and L. I. Zon. 2004. The 'definitive' (and 'primitive') guide to zebrafish hematopoiesis. *Oncogene* 23:7233-7246.
30. Lam, S. H., H. L. Chua, Z. Gong, T. J. Lam, and Y. M. Sin. 2004. Development and maturation of the immune system in zebrafish, Danio rerio: a gene expression profiling, in situ hybridization and immunological study. *Dev.Comp Immunol.* 28:9-28.
31. Van der Sar, A. M., O. W. Stockhammer, L. C. van der, H. P. Spaink, W. Bitter, and A. H. Meijer. 2006. MyD88 innate immune function in a zebrafish embryo infection model. *Infection and Immunity* 74:2436-2441.
32. Pressley, M. E., P. E. Phelan, III, P. E. Witten, M. T. Mellon, and C. H. Kim. 2005. Pathogenesis and inflammatory response to Edwardsiella tarda infection in the zebrafish. *Dev.Comp Immunol.* 29:501-513.
33. Clay, H., H. E. Volkman, and L. Ramakrishnan. 2008. Tumor necrosis factor signaling mediates resistance to mycobacteria by inhibiting bacterial growth and macrophage death. *Immunity* 29:283-294.
34. Levraud, J. P., P. Boudinot, I. Colin, A. Benmansour, N. Peyrieras, P. Herbomel, and G. Lutfalla. 2007. Identification of the zebrafish IFN receptor: implications for the origin of the vertebrate IFN system. *J Immunol* 178:4385-4394.
35. Phelps, H. A., and M. N. Neely. 2005. Evolution of the zebrafish model: from development to immunity and infectious disease. *Zebrafish* 2:87-103.
36. Meeker, N. D., and N. S. Trede. 2008. Immunology and zebrafish: spawning new models of human disease. *Developmental and comparative immunology* 32:745-757.
37. Lesley, R., and L. Ramakrishnan. 2008. Insights into early mycobacterial pathogenesis from the zebrafish. *Current opinion in microbiology* 11:277-283.
38. Chilcott, G. S., and K. T. Hughes. 2000. Coupling of flagellar gene expression to flagellar assembly in Salmonella enterica serovar typhimurium and Escherichia coli. *Microbiol Mol Biol Rev* 64:694-708.
39. Kimmel, C. B., W. W. Ballard, S. R. Kimmel, B. Ullmann, and T. F. Schilling. 1995. Stages of embryonic development of the zebrafish. *Dev.Dyn.* 203:253-310.
40. Beisvag, V., F. K. Junge, H. Bergum, L. Jolsum, S. Lydersen, C. C. Gunther, H. Ramampiaro, M. Langaas, A. K. Sandvik, and A. Laegreid. 2006. GeneTools--application for functional annotation and statistical hypothesis testing. *BMC bioinformatics* 7:470.
41. Dennis, G., Jr., B. T. Sherman, D. A. Hosack, J. Yang, W. Gao, H. C. Lane, and R. A. Lempicki. 2003. DAVID: Database for Annotation, Visualization, and Integrated Discovery. *Genome biology* 4:P3.
42. Jenner, R. G., and R. A. Young. 2005. Insights into host responses against pathogens from transcriptional profiling. *Nat Rev Microbiol* 3:281-294.
43. Dahlquist, K. D., N. Salomonis, K. Vranizan, S. C. Lawlor, and B. R. Conklin. 2002. GenMAPP, a new tool for viewing and analyzing microarray data on biological pathways. *Nature genetics* 31:19-20.
44. Roesner, A., T. Hankeln, and T. Burmester. 2006. Hypoxia induces a complex response of globin expression in zebrafish (Danio rerio). *The Journal of experimental biology* 209:2129-2137.
45. Thisse, C., B. Thisse, T. F. Schilling, and J. H. Postlethwait. 1993. Structure of the zebrafish snail1 gene and its expression in wild-type, spadetail and no tail mutant embryos. *Development* 119:1203-1215.
46. Medzhitov, R., P. Preston-Hurlburt, and C. A. Janeway, Jr. 1997. A human homologue of the Drosophila Toll protein signals activation of adaptive immunity. *Nature* 388:394-397.
47. Ohno, A., Y. Isii, K. Tateda, T. Matumoto, S. Miyazaki, S. Yokota, and K. Yamaguchi. 1995. Role of LPS length in clearance rate of bacteria from the bloodstream in mice. *Microbiology (Reading, England)* 141 (Pt 10):2749-2756.
48. Murray, G. L., S. R. Attridge, and R. Morona. 2003. Regulation of Salmonella typhimurium lipopolysaccharide O antigen chain length is required for virulence; identification of FepE as a second Wzz. *Molecular microbiology* 47:1395-1406.
49. Mansell, A., R. Smith, S. L. Doyle, P. Gray, J. E. Fenner, P. J. Crack, S. E. Nicholson, D. J. Hilton, L. A. O'Neill, and P. J. Hertzog. 2006. Suppressor of cytokine signaling 1 negatively regulates Toll-like receptor signaling by mediating Mal degradation. *Nature immunology* 7:148-155.
50. Frobose, H., S. G. Ronn, P. E. Heding, H. Mendoza, P. Cohen, T. Mandrup-Poulsen, and N. Billestrup. 2006. Suppressor of cytokine Signaling-3 inhibits interleukin-1 signaling by targeting the TRAF-6/TAK1 complex. *Molecular endocrinology (Baltimore, Md* 20:1587-1596.
51. Liew, F. Y., D. Xu, E. K. Brint, and L. A. O'Neill. 2005. Negative regulation of toll-like receptor-mediated immune responses. *Nature reviews* 5:446-458.
52. Kobayashi, K., L. D. Hernandez, J. E. Galan, C. A. Janeway, Jr., R. Medzhitov, and R. A. Flavell. 2002. IRAK-M is a negative regulator of Toll-like receptor signaling. *Cell* 110:191-202.
53. Hayashi, F., K. D. Smith, A. Ozinsky, T. R. Hawn, E. C. Yi, D. R. Goodlett, J. K. Eng, S. Akira, D. M. Underhill,

and A. Aderem. 2001. The innate immune response to bacterial flagellin is mediated by Toll-like receptor 5. *Nature* 410:1099-1103.

54. Smith, K. D., E. Andersen-Nissen, F. Hayashi, K. Strobe, M. A. Bergman, S. L. Barrett, B. T. Cookson, and A. Aderem. 2003. Toll-like receptor 5 recognizes a conserved site on flagellin required for protofilament formation and bacterial motility. *Nature immunology* 4:1247-1253.
55. Feuillet, V., S. Medjane, I. Mondor, O. Demaria, P. P. Pagni, J. E. Galan, R. A. Flavell, and L. Alexopoulou. 2006. Involvement of Toll-like receptor 5 in the recognition of flagellated bacteria. *Proceedings of the National Academy of Sciences of the United States of America* 103:12487-12492.
56. Seki, E., H. Tsutsui, H. Nakano, N. Tsuji, K. Hoshino, O. Adachi, K. Adachi, S. Futatsugi, K. Kuida, O. Takeuchi, H. Okamura, J. Fujimoto, S. Akira, and K. Nakanishi. 2001. Lipopolysaccharide-induced IL-18 secretion from murine Kupffer cells independently of myeloid differentiation factor 88 that is critically involved in induction of production of IL-12 and IL-1beta. *J Immunol* 166:2651-2657.
57. Balloy, V., J. M. Sallenave, Y. Wu, L. Touqui, J. P. Latge, M. Si-Tahar, and M. Chignard. 2008. Aspergillus fumigatus-induced interleukin-8 synthesis by respiratory epithelial cells is controlled by the phosphatidylinositol 3-kinase, p38 MAPK, and ERK1/2 pathways and not by the toll-like receptor-MyD88 pathway. *The Journal of biological chemistry* 283:30513-30521.
58. Zheng, J., J. Meng, S. Zhao, R. Singh, and W. Song. 2008. Campylobacter-induced interleukin-8 secretion in polarized human intestinal epithelial cells requires Campylobacter-secreted cytolethal distending toxin- and Toll-like receptor-mediated activation of NF-kappaB. *Infect Immun* 76:4498-4508.
59. Parks, W. C., C. L. Wilson, and Y. S. Lopez-Boado. 2004. Matrix metalloproteinases as modulators of inflammation and innate immunity. *Nat.Rev.Immunol.* 4:617-629.
60. Ramu, P., L. A. Lobo, M. Kukkonen, E. Bjur, M. Suomalainen, H. Raukola, M. Miettinen, I. Julkunen, O. Holst, M. Rhen, T. K. Korhonen, and K. Lahteenmaki. 2008. Activation of pro-matrix metalloproteinase-9 and degradation of gelatin by the surface protease PgtE of Salmonella enterica serovar Typhimurium. *Int J Med Microbiol* 298:263-278.
61. Taylor, J. L., J. M. Hattle, S. A. Dreitz, J. M. Troudt, L. S. Izzo, R. J. Basaraba, I. M. Orme, L. M. Matrisian, and A. A. Izzo. 2006. Role for matrix metalloproteinase 9 in granuloma formation during pulmonary Mycobacterium tuberculosis infection. *Infect Immun* 74:6135-6144.
62. Gomez-Gaviro, M., M. Dominguez-Luis, J. Canchado, J. Calafat, H. Janssen, E. Lara-Pezzi, A. Fourie, A. Tugores, A. Valenzuela-Fernandez, F. Mollinedo, F. Sanchez-Madrid, and F. Diaz-Gonzalez. 2007. Expression and regulation of the metalloproteinase ADAM-8 during human neutrophil pathophysiological activation and its catalytic activity on L-selectin shedding. *J Immunol* 178:8053-8063.
63. Matsuno, O., T. Kumamoto, and Y. Higuchi. 2008. ADAM8 in allergy. *Inflammation & allergy drug targets* 7:108-112.
64. Nomiyama, H., K. Hieshima, N. Osada, Y. Kato-Unoki, K. Otsuka-Ono, S. Takegawa, T. Izawa, A. Yoshizawa, Y. Kikuchi, S. Tanase, R. Miura, J. Kusuda, M. Nakao, and O. Yoshie. 2008. Extensive expansion and diversification of the chemokine gene family in zebrafish: identification of a novel chemokine subfamily CX. *BMC genomics* 9:222.
65. Meijer, A. H., F. J. Verbeek, E. Salas-Vidal, M. Corredor-Adamez, J. Bussman, A. M. van der Sar, G. W. Otto, R. Geisler, and H. P. Spaink. 2005. Transcriptome profiling of adult zebrafish at the late stage of chronic tuberculosis due to Mycobacterium marinum infection. *Molecular immunology* 42:1185-1203.
66. Zhu, Z., T. Zheng, R. J. Homer, Y. K. Kim, N. Y. Chen, L. Cohn, Q. Hamid, and J. A. Elias. 2004. Acidic mammalian chitinase in asthmatic Th2 inflammation and IL-13 pathway activation. *Science* 304:1678-1682.
67. Elias, J. A., R. J. Homer, Q. Hamid, and C. G. Lee. 2005. Chitinases and chitinase-like proteins in T(H)2 inflammation and asthma. *The Journal of allergy and clinical immunology* 116:497-500.

4 Transcriptome analysis of Traf6 function in the innate immune response of zebrafish embryos

Oliver W. Stockhammer[1], Han Rauwerda[2], Floyd R. Wittink[2], Timo M. Breit[2], Annemarie H. Meijer[1] and Herman P. Spaink[1]

1 Institute of Biology, Leiden University, Leiden, The Netherlands 2 MicroArray Department & Integrative Bioinformatics Unit, Swammerdam Institute for Life Sciences, University of Amsterdam, Amsterdam, The Netherlands

Abstract

TRAF6 is a key player at the cross-roads of development and immunity. The analysis of its *in vivo* molecular function is a great challenge since severe developmental defects and early lethality caused by *Traf6* deficiency in knock-out mice interfere with analyses of the immune response. In this study we have used a new strategy to analyse the function of Traf6 in a zebrafish-Salmonella infectious disease model. In our approach the effect of a Traf6 translation-blocking morpholino was titrated down to avoid developmental defects and the response to infection under these partial knock-down conditions was studied using the combination of microarray and next generation sequencing technology. Transcriptome profiling of the traf6 knock-down allowed the identification of a gene set whose responsiveness during infection is highly dependent on Traf6. Expression trend analysis based on the resulting data-sets identified nine clusters of genes with characteristic transcription response profiles, demonstrating Traf6 has a dynamic role as a positive and negative regulator. Among the Traf6-dependent genes was a large set of well known anti-microbial and inflammatory genes. Additionally, we identified several genes of which a role in the immune system was not previously known to be Traf6-dependent, such as the fertility hormone gene *gnrh2* and the DNA-damage regulated autophagy modulator 1 gene *dram1*. With the use of the zebrafish embryo model we have now dissected the *in vivo* function of Traf6 in the innate immune response without interference of adaptive immunity.

Introduction

Microbial infections usually elicit a rapid and strong response of the host innate immune system. Pattern recognition receptors (PRRs), such as Toll-like receptors (TLRs) and NOD-like receptors (NLRs), enable the host to recognize pathogens by detecting conserved molecular patterns such as lipopolysaccharide (LPS), flagellin or peptidoglycan (1). Activation of these receptors will initiate the induction of pro-inflammatory cytokines and as a result a complex network of underlying signalling pathways is activated leading to a tailored inflammatory response with the ultimate goal of eradicating the pathogen. An essential protein transducing the signals emanating from various PRRs and cytokine receptors, including the TNF superfamily, TGFβ, IL-1/Toll-like and NOD-like receptors, is the TNF receptor-associated factor 6 (TRAF6) (2-5).

Initial studies demonstrated the ability of TRAF6 to bind to CD40, RANK and IRAK-1 and showed that NF-κB signalling via TLR4 was abolished by a dominant-negative form of TRAF6 (6-12). Analysis of TRAF6 deficient mice revealed a critical role of TRAF6 in osteoclast development and function. Furthermore, these studies indicated an essential role of TRAF6 in IL-1 signalling, as the activation of NF-

κB and JNK in response to IL-1 were absent in embryonic fibroblasts derived from TRAF6-deficient mice. Moreover, bone marrow-derived macrophages from these mutants displayed a diminished response to LPS, and dendritic cell development and function was impaired (13-15).

The molecular mechanism underlying signal transduction by TRAF6 upon infection is that TRAF6 exerts its function as a K63-specific RING finger E3 ligase. Upon activation of the TLR or the IL-1 receptor pathway, the association of MyD88 with the cytosolic part of the receptor results in the phosphorylation of IRAK-1 by IRAK-4. Subsequently, activated IRAK1 will bind to TRAF6 that will form a complex with the ubiquitin-conjugating enzymes Ubc13 and Uev1a resulting in the attachment of non-degradative K63-linked ubiquitin chains to TRAF6 itself and to NEMO, the regulatory component of the IKK complex upstream of NF-κB. Ubiquitination of TRAF6 will recruit the TAB2/3-TAB1-TAK1 complex resulting in the activation of TAK1. Subsequent activation of the IKK complex and MAP kinase cascades by TAK1 lead to the induction of pro-inflammatory cytokines by the NF-κB and AP-1 transcription factor complexes, respectively (16-19). In addition to the role of TRAF6 in innate immunity, TRAF6 function was also placed in the context of adaptive immunity. Mice containing a T-cell specific deletion of TRAF6 showed the inability to maintain CD8 memory T-cells due to defective AMP-activated kinase activation and mitochondrial fatty acid oxidation after growth factor depletion (20).

Traf6 deficiency in mice causes severe developmental defects and early death at 17–19 days postnatal, making *in vivo* infection studies challenging. Therefore, we have used a zebrafish embryo model to perform *in vivo* infection experiments. In recent years the zebrafish (*Danio rerio*) embryo system has emerged as a model to study vertebrate innate immunity, offering several advantages that complement mammalian model systems. External development and the transparent character of the zebrafish embryo, in combination with fluorescently labeled immune cells and bacteria, allows for study of host microbe interaction and inflammation processes in the living organism (21-28). Analysis of the immune system of the zebrafish revealed a fully developed innate and adaptive immune system showing significant similarities to the human equivalent (29-33). An active innate immune system is detectable already at day one of zebrafish embryogenesis (21, 34, 35). By contrast, a functionally mature adaptive immune system is not active during the first three weeks of zebrafish development establishing a clear temporal separation of the innate and adaptive immune system in the zebrafish embryo. (36-38). Therefore, the zebrafish model provides a convenient system for the *in vivo* study of the vertebrate innate immune response to infection independently from the adaptive immune response. Furthermore, morpholino based knock-down experiments facilitate the functional analysis of genes in the zebrafish embryo that otherwise lead to lethal defects in gene knock-out studies in mice. Moreover, many infection systems for zebrafish have been developed lately, allowing the analysis of gene functions under infection conditions (32, 39, 40).

Here we report on the transcriptional analysis of the innate immune response in Traf6 knock-down and control embryos upon a bacterial infection using a previously described *Salmonella enterica* serovar *Typhimurium* (hereafter referred to as *S. typhimurium)* infection model (22, 33). By titrating down the concentration of a translation blocking morpholino we could avoid effects of Traf6 knock-down on embryo development and study the response to infection under these partial knock-down conditions. Multifactorial analysis of microarray data and confirmation by RNA deep sequencing allowed the identification of a gene set whose responsiveness to *S. typhimurium* infection is highly dependent on Traf6 function. Therefore, while our study indicates a role of Traf6 in developmental processes, it clearly illustrates its importance in the innate immune defence in the zebrafish embryo system.

Results

System for analysis of innate immune functions of Traf6

To accomplish *traf6* knock-down zebrafish embryos were injected at the one cell stage with an ATG morpholino to prevent *traf6* mRNA translation. Initial titration experiments of the *traf6* morpholino elicited a concentration-dependent effect on embryo development showing phenotypical defects, such as body axis truncation and brain malformation, when the administered morpholino concentration exceeded 1mM. To avoid the strong interference of developmental defects, all infection assays were performed using a concentration of 1mM *traf6* morpholino considered as an incomplete knock-down of *traf6*. To be able to discriminate between the specific effect of the *traf6* knock-down and possible aspecific morpholino effects in our assay a control group was treated with a 5bp mismatch *traf6* morpholino. At 27hpf both groups were either immune challenged by injection of 250 cfu of a *S. typhimurium* wild type strain or mock injected with PBS. The transcriptional response was subsequently analysed at 8 hours post infection (hpi) (Fig. 1A). Initial analysis of the datasets demonstrated a robust response to the infection in the control as well as in the *traf6* knock-down group. At the UniGene cluster level a total of 3720 genes ($p<0.05$ and a fold change < -1.2 and > 1.2) were regulated upon bacterial challenge in the control group. In contrast, a reduced response showing a total of 2840 differentially regulated genes ($p<0.05$ and a fold change < -1.2 and > 1.2) was noticeable in the *traf6* knock-down group (Fig. 1B, supplemental Table I). The *S. typhimurium*-induced expression signatures of both the control and the *traf6* knock-down groups were consistent with the published results of Stockhammer *et al.* and include all genes previously validated by Q-PCR in that study (33). As shown by projection of the microarray data on a GenMapp of the TLR-signalling pathway, the *S. typhimurium*-induced gene sets of both groups included several TLR pathway components and downstream targets (Fig. 2, supplemental Table II). Furthermore, GO-analysis on the zebrafish gene identifiers by master-target testing on the level of Biological

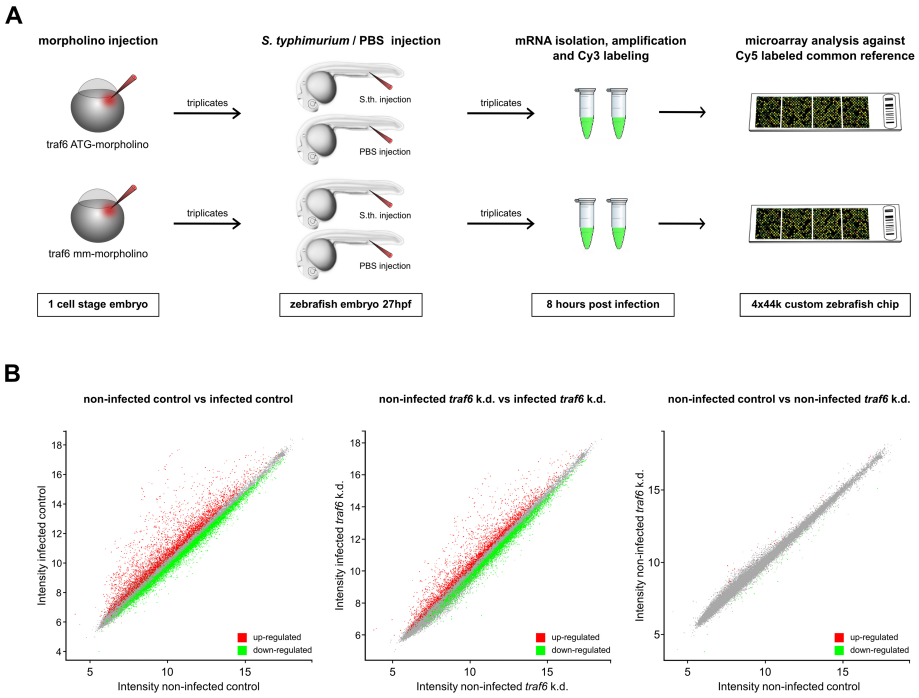
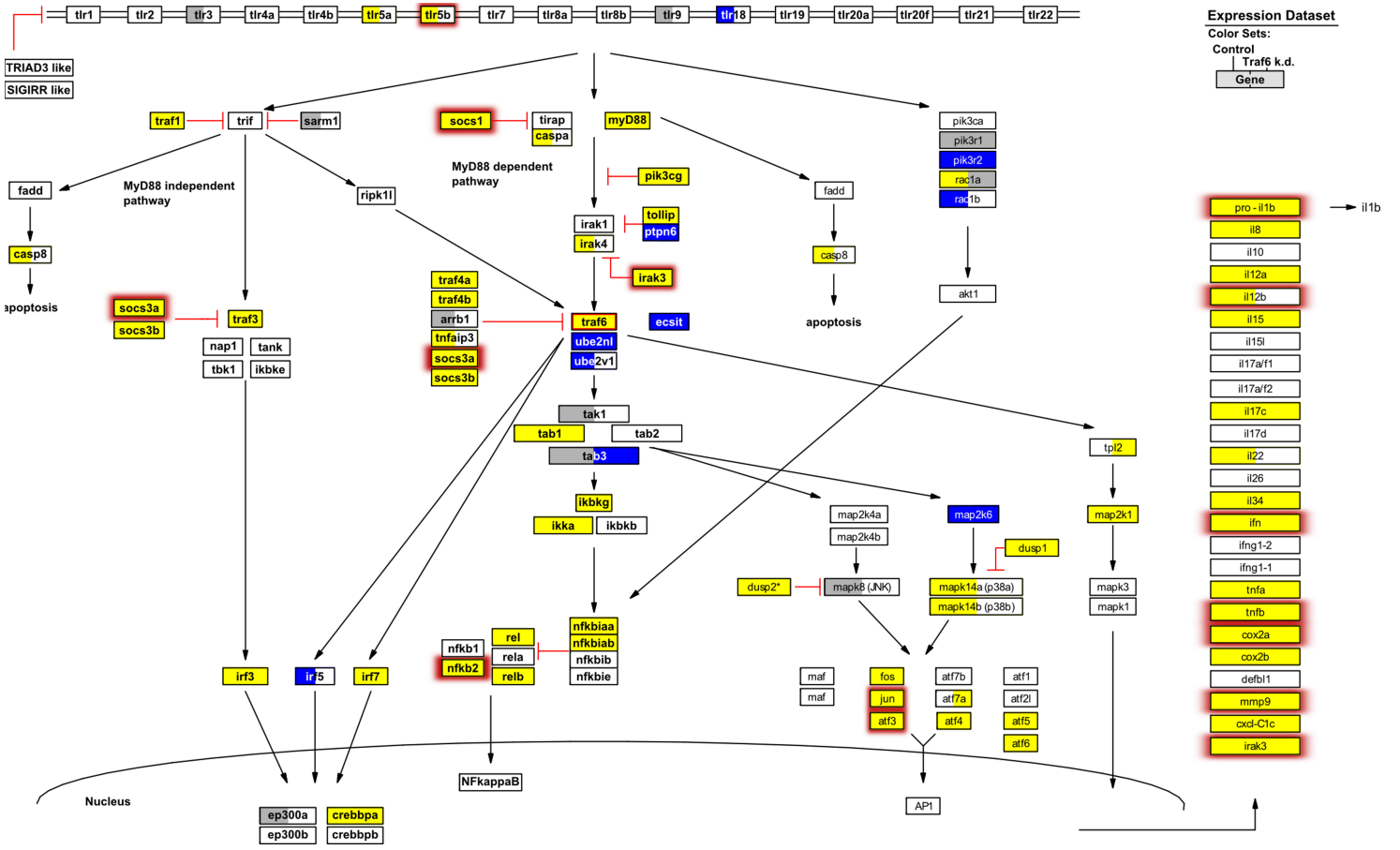


FIGURE 1. Schematic overview of the experimental setup (A) and scatter plot illustration of the transcriptional response of the various treatment groups (B). (A) Zebrafish embryos were either injected with a *traf6* ATG-morpholino or a 5bp mismatch (mm) morpholino at the first cell stage. At 27 hpf both groups were immune challenged by injection of 250 cfu of a *S. typhimurium* strain or mock injected with PBS. The transcriptional response was subsequently analysed at 8 hours post infection (hpi) using a common reference approach. The experiment was carried out in triplicate. (B) The scatter plots on the left side and in the middle show the transcriptional response upon *S. typhimurium* infection in the control (mm-morpholino) and *traf6* knock-down (k.d.) group respectively. The scatter plot on the right shows the response provoked by *traf6* knock-down independently of the infection.

Process revealed among others the GO-terms immune system process and response to stimulus as significantly ($p<0.05$) enriched in both groups (supplemental Table III). Interestingly, genes that were clustered under the GO-term reproduction were also significantly enriched in the up-regulated fraction. In contrast, only minor differences were provoked by *traf6* knock-down itself, indicating that our titration of the morpholino to avoid the developmental effect has been remarkably successful. In total 20 genes were up- and 35 genes were down-regulated by traf6 knock-down in the absence of infection ($p<0.05$, fold change $\leq$ -1.2 and $\geq$ 1.2) (Fig. 1B, supplemental Table IV). Among the group of up-regulated genes we identified genes such as *stc1 (stanniocalcin 1*, fc=2.62), a gene involved in $Ca2^{+}$ uptake in zebrafish, as well


tlr1
tlr2
tlr3
tlr4a
tlr4b
tlr5a
tlr5b
tlr7
tlr8a
tlr8b
tlr9
tlr18
tlr19
tlr20a
tlr20f
tlr21
tlr22
TRIAD3 like
SIGIRR like
traf1
trif
sarm1
socs1
tirap
caspa
myD88
pik3cg
fadd
MyD88 independent pathway
MyD88 dependent pathway
ripk1l
irak1
irak4
tollip
ptpn6
irak3
casp8
apoptosis
socs3a
socs3b
traf3
nap1
tank
tbk1
ikbke
traf4a
traf4b
arrb1
tnfaip3
socs3a
socs3b
traf6
ube2nl
ube2v1
ecsit
tak1
tab1
tab2
tab3
ikbkg
ikka
ikbkb
pik3ca
pik3r1
pik3r2
rac1a
rac1b
akt1
tpl2
map2k4a
map2k4b
map2k6
map2k1
dusp1
dusp2*
mapk8 (JNK)
mapk14a (p38a)
mapk14b (p38b)
mapk3
mapk1
irf3
irf5
irf7
nfkb1
nfkb2
rel
rela
relb
nfkbiaa
nfkbiab
nfkbib
nfkbie
maf
maf
fos
jun
atf3
atf7b
atf7a
atf4
atf1
atf2l
atf5
atf6
Nucleus
ep300a
ep300b
crebbpa
crebbpb
NFkappaB
AP1
Expression Dataset
Color Sets:
Control
Traf6 k.d.
Gene
pro - il1b
il1b
il8
il10
il12a
il12b
il15
il15l
il17a/f1
il17a/f2
il17c
il17d
il22
il26
il34
ifn
ifng1-2
ifng1-1
tnfa
tnfb
cox2a
cox2b
defb1
mmp9
cxcl-C1c
irak3

as *zgc:77734* (fc=2.57), showing similarities to the human DBI (diazepam binding inhibitor) gene. Examples of genes down-regulated by traf6 knock-down in the absence of infection are *or111-3* (fc=-3.8), a member of the fish odorant receptor family, and *he1a* (*hatching enzyme 1a*, fc=-2.68) as well as *rcv1* (*recoverin*, fc=-2.15) and *anterior gradient homolog 2* (*agr2*, fc=-1.89) (supplemental Table IV).

Statistical analysis of the effect of traf6 knock-down on the infection response

In order to find those genes that were specifically differentially regulated in the *traf6* knock-down group in comparison to the control group upon infection, the interaction term was analysed. Interaction is defined as the dependence of the effect of one factor (here gene knock-down by morpholino treatment) on the level of another factor (here immune challenge by infection). In terms of the analysis of variance (ANOVA) model, the interaction term measures the deviation from an expected value based on the additive combinations of the morpholino and infection means. A large positive deviation of this sort is called synergism, in which case the simultaneous morpholino and infection treatment gives rise to an expression level that deviates from the additive combination of the morpholino and infection treatment alone. A negative deviation, i.e. when the combined infection and morpholino application gives rise to a smaller effect than one could expect from the additive combination of the two effects separately, can be called interference. Synergy can be in the direction of overexpression or underexpression. In the former, a gene has a higher expression in the combined treatment than one could expect on the basis of the additive combination of the separate treatments. In the latter, a gene has an even lower expression in the combined treatment than one could expect on the basis of the additive combination of the separate treatments.

To specifically identify genes that were most highly dependent on Traf6 for their

FIGURE 2. GenMapp analysis of the immune response to *S. typhimurium* infection in the TLR pathway in control and traf6 knock-down embryos. Expression profiles of the control and *traf6* knock-down groups at the 8hpi time point (infected versus non infected, FDR corrected p-value <0.05 and fold changes ≥1.2 and ≤-1.2) were simultaneously mapped on the TLR pathway. Gene boxes are colour coded with the control morpholino treatment (Control) on the left and *traf6* knock-down (Traf6 k.d.) on the right side. Up-regulation is indicated in yellow, down-regulation in blue. The position of *traf6* in the pathway is highlighted by a red border of the gene box. Genes that failed the fold-change cut off are depicted in gray and genes that were not significantly regulated are represented in white. Highlighting of gene boxes by red shading indicates that the *S. typhimurium*-induced gene expression level was lower in *traf6* knock-down embryos than in control embryos, based on microarray expression trend analysis as well as RNAseq analysis. The pathway is based on knowledge of TLR signalling in mammalian species and it should be noted that most interactions remain to be experimentally confirmed in zebrafish.

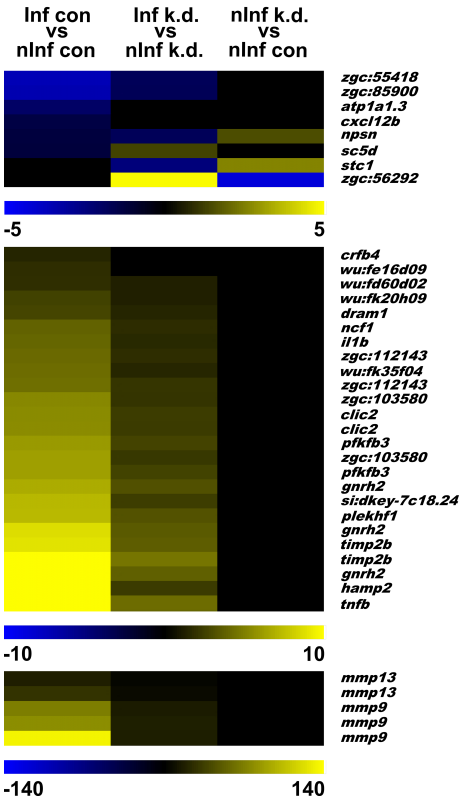


FIGURE 3. Heatmap showing the expression profiles of genes dependent on Traf6 during *S. typhimurium* infection as identified by interaction term analysis. Up-regulated expression is indicated in yellow, down-regulated expression in blue, and non-significantly changed expression in black. The level of up- or down-regulated expression is depicted by increasing brightness of yellow and blue colour, on three different scales for genes in different expression ranges. Note that several genes are represented by multiple probes on the microarray that showed significantly changed expression in the interaction term analysis. Gene descriptions and database identifiers are shown in Table 1. Column labels: infected control morpholino treated group (Inf con), noninfected control morpholino treated group (nInf con), infected *traf6* knock-down group (Inf k.d.), noninfected *traf6* knock-down group (nInf k.d.).

transcriptional response to a bacterial infection we examined all genes that were significant in the interaction term analysis with a stringent FDR-corrected p value smaller than 0.15 (Table I). The expression profiles of 28 identified genes corresponding to this criterion are shown in a heatmap (Fig.3). For the majority of these genes (20 out of 28) the *S. typhimurium*-induced gene expression levels were much lower in the *traf6* knock-down group than in the control group (Fig.3), indicating that the infection-mediated induction of these genes is dependent on *traf6*. Among these were several with a well established immune function like *hamp2*, *mmp9*, *mmp13*, *tnfb*, *il1b*, *ncf1*, *crfb4* and *zgc:103580*, the zebrafish ortholog of the human acute phase response gene serum Amyloid protein A. In addition to two members of the matrix metalloproteinase family (*mmp9* and *mmp13*), the group of 20 genes with a reduced infection response in *traf6* knock-down embryos also included the metalloproteinase inhibitor gene *timp2b* (*tissue inhibitor of metalloproteinase 2b*). This group also included *zgc:112143*, a gene homologous to the human *STEAP4* gene (also known as *TNFAIP9*, tumor necrosis factor alpha-induced protein 9), that we previously found to be induced with alternative splice forms during *Mycobacterium marinum* infection in adult zebrafish (41). On the other hand, the gene group showing a reduced infection response in *traf6* knock-down embryos also included genes that were pre-

Table I. Genes dependent on Traf6 during Salmonella infection*

Gene Symbol	Description	P-value	UniGene ID	ENS50 ID	K-means cluster	RNAseq
gnrh2	gonadotropin-releasing hormone 2	0.06	Dr.84757	ENSDARG00000044754	8	+
clic2	chloride intracellular channel 2	0.06	Dr.84618	ENSDARG00000010625	8	+
hamp2	hepcidin antimicrobial peptide 2	0.08	Dr.89447	ENSDARG00000053227	8	+
zgc:56292	similar to thyroid hormone receptor interactor 10	0.09	Dr.79814	ENSDARG00000028524	1	n.d.
pfkfb3	6-phosphofructo-2-kinase/fructose-2,6-biphosphatase 3	0.09	Dr.78868	ENSDARG00000001953	8	+
timp2b	tissue inhibitor of metalloproteinase 2b	0.09	Dr.81512	ENSDARG00000075261	8	+
dram1	DNA-damage regulated autophagy modulator 1	0.09	Dr.77501	ENSDARG00000045561	7	+
zgc:112143	STEAP family member 4 homolog	0.09	Dr.76505	ENSDARG00000055901	7	+
crfb4	cytokine receptor family member b4	0.11	Dr.14717	ENSDARG00000068711	7	+
wu:fk20h09	similar to pyruvate dehydrogenase complex, component X	0.11	Dr.140666		7	n.a.
zgc:103580	serum amyloid A1 homolog	0.11	Dr.13131	ENSDARG00000045999	7	+
cxcl12b	chemokine (C-X-C motif) ligand 12b	0.11	Dr.27045	ENSDARG00000055100	9	+
il1b	interleukin 1, beta	0.11	Dr.30443	ENSDARG00000005419	7	+
sc5d	sterol-C5-desaturase	0.11	Dr.119848	ENSDARG00000044642	4	-
mmp13	matrix metalloproteinase 13	0.12	Dr.81475	ENSDARG00000012395	7	+
mmp9	matrix metalloproteinase 9	0.12	Dr.76275	ENSDARG00000042816	8	+
tnfb	tumor necrosis factor b	0.12	Dr.94015	ENSDARG00000013598	8	+
wu:fk35f04	hypothetical protein containing S-100 domain	0.12	Dr.148687		7	n.a.
stc1	stanniocalcin 1	0.12	Dr.88421	ENSDARG00000058476	2	+
atp1a1a.3	ATPase, Na+/K+ transporting, alpha 1a.3 polypeptide	0.12	Dr.10713	ENSDARG00000039131	9	+
npsn	nephrosin	0.12	Dr.79156	ENSDARG00000010423	2	-
wu:fd60d02	transcribed locus	0.12	Dr.79931		8	n.a.
wu:fe16d09	transcribed locus	0.12	Dr.80006		7	n.a.
zgc:55418	similar to ABI gene family, member 3 (NESH) binding protein	0.12	Dr.14064	ENSDARG00000071095	9	+
zgc:85900	olfactomedin 2 like	0.14	Dr.85843	ENSDARG00000007015	9	+
ncf1	neutrophil cytosolic factor 1	0.14	Dr.2973	ENSDARG00000033735	8	+
plekhf1	pleckstrin homology domain containing, family F	0.14	Dr.80998	ENSDARG00000027852	8	+
si:dkey-7c18.24	hypotetical protein	0.14	Dr.104301	ENSDARG00000041433	7	+

* Listed genes were identified by interaction term analysis. Significance cut off values were set to p<0.15 (FDR). All genes indicated as + were confirmed by RNAseq analysis, whereas genes indicated as – were not. Four genes indicated as not applicable (n.a.) lacked an ENSDART identifier and could therefore not be verified by RNAseq analysis. For one gene indicated as not detectable (n.d.) not enough RNA sequence reads were obtained (< 1 mapped reads per million total reads). K-means cluster identifiers refer to Figure 5.

viously not linked to immune function or TRAF6 signalling like *plekhf1* (*pleckstrin homology domain containing, family F*), *clic2* (*chloride intracellular channel 2*), *pfkfb3* (*6-phosphofructo-2-kinase/fructose-2,6-biphosphatase 3*), *gnrh2* (*gonadotropin-releasing hormone 2*), and *dram1* (DNA-damage regulated autophagy modulator 1).

In addition to the 20 genes showing a reduced infection-mediated induction in *traf6* knock-down embryos, the statistical analysis also identified 4 genes (*cxcl12b*, *atp1a1a.3*, *zgc:55418* and *zgc:85900*) that appeared to be dependent on Traf6 for their negative regulation during infection. These genes were down-regulated by infection in control embryos but not or to a lower extent in *traf6* knock-down embryos (Fig.3, Table I). Four other genes showed a more complex dependency on Traf6, with opposite regulation in knock-down embryos and controls (*sc5d*) or with expression levels affected both in the absence and presence of infection (*zgc:56292*, *stc1*, *npsn*).

In conclusion, based on the interaction term analysis we identified genes that are dependent on Traf6 activity for their positive or negative regulation during *S. typhimurium* infection of zebrafish embryos.

Confirmation of Traf6-dependent genes by RNA deep sequencing

In order to confirm the microarray data we subjected the pooled RNA samples of

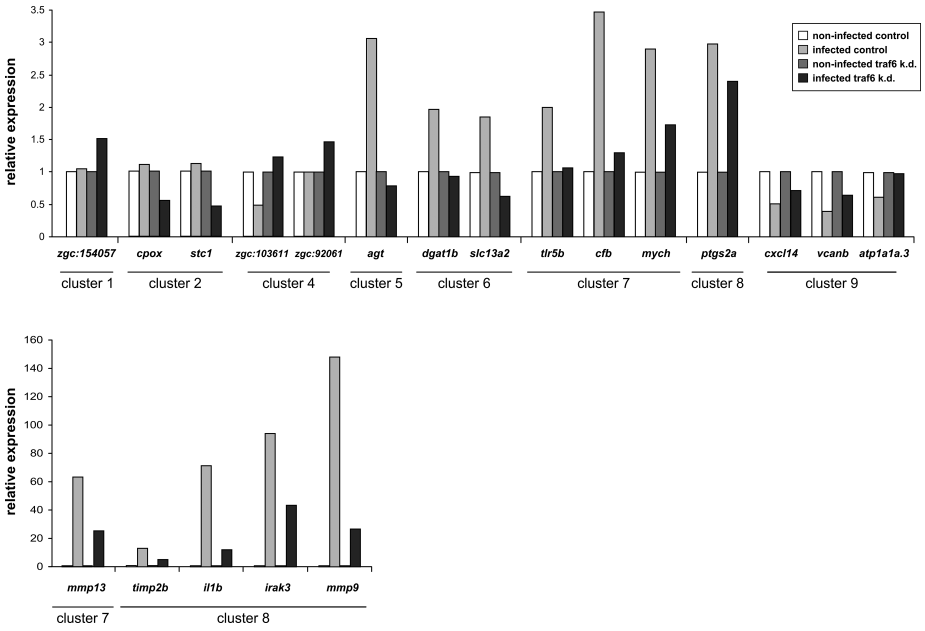


FIGURE 4. RNAseq validation of microarray results. RNAseq data are shown for representative examples of genes for which the microarray expression trend was confirmed by RNAseq read counts of the four treatment groups (non-infected control, infected control, non-infected *traf6* knock-down, infected *traf6* knock-down). Bars indicate the relative expression of the different treatment groups based on the number of mapped sequence reads per million of total reads. For every gene the value of the uninfected control group is set to 1 and the expression level of the gene in the treatment group is calculated relative to the control value. Two different scales are used for genes in different ranges of induction level upon *S. typhimurium* infection. Cluster numbers refer to the K-means clustering in Fig.5. The complete overview of genes for which the microarray expression trend was confirmed by RNAseq is given in supplemental Table VI

the three biological replicates of each treatment group to Illumina RNA sequencing (RNAseq). Approximately 15 million reads were obtained for each of the four RNAseq libraries (control, control infected, *traf6* knock-down, *traf6* knock-down infected) and approximately 10 million reads per library could be mapped to the Ensembl transcript database based on the Zv8 genome sequence. Next we compared the sequence read counts (mapped reads per million total reads) between the treatment groups (supplemental Table VI). For 21 of the 28 genes that were significant in the interaction term analysis, we found that the RNAseq data confirmed the microarray results. This included 16 of the 20 genes positively dependent on Traf6 during infection and all 4 of the genes negatively dependent on Traf6 during infection. Representative examples of these positively (*il1b*, *mmp9*, *mmp13*, *timp2b*) and negatively (*atp1a1a.3*, *cxcl12b*) regulated genes are shown in Fig. 4. In five cases the micro-

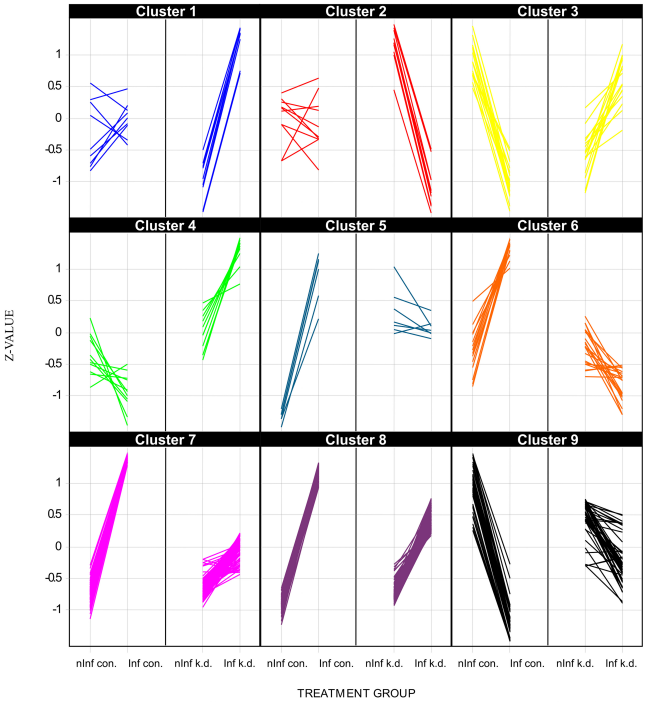


FIGURE 5. Trend analysis of the interaction term by K-means clustering. For a broader analysis of the effects of *traf6* knock-down all retrieved probes with an FDR-corrected p-value lower than 0.4 were clustered using the K-means cluster function in SPOTFIRE. All probes lacking a valid annotation were excluded from the analysis resulting in a final set of 376 probes. The identified trend in the control group is illustrated on the left side of each cluster expressed by the z-score of each probe between the noninfected (nInf con) and the infected (Inf con) control morpholino treated group. On the right side the corresponding trend of the noninfected (nInf k.d.) versus the infected (Inf k.d.) group under the *traf6* knock-down condition is illustrated. All probes that contribute to the distinct clusters are listed in supplemental table VI.

array data could not be validated by RNAseq because transcripts for these genes were not present in the Ensembl database or not enough RNAseq reads were obtained (< 1 mapped reads per million total reads). In only two cases, the RNAseq data did not confirm the microarray data. Both these cases (*sc5d*, *npsn*) were genes showing a complex dependency on Traf6 as described above. In conclusion, RNAseq analysis validated the interaction term analysis for most of the genes whose induction or repression during *S. typhimurium* infection was found to be dependent on Traf6.

Expression trend analysis

Since the knock-down conditions of Traf6 can be considered to be incomplete, we also wanted a broader overview of the effects of *traf6* knock-down in an expression

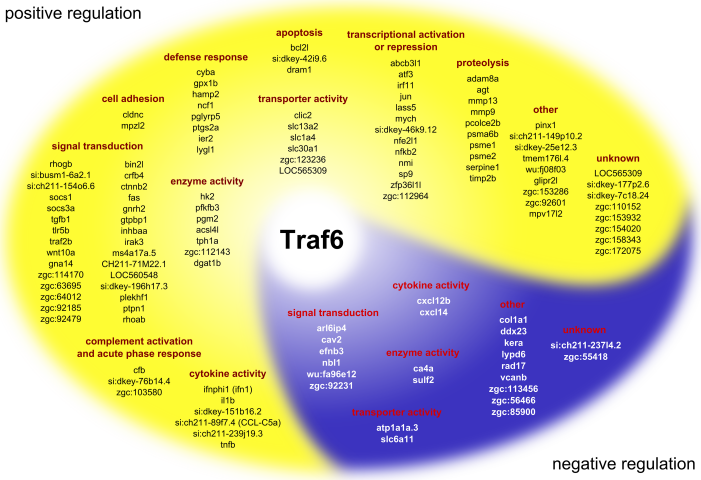


FIGURE 6. Schematic overview of the Traf6-dependent gene groups during *S. typhimurium* infection. Genes that are dependent on Traf6 for their induction during infection (positive regulation) are in the yellow area of the scheme and genes that depend on Traf6 for their repression (negative regulation) during infection are in the blue area. Genes positively regulated by Traf6 belong to clusters 5-8 in the microarray expression trend analysis in Figure 5, and genes negatively regulated by Traf6 belong to cluster 9. The microarray expression trend of all genes in the scheme was in agreement with RNAseq data.

trend analysis of the microarray data using a less stringent criterion: a FDR-corrected p-value of smaller than 0.4 retrieved from the interaction term. First, we analysed these probes by enrichment analysis based on Gene Ontology (GO) annotation. A significant enrichment was demonstrated for genes clustering under the biological process GO-terms immune system process ($p<0.05$), response to stimulus ($p<0.05$), and multi-organism process ($p<0.05$), demonstrating a clear effect of *traf6* knock-down on the immune response to *S. typhimurium* (supplemental Table V).

Following up the GO-term analysis, we subjected the selected probes to K-means cluster analysis, allowing for the visual discrimination between synergism and interference of the interaction term. Probes missing a valid annotation were excluded from the analysis. The remaining 376 probes, representing 233 genes, were categorized into 9 clusters (Fig. 5, supplemental table V). The microarray expression trends of 246 of these probes, representing 146 genes, were confirmed by the RNAseq data (supplemental table VI, with representative examples in Fig.4), indicating the validity of these results despite the use of a less stringent criterion in the interaction term analysis.

Genes indicated by clusters 1 and 2 were respectively up- or down-regulated upon infection under the *traf6* knock-down condition, whereas only minor and in the ma-

jority not significant changes were observed in the control group. These two clusters contain such genes as *zgc:1154057* (*transcriptional adaptor 2-like*) in cluster 1, and *cpox (coproporphyrinogen oxidase)* and *stc1* (*stanniocalcin 1*) in cluster 2 (supplemental Table VI, Fig. 4). Clusters 3 and 4 show an opposing trend in gene regulation upon infection between the control and *traf6* knock-down groups. Cluster 3 was not considered further, since regulation of genes in this cluster was generally not confirmed by the RNAseq data. Genes in cluster 4 were consistently up-regulated in the *traf6* knock-down group upon infection, while down-regulated or non-responsive in the control group, with examples such as *zgc:92061* (similar to keratin 17) and *tm7sf2* (transmembrane 7 superfamily member 2) (supplemental Table VI, Fig. 4). A common trend in gene regulation is observed in clusters 5 to 8, where infection leads to a consistent up-regulation in the control groups and weaker up-regulation (clusters 7 and 8) or unchanged expression (clusters 5 and 6) in the *traf6* knock-down groups. Finally, cluster 9 consists of those genes that were strongly down-regulated by infection in the controls, while showing a weaker or no down-regulation in *traf6* knock-down embryos.

For further analysis we concentrated on the genes that were dependent on Traf6 for their induction (clusters 5-8) or repression (cluster 9) during *S. typhimurium* infection. From the total of 124 genes with Traf6-dependent induction and 32 genes with Traf6-dependent repression, the microarray expression trend of 105 and 22 genes, respectively, could be confirmed by the RNAseq data (supplemental table VI, with representative examples in Fig.4). We categorized these Traf6-dependent genes into functional groups based on gene ontology terms and using references to gene function of their mammalian homologs in the NCBI Entrez Gene database (Fig.6). A notable fraction of the Traf6-dependent infection-induced genes play a well established role in the immune response, for example as cytokines or interferons (e.g. *il1b*, *tnfb*, *CCL-C5a*, *ifnphi1*), in complement activation or the acute phase response (e.g. *cfb*, *zgc:103580*), in prostaglandin biosynthesis (*pgts2a*), or in microbial killing (e.g. *ncf1*, *hamp2*). Many of the Traf6-dependent infection-induced genes are involved in signal transduction and transcriptional activation or repression. This includes the *tlr5b* gene, important for the response to flagellin, negative regulators of TLR-signaling (*irak3*, *socs3a*) as well as transcription factors (*atf3*, *jun*, *nfkb2*) activated by the TLR pathway (Fig.2, Fig.6). Other examples of Traf6-dependent signal transduction genes include *fas* (*TNF receptor superfamily, member 6*), *tgfb1* (*transforming growth factor, beta 1*), *ctnnb2* (beta-catenin2), *wnt10*a, and small gtpase genes (*rhogb*, *rhoab*). In addition to the above-mentioned Traf6-dependent members of the matrix metalloproteinase family (*mmp9* and *mmp13*) and metalloproteinase inhibitor gene (*timp2b*), the induction of several other genes involved in proteolysis was Traf6-dependent (e.g. *adam8a*, *agt*, *psme1/2*, *serpine1*). Finally, Traf6-dependent infection-induced gene groups were linked to apoptosis (e.g. *bcl2l*, *dram1*), cell adhesion (e.g. *cldnc*), transporter activity (e.g. *clic2*, *slc13a2*), or encoded enzymes involved in metabolic processes (e.g. *acsl4l*, *pfkfb3*, *dgat1b*) (Fig. 6).

Not only the infection-induced gene groups, but also the gene groups that were dependent on Traf6 for their repression during infection included genes for cytokines (*cxcl12b*, *cxcl14*), transporters (*atp1a1a.3*, *slc56a11*), enzymes (*ca4a*, *sulf2*) and signal transduction proteins (e.g. *efnb3*, *nbl1*). In addition, several other genes, for example *vcanb*, encoding a member of the hyaluronan (HA)-binding proteoglycans, were repressed by infection in a Traf6-dependent manner (Fig.6).

Taken together, based on the expression trend analysis of the microarray data and validation by RNAseq, we conclude that Traf6 has a dynamic role as a positive and negative regulator of genes responsive to *S. typhimurium* infection in zebrafish embryos, including a large set of well known anti-microbial and inflammatory genes as well as genes not previously linked to the immune response or to Traf6 function.

Discussion

The fact that TRAF6 is a key player at the cross-roads of development and immunity makes the analysis of its *in vivo* molecular function a great challenge (13, 14, 47). Severe developmental defects and early lethality caused by *Traf6* deficiency in knock-out mice interfere with analyses of the immune response. In this study we have developed a new approach to analyse the function of Traf6 in a zebrafish acute infectious disease model. In this approach the effect of a Traf6 translation-blocking morpholino was titrated in such a way that developmental defects were brought back to an identifiable non-dominant factor in the transcriptome analyses. The results show that, even under partial knock-down conditions, it was possible to identify a gene set (Table I) whose responsiveness during *S. typhimurium* infection is highly dependent on Traf6. In addition, expression trend analysis identified nine clusters of genes with characteristic transcription response profiles, demonstrating that Traf6 has a dynamic role as a positive and negative regulator. We have confirmed the data from microarray experiments with whole transcriptome shotgun sequencing (RNA-seq). This is one of the first times that this novel deep sequencing approach has been used for quantitative transcriptome profiling (48, 49). The results show that this complementary technique gives good support for the identified Traf6-dependent infection-responsive gene set, confirming Traf6-dependent induction of 105 genes and Traf6-dependent repression of 22 genes during *S. typhimurium* infection. In addition, especially since this is the first time that RNA-seq technology is used for infectious disease studies, these data represent a great wealth of disease-induced transcript information that will be of great value for future studies.

Among the genes that are highly dependent on Traf6 for their induction in response to *S. typhimurium* infection a subset of well known immune system-associated genes such as *il1b*, *mmp9, mmp13*, *hamp2,* and *tnfb* was found, demonstrating a specific *in vivo* effect of Traf6 on the innate immune response. Previously we could show that *il1b* and *mmp9* are downstream targets of the zebrafish TLR-pathway. The

dependency of the expression of these genes on Traf6 is consistent with this study and supports the specificity of the morpholino knock-down (33). It was shown in mouse that MMP-9 can also be activated upon RANKL stimulation via TRAF6, p38 and ERK1/2 (50). RANKL is a member of the tumor necrosis factor (ligand) superfamily and is an important activator of osteoclasts, cells involved in bone resorption. Although osteoclasts only develop in zebrafish larvae after several weeks it is not unlikely that these pathways are conserved during embryonic development (51). Several of the other Traf6-dependent genes that are linked to the TLR/IL1R-pathway are also corroborated in other model systems. It was shown that the regulation of hepcidin (HAMP1) is facilitated via the TLR-pathway in mice-derived macrophages upon bacterial infection (52). Another example shown in mouse is that activation of MMP-13 through the IL1-signalling pathway was strongly impaired after *traf6* knock-down (53). Interestingly, also the induction of a tissue inhibitor of metalloproteinase function, Timp2b was dependent of Traf6 during zebrafish embryo infection. The expression of *timp2b* was also found to be induced during mycobacterium infection in zebrafish embryos, which was suggested to function as a compensatory response to increased *mmp9* activity (54). Furthermore, human TIMP2 has been linked to cancer progression and has been found to be a marker for dendritic cell response to HIV infection (55). The known immune response genes that we showed to be induced in a Traf6-dependent manner also included components of the TLR-signalling pathway, such as *tlr5b* and *irak3*. It remains a question whether the regulation of the above mentioned genes is mediated via the TLR-pathway itself or via another Traf6-directed pathway. For instance Salmonella infection also regulated *tgfb1* in the TGF-beta pathway in a Traf6-dependent manner. Therefore, the poorly understood interrelatedness of the TGF-beta and TLR signaling pathways remains an important subject for future investigations.

Other Traf6-dependent infection induced genes, such as *dram1* (*DNA-damage regulated autophagy modulator 1*) and *gnrh2* (*gonadotropin releasing hormone 2)*, have until know not been directly associated with TRAF6 function. Human homologs of *dram1* are activated by p53 as a requirement to induce autophagy and damage-induced programmed cell death (56, 57). As recently highlighted in several studies, the autophagy pathway is also important for the control of intracellular pathogens and therefore the link with Traf6 function is relevant for Salmonella infection (58, 59). In the zebrafish embryo *gnrh2* has been linked to central nervous system development (60). However, next to the well established function of GnRH in mammalian reproduction, an immune regulatory function was suggested as well (61, 62). In fact, Tanriverdi et al. have discussed that immune and reproductive function are intrinsically linked in a so-called hypothalamic-pitutary-gonadal axis (60). Recently it was shown that GnRH treatment of mice macrophages *in vitro* leads to elevated Ca2+ uptake and an impaired generation of NO and suppression of iNOS after LPS/INF-γ treatment (63). A function of Traf6 in Ca2+ homeostasis is suggested by the fact that there is an interference effect of *traf6* knock-down and *S. typhimurium* in-

fection on *stanniocalcin* (*stc1*) regulation. The mammalian homolog of *stanniocalcin* is involved in inhibition of transendothelial migration of human macrophages and T-lymphocytes (64). In addition *stanniocalcin* was also shown to stimulate osteoblast differentiation in rat calvaria cells (65). In a broader sense, Traf6 is probably involved in other ion transport processes. For instance the induction of *chloride intracellular channel 2* (*clic2*) by Salmonella infection is highly dependent of Traf6 function. Furthermore, the negative regulation of *ATPase, Na+/K+ transporting, alpha 1a.3 polypeptide* (*atp1a1a.3*) during *S. typhimurium* infection is blocked by *traf6* knockdown.

In addition to the annotated genes we also have identified Traf6 targets of which no annotation could be derived either for zebrafish, mouse or human orthologs (Supplemental Tab. VI, Fig. 6). Even domain searches could not identify a possible function. Since the expression levels of some of these genes are both strongly affected by Salmonella induction at early time points (33) and are strongly dependent on Traf6 function, the further study of the function of these genes in the vertebrate immune system is of great interest.

Interestingly, we find the induction of several metabolic genes to be dependent on Traf6 function during Salmonella infection in one-day old embryos, suggesting a possible role in the immune response. For example, expression of *6-phosphofructo-2-kinase* (*pfkfb3*), *hexokinase 2* (*hk2*), and *diacylglycerol O-acyltransferase homolog 1b* (*dgat1b*) were induced during infection in a Traf6-dependent manner. Furthermore, the induction of an ortholog of STEAP4 (*zgc:112143*), which has been shown to play a role in integration of inflammatory and metabolic responses, is also dependent on Traf6 (66). We previously found this gene also to be induced by mycobacterium infection in zebrafish (41). The expression trend analysis shows that *pfkb3*, *hk2* and *zgc:111243* cluster together with several of the above mentioned inflammatory genes such as *mmp9*, *mmp13*, *il1b* and *tnfb* (Fig. 5). Other metabolic functions might also play a role during infection since our analyses only show the minimal contribution of Traf6 to immunity. This is because functions that play an equally important role in immunity and development cannot confidently be analyzed in our method since we have titrated down the effect of the morpholino treatment to have a low effect on development.

It does not come as a surprise that after knock-down of Traf6 there is still a strong immune response to Salmonella infection, not only because the knock-down was incomplete but also because it can be expected that there are innate immune responses to Salmonella infection that are independent of Traf6, for example the chemotactic response to the bacterial infection site via G-protein coupled receptors. Furthermore, also within the TLR-dependent pathway there are possible signaling routes that might not be dependent on Traf6. For instance, the pathway of TLR4 signaling can lead to TRAF3 activation and subsequent stimulation of the interferon pathway via the IRF3 protein. It would therefore also be interesting to use our method to analyze other key factors such as TRAF3 and partners immediately downstream of the TRAF

family proteins such as TBK1 and TAB1/2/3. Such studies could show whether any of these factors might be partially redundant during the innate immune response.

Materials and Methods

Bacterial strains and growth conditions

S. typhimurium wild type (wt) strain SL1027, containing the DsRed expression vector pGMDs3, was used for the infection of zebrafish embryos (22). Bacteria were freshly grown overnight on LB agar plates supplemented with 100µg/ml carbenicillin and resuspended in phosphate-buffered saline (PBS) prior to injection.

Zebrafish husbandry

Zebrafish were handled in compliance with the local animal welfare regulations and maintained according to standard protocols (http://ZFIN.org). Embryos were grown at 28,5 -30 °C in egg water (60µg/ml Instant Ocean sea salts). For the duration of bacterial injections embryos were kept under anaesthesia in egg water containing 0.02% buffered 3-aminobenzoic acid ethyl ester (tricaine, Sigma).

Morpholino knock-down experiments

For morpholino knockdown experiments, morpholino oligonucleotides (Gene Tools) were diluted to desired concentrations in 1x Danieu's buffer [58 mM NaCl, 0.7 mM KCl, 0.4 mM $MgSO_4$, 0.6 mM $Ca(NO_3)2$, 5.0 mM HEPES; pH 7.6] containing 1% Phenol red (Sigma). To block translation of *traf6* mRNA we injected 1 nl (1 mM) per embryo of a morpholino specifically targeting the 5' UTR region including the start codon of *traf6* (5' GCCATATTGGCTCGGTACGGCCTC). To control for aspecific morpholino effects we used a 5 bp mismatch morpholino (1mM, 5' GCaATATTcGCTaGGTACaGCgTC).

Experimental design of the infection study

All infection experiments were performed using mixed egg clutches of ABxTL strain zebrafish. Embryos injected with the *traf6* morpholino and the 5bp mismatch morpholino were staged at 27 hours post fertilization (hpf) by morphological criteria and approximately 250 cfu of DsRed expressing *S. typhimurium* wild type bacteria were injected into the caudal vein close to the urogenital opening as described in Stockhammer et al. (33). As a control an equal volume of PBS was likewise injected. Pools of 20-40 infected and control embryos were collected 8 hours post infection (hpi). For the microarray analysis, the whole procedure was performed in triplicate on separate days.

RNA extraction

Embryos for RNA isolation were snap frozen in liquid nitrogen and subsequently

stored at -80°C. Total RNA from each sample was extracted using TRIZOL followed by a cleanup procedure with Rneasy Mini kit (Qiagen, Valencia, CA, USA), and a DNase treatment with RNase-Free DNase Set (Qiagen Valencia, CA, USA)). The RNA concentration was measured on a nanodrop ND-100 (NanoDrop Technologies Inc., Wilmington, DE, USA) and RNA quality was checked on an Agilent 2100 BioAnalyzer (Agilent Technologies, Palo Alto, CA, USA). Total RNA samples with an RNA integrity number (RIN) > 7 were used for further analysis. These assays were performed according to the manufacturer's protocols.

Illumina RNA sequencing

The total RNA of the three biological samples of each treatment group, previously used for the microarray analysis, was pooled using equal amounts of RNA. To perform transcriptome sequencing, RNAseq libraries were made from 4 µg of each sample, using the Illumina mRNA-Seq Sample Preparation Kit according to the manufacturer's instructions (Illumina, Inc. San Diego). An amount of 4 pmol of each library was sequenced in one lane with a read length of 51 nt on an Illumina GAII instrument (Illumina, Inc. San Diego). The raw data were deposited in the GEO database under submission number GSE21024. Sequence reads were mapped to Ensembl transcripts (Zv8. 56) using the CLCbio Genomics Workbench version 3.6.5 (www.clcbio.com).

Microarray design and hybridization

A custom zebrafish genome 4 x 44 K microarray (Agilent) containing slight modifications in regard to a previous described design was used (accession no. GPL10042 in the GEO database) (33). In short, a total of 600 new features based on deep sequencing results were added to the existing chip design resulting in 45219 features, including 43801 well-characterized genes and 1418 controls (41). The probes of the custom manufactured Agilent array have been reannotated by mapping all probes to the Unigene 114 (unique) sequences and the Ensembl 50 and Vega 32 transcripts using the BLAST algorithm. Technical handling of the microarrays was performed at the MicroArray Department (MAD) of the University of Amsterdam (Amsterdam, The Netherlands). In short, cyanine 3 and cyanine 5 labeled cRNA samples were prepared as described in the Amino allyl message AMP II manual (Ambion) using 0.5 ug purified total RNA as template for the reaction. Test samples were labelled with Cy3 and the common reference was labeled with Cy5. The common reference was composed by combining 1 ug of cRNA from each sample and chemical coupling of this pool with Cy5. Hybridization of 825 ng of Cy3 labeled test sample and 825 ng of Cy5 labeled common reference was performed overnight according to Agilent protocols at 65° C. Images of the arrays were acquired using an Agilent DNA MicroArray Scanner (Agilent Technologies, Palo Alto, CA, USA).

Data extraction and statistical analysis

Spot intensities were quantified with Feature Extraction 9.5.1 (Agilent) as the foreground median signal intensity. Further processing of the data was performed using R (version 2.5.0), the Bioconductor MAANOVA package (version 1.6.0) (42) and Spotfire (version 7.3).

All slides were subjected to a set of quality control checks, i.e. visual inspection of the scans, examining the consistency among the replicated samples by principal components analysis, testing against criteria for signal to noise ratios, testing for consistent performance of the labeling dyes, and visual inspection of pre- and post-normalized data with box plots and RI plots.

The data set concerned a two-factorial Latin square design, with the factors 'Morpholino treatment' (2 levels: treated and not treated) and 'Infection' (2 levels: treated and not treated). The design was completely balanced with 3 replicates each, so the experiment involved 12 observations per gene.

After log2 transformation the data was normalized by a global LOWESS smoothing procedure. The data was analyzed using a two-stage mixed analysis of variance (ANOVA) model (43). First, array, dye, and array-by-dye effects were modeled globally. Next, the residuals from this first model were fed into a gene-by-gene model in which we took 'Group', 'Array', and 'Dye' as factors of which 'Array' was modeled as random factor. 'Group' is defined by each unique Morpholino and Infection treatment combination. These residuals can be considered normalized expression values and used in the graphs to depict gene expression profiles. All changes were calculated from the model coefficients. For hypothesis testing a permutation based Fs test, which allows relaxation of the assumption that the data are normally distributed, was used (2,000 permutations). The significance of the differences between factor level means was tested using contrasts. To account for multiple testing, all P values were adjusted to represent a false discovery rate using the method of Benjamini and Hochberg (44). The raw data were submitted to the GEO database under accession number GSE20310.

Gene Ontology, pathway and cluster analysis

K-means clustering was performed using Spotfire (version 7.3) Cluster initialization was set to data centroid based search and similarity measure was set to Euclidian distance. Analysis was performed on the probes retrieved by interaction term analysis with a p-value lower than or equal to 0.4. All identifiers lacking a valid annotation were excluded from the analysis leading to a dataset of 376 probes.

Gene ontology (GO) analysis was performed using the GeneTools eGOn v2.0 web-based gene ontology analysis software (www.genetools.microarray.ntnu.no) (45). Master-target analysis was performed at the level of Unigene clusters (UniGene build #105). To test for enrichment or under representation at the level of GO criteria for Biological Process (BP) we compared the UniGene identifiers retrieved from

our analysis (targets) to all identifiers present on the chip (master). Identifiers tested are listed in supplemental Table I and IV for those genes that were regulated after infection in the control and *traf6* knock-down group as well as due to *traf6* knock-down alone. All identifiers that were retrieved from the interaction term analysis are listed in supplemental Table VI.

Pathway analysis was performed using the GenMapp software package (www.genmap.org) (46). Analysis was done at the level of UniGene clusters (*D.rerio* UniGene build #114). Significance cut-off was set at 1.2 fold change at P <0.05. Zebrafish homologs of the genes contributing to the TLR pathway were identified by either searching the ZFIN (http://zfin.org) database or the Gene and HomoloGene database of NCBI (http://www.ncbi.nlm.nih.gov) (supplemental Table II).

The following link has been created to allow review of record GSE21024:
http://www.ncbi.nlm.nih.gov/geo/query/acc.cgi?token=jhwzvcicksqqabm&acc=GSE21024
The following link has been created to allow review of record GSE20310:
http://www.ncbi.nlm.nih.gov/geo/query/acc.cgi?token=rxcjnswseookuvk&acc=GSE20310

Acknowledgments

We are grateful to Christiaan Henkel and Hans Jansen (ZFscreens B.V., the Netherlands) for help with RNAseq analysis and thank our group members for helpful discussions. We are also grateful to Davy de Witt, Ulrike Nehrdich and Karen Bosma for fish maintenance. This work was financially supported by the European Commission 6th Framework Programs ZF-TOOLS (LSHG-CT-2006-037220)

Supplementary Data

Supplementary tables can be found online at: http://www.mediafire.com/?sharekey=686efof919604e919bf8d6369220dcab43aecfabc95fc71da7b01fe6e4055ae3

References

1. Mogensen, T. H. 2009. Pathogen recognition and inflammatory signaling in innate immune defenses. *Clin Microbiol Rev* 22:240-273, Table of Contents.
2. Abbott, D. W., Y. Yang, J. E. Hutti, S. Madhavarapu, M. A. Kelliher, and L. C. Cantley. 2007. Coordinated regulation of Toll-like receptor and NOD2 signaling by K63-linked polyubiquitin chains. *Mol Cell Biol* 27:6012-6025.
3. Kobayashi, T., M. C. Walsh, and Y. Choi. 2004. The role of TRAF6 in signal transduction and the immune response. *Microbes Infect* 6:1333-1338.
4. Sorrentino, A., N. Thakur, S. Grimsby, A. Marcusson, V. von Bulow, N. Schuster, S. Zhang, C. H. Heldin, and M. Landstrom. 2008. The type I TGF-beta receptor engages TRAF6 to activate TAK1 in a receptor kinase-independent manner. *Nat Cell Biol* 10:1199-1207.
5. Yamashita, M., K. Fatyol, C. Jin, X. Wang, Z. Liu, and Y. E. Zhang. 2008. TRAF6 mediates Smad-independent activation of JNK and p38 by TGF-beta. *Mol Cell* 31:918-924.
6. Cao, Z., J. Xiong, M. Takeuchi, T. Kurama, and D. V. Goeddel. 1996. TRAF6 is a signal transducer for interleukin-1. *Nature* 383:443-446.
7. Ishida, T., S. Mizushima, S. Azuma, N. Kobayashi, T. Tojo, K. Suzuki, S. Aizawa, T. Watanabe, G. Mosialos, E. Kieff, T. Yamamoto, and J. Inoue. 1996. Identification of TRAF6, a novel tumor necrosis factor receptor-associated factor protein that mediates signaling from an amino-terminal domain of the CD40 cytoplasmic region. *J Biol Chem* 271:28745-28748.
8. Galibert, L., M. E. Tometsko, D. M. Anderson, D. Cosman, and W. C. Dougall. 1998. The involvement of multiple tumor necrosis factor receptor (TNFR)-associated factors in the signaling mechanisms of receptor activator of NF-kappaB, a member of the TNFR superfamily. *J Biol Chem* 273:34120-34127.
9. Muzio, M., G. Natoli, S. Saccani, M. Levrero, and A. Mantovani. 1998. The human toll signaling pathway: divergence of nuclear factor kappaB and JNK/SAPK activation upstream of tumor necrosis factor receptor-associated factor 6 (TRAF6). *J Exp Med* 187:2097-2101.
10. Wong, B. R., R. Josien, S. Y. Lee, M. Vologodskaia, R. M. Steinman, and Y. Choi. 1998. The TRAF family of signal transducers mediates NF-kappaB activation by the TRANCE receptor. *J Biol Chem* 273:28355-28359.
11. Darnay, B. G., J. Ni, P. A. Moore, and B. B. Aggarwal. 1999. Activation of NF-kappaB by RANK requires tumor necrosis factor receptor-associated factor (TRAF) 6 and NF-kappaB-inducing kinase. Identification of a novel TRAF6 interaction motif. *J Biol Chem* 274:7724-7731.
12. Tsukamoto, N., N. Kobayashi, S. Azuma, T. Yamamoto, and J. Inoue. 1999. Two differently regulated nuclear factor kappaB activation pathways triggered by the cytoplasmic tail of CD40. *Proc Natl Acad Sci U S A* 96:1234-1239.
13. Lomaga, M. A., W. C. Yeh, I. Sarosi, G. S. Duncan, C. Furlonger, A. Ho, S. Morony, C. Capparelli, G. Van, S. Kaufman, A. van der Heiden, A. Itie, A. Wakeham, W. Khoo, T. Sasaki, Z. Cao, J. M. Penninger, C. J. Paige, D. L. Lacey, C. R. Dunstan, W. J. Boyle, D. V. Goeddel, and T. W. Mak. 1999. TRAF6 deficiency results in osteopetrosis and defective interleukin-1, CD40, and LPS signaling. *Genes Dev* 13:1015-1024.
14. Naito, A., S. Azuma, S. Tanaka, T. Miyazaki, S. Takaki, K. Takatsu, K. Nakao, K. Nakamura, M. Katsuki, T. Yamamoto, and J. Inoue. 1999. Severe osteopetrosis, defective interleukin-1 signalling and lymph node organogenesis in TRAF6-deficient mice. *Genes Cells* 4:353-362.
15. Kobayashi, T., P. T. Walsh, M. C. Walsh, K. M. Speirs, E. Chiffoleau, C. G. King, W. W. Hancock, J. H. Caamano, C. A. Hunter, P. Scott, L. A. Turka, and Y. Choi. 2003. TRAF6 is a critical factor for dendritic cell maturation and development. *Immunity* 19:353-363.
16. Deng, L., C. Wang, E. Spencer, L. Yang, A. Braun, J. You, C. Slaughter, C. Pickart, and Z. J. Chen. 2000. Activation of the IkappaB kinase complex by TRAF6 requires a dimeric ubiquitin-conjugating enzyme complex and a unique polyubiquitin chain. *Cell* 103:351-361.
17. Wang, C., L. Deng, M. Hong, G. R. Akkaraju, J. Inoue, and Z. J. Chen. 2001. TAK1 is a ubiquitin-dependent kinase of MKK and IKK. *Nature* 412:346-351.
18. Kanayama, A., R. B. Seth, L. Sun, C. K. Ea, M. Hong, A. Shaito, Y. H. Chiu, L. Deng, and Z. J. Chen. 2004. TAB2 and TAB3 activate the NF-kappaB pathway through binding to polyubiquitin chains. *Mol Cell* 15:535-548.
19. Kawai, T., and S. Akira. 2007. TLR signaling. *Semin Immunol* 19:24-32.
20. Pearce, E. L., M. C. Walsh, P. J. Cejas, G. M. Harms, H. Shen, L. S. Wang, R. G. Jones, and Y. Choi. 2009. Enhancing CD8 T-cell memory by modulating fatty acid metabolism. *Nature* 460:103-107.
21. Davis, J. M., H. Clay, J. L. Lewis, N. Ghori, P. Herbomel, and L. Ramakrishnan. 2002. Real-time visualization of mycobacterium-macrophage interactions leading to initiation of granuloma formation in zebrafish embryos. *Immunity* 17:693-702.
22. van der Sar, A. M., R. J. Musters, F. J. van Eeden, B. J. Appelmelk, C. M. Vandenbroucke-Grauls, and W. Bitter. 2003. Zebrafish embryos as a model host for the real time analysis of Salmonella typhimurium infections. *Cell Microbiol* 5:601-611.
23. Ward, A. C., D. O. McPhee, M. M. Condron, S. Varma, S. H. Cody, S. M. Onnebo, B. H. Paw, L. I. Zon, and G. J. Lieschke. 2003. The zebrafish spi1 promoter drives myeloid-specific expression in stable transgenic fish. *Blood* 102:3238-3240.

24. Mathias, J. R., B. J. Perrin, T. X. Liu, J. Kanki, A. T. Look, and A. Huttenlocher. 2006. Resolution of inflammation by retrograde chemotaxis of neutrophils in transgenic zebrafish. *J Leukoc Biol* 80:1281-1288.
25. Redd, M. J., G. Kelly, G. Dunn, M. Way, and P. Martin. 2006. Imaging macrophage chemotaxis in vivo: studies of microtubule function in zebrafish wound inflammation. *Cell Motil Cytoskeleton* 63:415-422.
26. Renshaw, S. A., C. A. Loynes, D. M. Trushell, S. Elworthy, P. W. Ingham, and M. K. Whyte. 2006. A transgenic zebrafish model of neutrophilic inflammation. *Blood* 108:3976-3978.
27. Meijer, A. H., A. M. van der Sar, C. Cunha, G. E. Lamers, M. A. Laplante, H. Kikuta, W. Bitter, T. S. Becker, and H. P. Spaink. 2008. Identification and real-time imaging of a myc-expressing neutrophil population involved in inflammation and mycobacterial granuloma formation in zebrafish. *Dev Comp Immunol* 32:36-49.
28. Hall, C., M. V. Flores, K. Crosier, and P. Crosier. 2009. Live cell imaging of zebrafish leukocytes. *Methods Mol Biol* 546:255-271.
29. Meijer, A. H., S. F. Gabby Krens, I. A. Medina Rodriguez, S. He, W. Bitter, B. Ewa Snaar-Jagalska, and H. P. Spaink. 2004. Expression analysis of the Toll-like receptor and TIR domain adaptor families of zebrafish. *Mol Immunol* 40:773-783.
30. Murayama, E., K. Kissa, A. Zapata, E. Mordelet, V. Briolat, H. F. Lin, R. I. Handin, and P. Herbomel. 2006. Tracing hematopoietic precursor migration to successive hematopoietic organs during zebrafish development. *Immunity* 25:963-975.
31. Stein, C., M. Caccamo, G. Laird, and M. Leptin. 2007. Conservation and divergence of gene families encoding components of innate immune response systems in zebrafish. *Genome Biol* 8:R251.
32. Meeker, N. D., and N. S. Trede. 2008. Immunology and zebrafish: spawning new models of human disease. *Dev Comp Immunol* 32:745-757.
33. Stockhammer, O. W., A. Zakrzewska, Z. Hegedus, H. P. Spaink, and A. H. Meijer. 2009. Transcriptome profiling and functional analyses of the zebrafish embryonic innate immune response to Salmonella infection. *J Immunol* 182:5641-5653.
34. Herbomel, P., B. Thisse, and C. Thisse. 1999. Ontogeny and behaviour of early macrophages in the zebrafish embryo. *Development* 126:3735-3745.
35. Herbomel, P., B. Thisse, and C. Thisse. 2001. Zebrafish early macrophages colonize cephalic mesenchyme and developing brain, retina, and epidermis through a M-CSF receptor-dependent invasive process. *Dev Biol* 238:274-288.
36. Willett, C. E., A. Cortes, A. Zuasti, and A. G. Zapata. 1999. Early hematopoiesis and developing lymphoid organs in the zebrafish. *Dev Dyn* 214:323-336.
37. Davidson, A. J., and L. I. Zon. 2004. The 'definitive' (and 'primitive') guide to zebrafish hematopoiesis. *Oncogene* 23:7233-7246.
38. Lam, S. H., H. L. Chua, Z. Gong, T. J. Lam, and Y. M. Sin. 2004. Development and maturation of the immune system in zebrafish, Danio rerio: a gene expression profiling, in situ hybridization and immunological study. *Dev Comp Immunol* 28:9-28.
39. Phelps, H. A., and M. N. Neely. 2005. Evolution of the zebrafish model: from development to immunity and infectious disease. *Zebrafish* 2:87-103.
40. Lesley, R., and L. Ramakrishnan. 2008. Insights into early mycobacterial pathogenesis from the zebrafish. *Curr Opin Microbiol* 11:277-283.
41. Hegedus, Z., A. Zakrzewska, V. C. Agoston, A. Ordas, P. Racz, M. Mink, H. P. Spaink, and A. H. Meijer. 2009. Deep sequencing of the zebrafish transcriptome response to mycobacterium infection. *Mol Immunol* 46:2918-2930.
42. Wu, H., K. Kerr, X. Cui, and G. A. Churchill. 2003. MAANOVA: A Sofware Package for the Analysis of Spotted cDNA Microarray Experiments.
43. Kerr, M. K., M. Martin, and G. A. Churchill. 2000. Analysis of variance for gene expression microarray data. *J Comput Biol* 7:819-837.
44. Benjamini, Y., and Y. Hochberg. 1995. Controlling the False Discovery Rate: a Practical and Powerful Approach to Multiple Testing. *J.R. Statist. Coc. B.* 57:289-300.
45. Beisvag, V., F. K. Junge, H. Bergum, L. Jolsum, S. Lydersen, C. C. Gunther, H. Ramampiaro, M. Langaas, A. K. Sandvik, and A. Laegreid. 2006. GeneTools--application for functional annotation and statistical hypothesis testing. *BMC Bioinformatics* 7:470.
46. Dahlquist, K. D., N. Salomonis, K. Vranizan, S. C. Lawlor, and B. R. Conklin. 2002. GenMAPP, a new tool for viewing and analyzing microarray data on biological pathways. *Nat Genet* 31:19-20.
47. Xiao, C., J. H. Shim, M. Kluppel, S. S. Zhang, C. Dong, R. A. Flavell, X. Y. Fu, J. L. Wrana, B. L. Hogan, and S. Ghosh. 2003. Ecsit is required for Bmp signaling and mesoderm formation during mouse embryogenesis. *Genes Dev* 17:2933-2949.
48. Mortazavi, A., B. A. Williams, K. McCue, L. Schaeffer, and B. Wold. 2008. Mapping and quantifying mammalian transcriptomes by RNA-Seq. *Nat Methods* 5:621-628.
49. Asmann, Y. W., M. B. Wallace, and E. A. Thompson. 2008. Transcriptome profiling using next-generation sequencing. *Gastroenterology* 135:1466-1468.
50. Sundaram, K., R. Nishimura, J. Senn, R. F. Youssef, S. D. London, and S. V. Reddy. 2007. RANK ligand signal-

ing modulates the matrix metalloproteinase-9 gene expression during osteoclast differentiation. *Exp Cell Res* 313:168-178.

51. Witten, P. E., A. Hansen, and B. K. Hall. 2001. Features of mono- and multinucleated bone resorbing cells of the zebrafish Danio rerio and their contribution to skeletal development, remodeling, and growth. *J Morphol* 250:197-207.
52. Koening, C. L., J. C. Miller, J. M. Nelson, D. M. Ward, J. P. Kushner, L. K. Bockenstedt, J. J. Weis, J. Kaplan, and I. De Domenico. 2009. Toll-like receptors mediate induction of hepcidin in mice infected with Borrelia burgdorferi. *Blood* 114:1913-1918.
53. Ahmad, R., J. Sylvester, and M. Zafarullah. 2007. MyD88, IRAK1 and TRAF6 knockdown in human chondrocytes inhibits interleukin-1-induced matrix metalloproteinase-13 gene expression and promoter activity by impairing MAP kinase activation. *Cell Signal* 19:2549-2557.
54. Volkman, H. E., T. C. Pozos, J. Zheng, J. M. Davis, J. F. Rawls, and L. Ramakrishnan. Tuberculous granuloma induction via interaction of a bacterial secreted protein with host epithelium. *Science* 327:466-469.
55. Solis, M., P. Wilkinson, R. Romieu, E. Hernandez, M. A. Wainberg, and J. Hiscott. 2006. Gene expression profiling of the host response to HIV-1 B, C, or A/E infection in monocyte-derived dendritic cells. *Virology* 352:86-99.
56. O'Prey, J., J. Skommer, S. Wilkinson, and K. M. Ryan. 2009. Analysis of DRAM-related proteins reveals evolutionarily conserved and divergent roles in the control of autophagy. *Cell Cycle* 8:2260-2265.
57. Crighton, D., S. Wilkinson, J. O'Prey, N. Syed, P. Smith, P. R. Harrison, M. Gasco, O. Garrone, T. Crook, and K. M. Ryan. 2006. DRAM, a p53-induced modulator of autophagy, is critical for apoptosis. *Cell* 126:121-134.
58. Munz, C. 2009. Enhancing immunity through autophagy. *Annu Rev Immunol* 27:423-449.
59. Kumar, D., L. Nath, M. A. Kamal, A. Varshney, A. Jain, S. Singh, and K. V. Rao. genome-wide analysis of the host intracellular network that regulates survival of Mycobacterium tuberculosis. *Cell* 140:731-743.
60. Wu, S., L. Page, and N. M. Sherwood. 2006. A role for GnRH in early brain regionalization and eye development in zebrafish. *Mol Cell Endocrinol* 257-258:47-64.
61. Chen, H. F., E. B. Jeung, M. Stephenson, and P. C. Leung. 1999. Human peripheral blood mononuclear cells express gonadotropin-releasing hormone (GnRH), GnRH receptor, and interleukin-2 receptor gamma-chain messenger ribonucleic acids that are regulated by GnRH in vitro. *J Clin Endocrinol Metab* 84:743-750.
62. Tanriverdi, F., L. F. Silveira, G. S. MacColl, and P. M. Bouloux. 2003. The hypothalamic-pituitary-gonadal axis: immune function and autoimmunity. *J Endocrinol* 176:293-304.
63. Min, J. Y., M. H. Park, J. K. Lee, H. J. Kim, and Y. K. Park. 2009. Gonadotropin-releasing hormone modulates immune system function via the nuclear factor-kappaB pathway in murine Raw264.7 macrophages. *Neuroimmunomodulation* 16:177-184.
64. Chakraborty, A., H. Brooks, P. Zhang, W. Smith, M. R. McReynolds, J. B. Hoying, R. Bick, L. Truong, B. Poindexter, H. Lan, W. Elbjeirami, and D. Sheikh-Hamad. 2007. Stanniocalcin-1 regulates endothelial gene expression and modulates transendothelial migration of leukocytes. *Am J Physiol Renal Physiol* 292:F895-904.
65. Yoshiko, Y., N. Maeda, and J. E. Aubin. 2003. Stanniocalcin 1 stimulates osteoblast differentiation in rat calvaria cell cultures. *Endocrinology* 144:4134-4143.
66. Wellen, K. E., R. Fucho, M. F. Gregor, M. Furuhashi, C. Morgan, T. Lindstad, E. Vaillancourt, C. Z. Gorgun, F. Saatcioglu, and G. S. Hotamisligil. 2007. Coordinated regulation of nutrient and inflammatory responses by STAMP2 is essential for metabolic homeostasis. *Cell* 129:537-548.

5 Transcriptome analysis of Traf6 function in early zebrafish embryogenesis

Oliver W. Stockhammer[1], Han Rauwerda[2], Martijs J. Jonker[2], Floyd R. Wittink[2], Timo M. Breit[2], Annemarie H. Meijer[1] and Herman P. Spaink[1]

1 Institute of Biology, Leiden University, Leiden, The Netherlands
2 MicroArray Department & Integrative Bioinformatics Unit, Swammerdam Institute for Life Sciences, University of Amsterdam, Amsterdam, The Netherlands

Abstract

TRAF6 is an essential signal transduction factor that not only mediates signals emanating from the TNF-receptor family but also from the TLR/IL-1 receptors and the TGF-beta receptors. In order to analyse the function of Traf6 during early zebrafish embryogenesis, transcriptome analysis was performed at 30% epiboly using a morpholino based knock-down approach. This approach turned out to be very challenging since non-specific effects of control morpholinos also appeared to trigger many responses at the transcriptome level. However, using different morpholinos directed against *traf6* mRNA and by comparisons to two control morpholinos we were able to identify a large gene set that is specifically controlled by Traf6 during embryogenesis. Using GO and pathway analyses we were able to give new insights into the diverse functions of Traf6. We compared the gene set that we found to be dependent on Traf6 during early embryogenesis with a previously identified set of genes dependent on Traf6 in the context of infection of one-day-old embryos and found that only a set of 14 genes was overlapping. This limited overlap shows that the function of Traf6 is modulated from a control factor of developmental genes to a control factor of a largely different set of genes involved in functions in infectious disease. In addition, we can conclude that there is a general effect of all morpholino injections on *tlr3* expression that is not dependent on Traf6. In contrast, there is a response of *tlr4a*, *tlr4b* and *tlr9* to morpholino injections in general that appears to be dependent on Traf6. These results prompt further investigations into the function of Traf6 in mediating responses to immunogenic stimuli at very early stages of embryogenesis.

Introduction

The members of the tumor necrosis factor receptor-associated factor (TRAF) family are essential signal transduction proteins that play a role in a wide range of physiological processes ranging from cell growth to immune responses and to programmed cell death. They were originally discovered as adapter proteins that mediate signals emanating from the TNF-receptor family. To date, seven members, named TRAF1 to TRAF7, have been identified in mammals (1, 2). All TRAF proteins are characterised by a TRAF domain at the carboxyl-terminus of the protein that can be further subdivided into a highly conserved TRAF-C domain and a less conserved coiled-coil domain referred to as TRAF-N domain. In addition all TRAF proteins, with the exception of TRAF1, contain a RING finger domain and several zinc finger motifs at the N-terminus. Self-association and interaction with TNF-receptors and other adaptor proteins is mediated by the TRAF-domain whereas downstream signalling is relying on the conserved domains of the N-terminus (2).

Among all members of the TRAF-family, TRAF6 holds a unique position, as TRAF6 is not only mediating signals emanating from the TNF-receptor family but

also from the TLR/IL-1 receptors and the TGF-beta receptors, eventually leading to the activation of the AP-1 and NF-κB transcription factor complexes (3, 4). Analysis of TRAF6 function by gene knock-down studies in mice revealed a critical role of TRAF6 in lymph node and exocrine gland organogenesis as well as in apoptosis and osteoclast development and function (5-8). TRAF6 was shown to bind to the receptor activator of NF-κB (RANK) and upon stimulation of RANK by the associated ligand RANKL, TRAF6 forms a complex with TAB1, TAB2 and TAK1, eventually leading to the activation of NF-κB, JNK and p38, thereby promoting osteoclast differentiation, function and survival (9-11). Similarly, following TLR receptor activation, TRAF6 also activates NF-κB through TAB1-TAB2-TAK1 complex formation. Furthermore, it was demonstrated that JNK and p38 activation is also mediated by TRAF6 upon activation of the TGF-beta receptor as well as the TLR-pathways (3, 12, 13). To activate JNK and p38 after TLR stimulation TRAF6 forms a complex with the protein ECSIT (12). In mouse embryonal carcinoma (EC) cells ECSIT was shown to be involved in BMP signalling by forming complexes with nuclear Smads on the *Tlx2* enhancer (13). TGF-beta signalling via TRAF6 was shown to be Smad-independent. However, whether TRAF6 is also involved in Smad-dependent BMP signalling events via ECSIT is still unknown. Recently it was demonstrated that TRAF6 also functions as a transcriptional cofactor in osteoclasts promoting FHL2 gene expression, further demonstrating the diverse functions of TRAF6 (14).

The zebrafish embryo is an extensively used model organism to study the molecular processes underlying vertebrate developmental, organogenesis and immune function. We could previously demonstrate the role of Traf6 in the immune response towards a bacterial infection of zebrafish embryos (Chapter 4). Initial experiments of morpholino mediated *traf6* knock-down revealed developmental defects during zebrafish embryogenesis. To investigate the role of Traf6 in early zebrafish development and to elucidate the implication of *traf6* knock-down on the transcription profile we performed a microarray based transcriptome analysis during early zebrafish embryogenesis. By using several control morpholino experiments we could show that Traf6 directs the transcription of a large set of genes during early embryogenesis. These sets were further characterized using ontology and pathway analyses, showing that Traf6 has a role in many fundamental biological processes. We have also compared our results with the infection data obtained in chapter 4.

Results

Phenotypic alterations after *traf6* knock-down

For functional analysis of *traf6* in zebrafish embryogenesis we designed two non-overlapping translation-blocking morpholinos targeted against the 5' UTR of the *traf6* transcript and tested these in at doses of 0.5 mM, 1 mM and 2 mM. Phenotypic effects of *traf6* knock-down at 30% epiboly were only observed after *traf6*-mor-

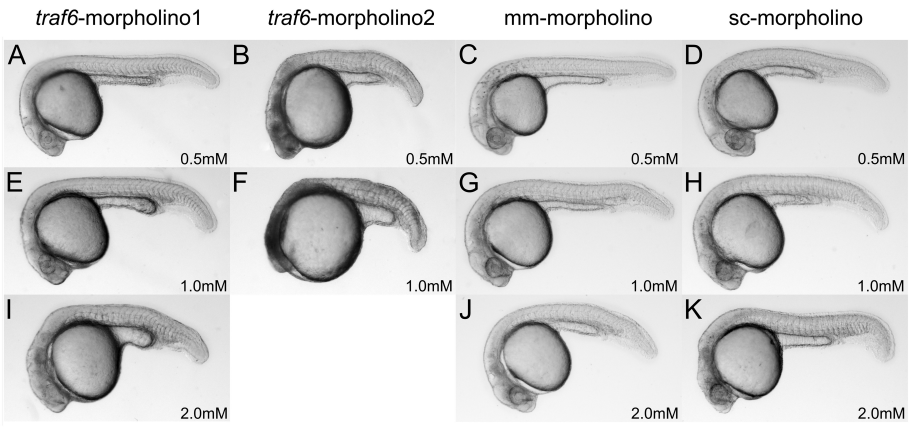


FIGURE 1. Overview of representative phenotypes upon morpholino treatment. Zebrafish embryos were injected with two translation-blocking morpholinos specifically targeting *traf6* (traf6-morpholino1 and 2) and two control morpholinos; 5bp mismatch (mm) and standard control-morpholino (sc) (A-K). (A, E, I) Morphology of zebrafish embryos injected with 0.5 mM, 1 mM and 2 mM of traf6-morpholino-1 and (B, F) traf6-morpholino-2 at 24hpf. Injection of 2 mM traf6-morpholino-2 resulted in 100% lethality at 24hpf. (C, G, J) Morphology of mm-morpholino injected embryos and (D, H, K) sc-morpholino injected embryos at 24 hpf. Zebrafish embryos are shown in lateral view with the anterior side to the left and dorsal to the top.

pholino-2 injection at the highest concentration. At this stage we observed a delay of at least 2 hours in epiboly progression as compared to normal development. However, at 24 hpf phenotypic changes were observed with both morpholinos as shown in figure 1. The results show that injection with *traf6*-morpholino-2 results in high mortality at the 2 mM concentration and shortening of the anterior-posterior (AP) axis and strong necrosis in the developing nervous system at the lower concentrations (Fig. 1 B, F). With *traf6*-morpholino-1 we observed a shortening of the AP axis at 1 and 2 mM (Fig. 1 E, I). We have also designed a control morpholino that contains 5bp mismatches (mm) as compared to *traf6*-morpholino-1. We furthermore tested a standard control morpholino (sc) that has previously been used in other studies and which is assumed not to target zebrafish genes (20). Control experiments with these morpholinos at various concentrations did not show phenotypes at 24 hpf that were comparable to the observed effects of *traf6*-morpholinos-1 and -2 treatment at 0.5 and 1 mM concentrations (Fig. 1 C, D, G, H). However, at 2 mM concentration necrosis in the head area and malformation of the somites posterior to the yolk sac extension was observed (Fig. 1 J, K)

Transcriptome analysis of Traf6 knock-down compared to control experiments

As studies in human and mammalian models have shown TRAF6 to be involved as

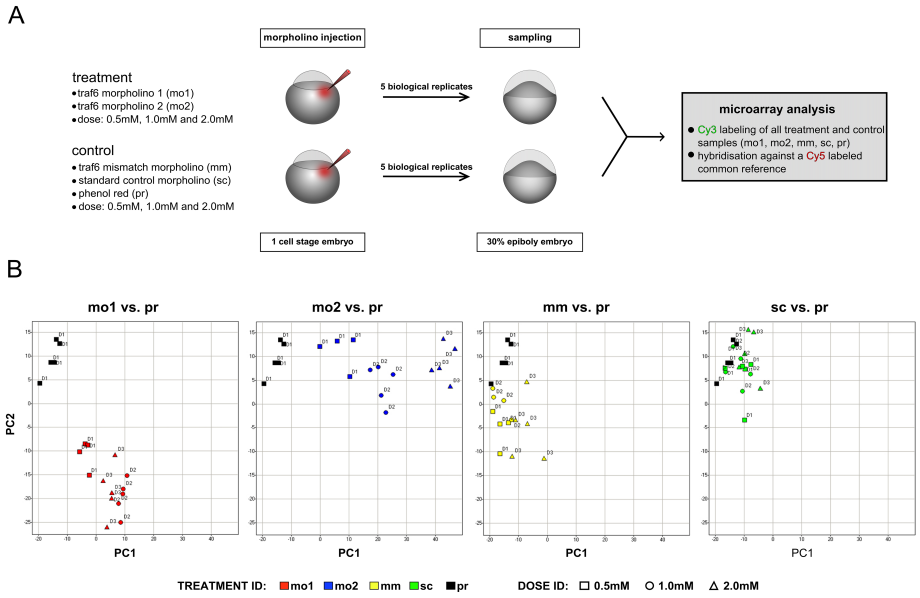


FIGURE 2. Schematic overview of the experimental setup (A) and principal component analysis (PCA) of the transcriptome responses (B). (A) Zebrafish embryos were injected at the one cell stage with two morpholinos specifically targeting traf6 mRNA indicated as traf6-morpholino1 and traf6-morpholino2 respectively (treatment). In addition a 5bp mismatch morpholino (mm) and a standard control morpholino (sc) were injected to control for general morpholino effects and phenol red (pr) as a control for the injection process in general. The transcriptional response was analysed at 30% epiboly using a common reference approach. The experiment was carried out in quintuplicate. (B) Transcriptome responses after morpholino and control treatment were analysed by PCA.

a signal transducer in various pathways, the observed knock-down phenotypes are hard to investigate with *in situ* gene pattern analyses methods. In order to get an overview of the signal transduction processes that are affected by *traf6* knock-down we decided to perform transcriptome expression profiling using custom-designed Agilent micro-arrays containing 43,371 probes. As above, zebrafish embryos at the one cell stage were injected with *traf6*-morpholinos-1 and -2 and with the mismatch and standard control morpholinos at concentrations of 0.5, 1, and 2 mM. In addition we also injected Phenol red as a general control for the injection per se (Fig.2 A). The assay was performed in biological quintuplicate and analysis of the transcriptome took place at 30% epiboly to minimise the accumulation of secondary effects caused by *traf6* knock-down. Principal component analysis (PCA) demonstrated good separation of the biological replicates of the two specific *traf6*-morpholinos (*traf6*-morpholino-1, *traf6*-morpholino-2) along the concentration range (Fig.2 B). Treatments with traf6-morpholino-2 showed a good correlation between the strength of response and the increase of the treatment dose whereas for *traf6*-morpholino-1 we found the

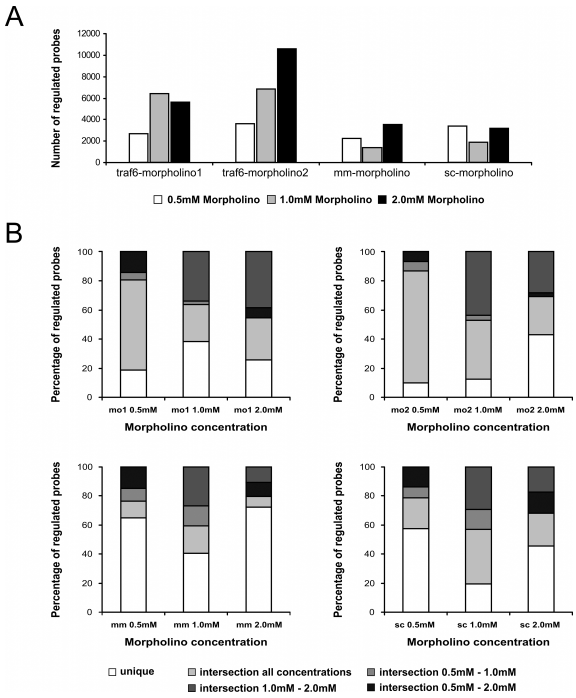


FIGURE 3. Analysis of the transcriptional response. (A) Bar graph representation of the dose-response relationship after traf6- and control morpholino treatment. The transcriptional response of traf6- and control morpholino treatment groups was analysed against the phenol red transcriptome response. Significance cut-off was set to p <0.05. To account for multiple testing, all P values were FDR adjusted. (B) Illustration of relative overlap in each treatment group along the concentration range. mo1, traf6-morpholino1; mo2, traf6-morpholino2; mm, 5bp mismatch morpholino; sc, standard control morpholino treatment

strongest effect to be elicited at a concentration of 1 mM. In contrast, only a poor separation was shown for the 5bp mismatch morpholino and no separation for the standard control morpholino, indicating a concentration independent effect at that stage. For the control morpholino treatments, in particular for the sc-morpholino treated group, we observed less deviation from the phenol red treatments.

In agreement with the results of the PCA analysis we found an increasing number of probes in the signature set of *traf6*-morpholino-2 treatment, ranging from 3578 at 0.5 mM up to 10539 at 2 mM (Fig.3 A, Supplemental Tab. I). The strongest response after *traf6*-morpholino-1 treatment was observed at a dose of 1 mM with a total of 6358 probes in the signature set. At a dose of 0.5 mM the signature set contained 2624 regulated probes whereas it contained 5623 probes at a dose of 2 mM. The two control groups were very similar to each other regarding the number of regulated genes and the distribution over the concentration range. In both cases we observed a decrease in the number of regulated genes at 1 mM, followed by an increase at the 2 mM dose (Fig.3 A).

In order to define a *traf6* knock-down specific transcription profile we first identified subsets of the individual treatment groups that were consistently regulated (FDR adjusted P-value <0.05 for at least two concentrations) along the concentration range (Fig.3 B). Analysis of the *traf6*-morpholino treatment groups demonstrated that a high percentage of the probes were overlapping along the concentration range, indicating a specific effect of the morpholinos. For *traf6*-morpholino-2 treatment we

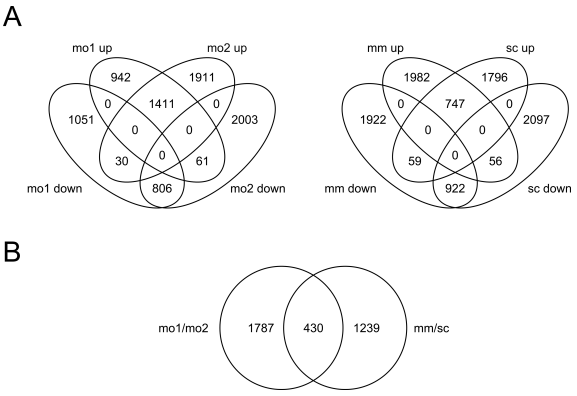


FIGURE 4. Identification of specific *traf6* knock-down and general morpholino effects. (A) Upper Venn diagram illustrates the overlap of the response signatures between *traf6* specific morpholino-1 and -2. Lower Venn diagram illustrates the overlap between the mm- and sc-morpholino response signatures. Overlap of *traf6* specific morpholino-1 and -2 response signature was defined for all probes that were significantly regulated ($p<0.05$) in at least 2 out of 3 concentrations. Overlap of mm- and sc-morpholino response signature was defined in a less stringent way by taking all probes that were significant in at least one concentration of each treatment. (B) Identification of *traf6* knock-down specific expression profile and general morpholino response profile. mo1, traf6-morpholino1; mo2, traf6-morpholino2; mm, 5bp mismatch morpholino; sc, standard control morpholino treatment; mo1/mo2, overlap traf6-morpholino1 and -2 response ; mm/sc, overlap mm- and sc-morpholino response

found an overlap ranging from a total of 90% of all significantly regulated probes at 0.5 mM over 88% at 1 mM down to 57% at 2 mM. In the case of *traf6*-morpholino-1 treatment the smallest overlap was observed at 1 mM with 62% and the maximum at 0.5 mM with 81% of all regulated probes. For both treatments we furthermore observed that the expression of large probe sets was affected by the morpholino treatment at all concentrations: 1628 probes for *traf6*-morpholino-1 and 2760 probes for *traf6*-morpholino-2 (Supplemental Tab. II and III). An overall much weaker response was observed for the control groups and there was also considerable smaller percentage of regulated probes overlapping along the concentration range. In the mm-morpholino as well as the sc-morpholino treated groups the highest overlap was present at the 1 mM dose reaching 60% after mm-morpholino treatment and 80% upon sc-morpholino treatment. However, a substantially smaller overlap was evident at 0.5 mM and 2 mM in both cases, ranging between 35 and 55%. Furthermore, the expression of only a small probe set of 260 for the mm-morpholino group and 706 for the sc-morpholino group was consistently changed after treatment with each concentration of morpholinos (Supplemental Tab. IV and V).

Definition of specific sets for *traf6* knock-down and control effects

We specified the common signature of *traf6*-morpholino1 and 2 by determining the overlap of the above described subsets, i.e. the number of probes consistently changed in the same direction for both morpholinos and at least two concentrations for each morpholino (Fig. 3 B). We found a total of 1411 probes to be commonly up-regulated

Table I. Master-target test of GO analysis for Biological Process of the overlap between mismatch and standard control morpholino*

GO-term	Name	MASTER	UP	DOWN
GO:0008150	biological_process	5265	136	158
GO:0065007	biological regulation	1009	24	32
GO:0009987	cellular process	3042	79	108
GO:0051301	cell division	42	1	4
GO:0044237	cellular metabolic process	2053	51	76
GO:0032502	developmental process	742	22	29
GO:0009790	embryonic development	217	9	12
GO:0007389	pattern specification process	133	6	10
GO:0051234	establishment of localization	574	15	13
GO:0040007	growth	53	0	2
GO:0002376	immune system process	92	2	6
GO:0006955	immune response	55	1	5
GO:0051179	localization	648	18	15
GO:0051641	cellular localization	145	8	3
GO:0008152	metabolic process	2402	60	90
GO:0009058	biosynthetic process	1041	21	42
GO:0044237	cellular metabolic process	2053	51	76
GO:0044238	primary metabolic process	2022	49	74
GO:0051704	multi-organism process	24	0	2
GO:0032501	multicellular organismal process	714	18	29
GO:0048519	negative regulation of biological process	98	5	4
GO:0043473	pigmentation	11	1	1
GO:0048518	positive regulation of biological process	89	2	1
GO:0050789	regulation of biological process	922	23	30
GO:0000003	reproduction	21	0	1
GO:0050896	response to stimulus	282	8	11
GO:0006955	immune response	55	1	5

* A master-target statistical test using eGOn software was performed with input gene lists of zebrafish UniGene identifiers. The master input lists contained all UniGene identifiers present on the microarray. The target lists contained the UniGene identifiers that were retrieved by the intersection analysis of the mismatch and standard-control morpholino response signatures with an FDR adjusted P-value lower than 0.05. The table indicates the number of genes in each list that are associated with the indicated GO-terms. Numbers highlighted in grey are significantly enriched in the target list compared to the master whereas all numbers indicated in black demonstrated a significant underrepresentation in the target list compared to the master ($p < 0.05$).

upon *traf6*-morpholino treatment and 806 to be commonly down-regulated (Fig.4 A). The response of a small group of 91 probes was anti-correlated (Supplemental Tab. VI). In addition, we were interested in a probe set that was responsive both to the mismatch and standard-control morpholinos, reasoning that this set would most likely characterize a general response to morpholino treatments. Taking into consideration the low consistency of the control groups along the concentration range, and the therefore largely dose-independent response, we decided to take a less restrictive selection criterion than for the comparison between *traf6*-morpholinos and compared all probes that were significantly (FDR adjusted P-value <0.05) regulated by the mismatch and standard control morpholinos at minimally one of the applied doses. A total of 747 commonly up-regulated probes and 922 commonly down-regulated probes were found (Fig.4 A). In addition we observed 115 anti-correlated probes (Supplemental Tab. VII). In a next step we determined the overlap between the common *traf6* knock-down and control signature and subtracted this set, leading to a *traf6* knock-down signature of 1787 regulated probes representing 868 genes (Fig. 4B, supplemental Tab. VIII).

Table II. Master-target test of GO analysis for Biological Process for the overlap between traf6 morpholino1 and 2*

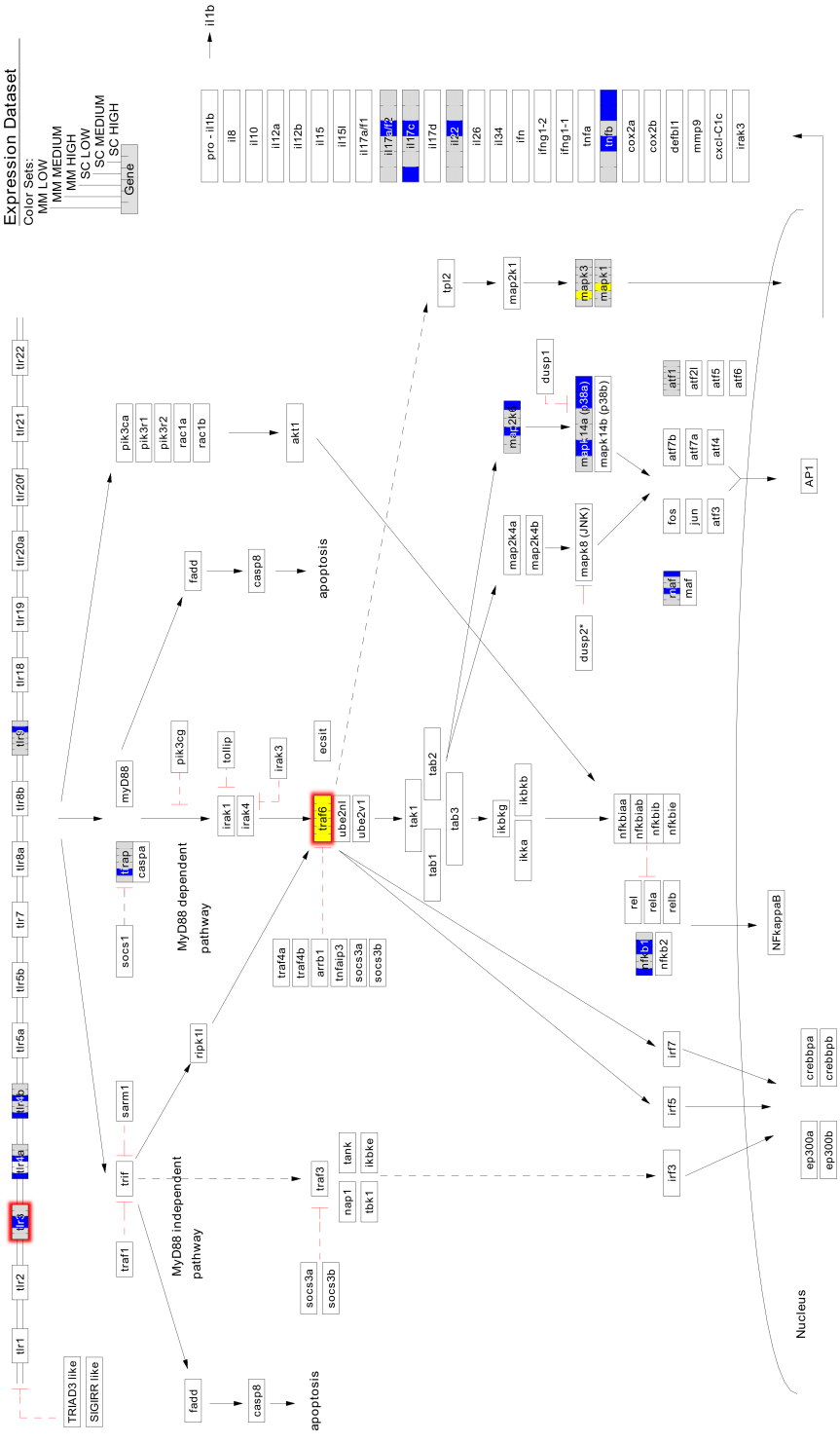
GO-term	Name	master	UP	DOWN
GO:0008150	biological_process	5265	286	116
GO:0022610	biological adhesion	83	2	1
GO:0065007	biological regulation	1009	47	19
GO:0009987	cellular process	3042	151	75
GO:0010467	gene expression	921	29	23
GO:0050794	regulation of cellular process	864	35	17
GO:0032502	developmental process	742	30	19
GO:0048856	anatomical structure development	506	16	10
GO:0016265	death	81	10	4
GO:0007275	multicellular organismal development	648	19	14
GO:0051234	establishment of localization	574	40	9
GO:0040007	growth	53	1	1
GO:0002376	immune system process	92	1	2
GO:0051179	localization	648	43	10
GO:0008152	metabolic process	2402	129	57
GO:0009056	catabolic process	139	17	5
GO:0019222	regulation of metabolic process	711	26	13
GO:0051704	multi-organism process	24	0	0
GO:0032501	multicellular organismal process	714	20	15
GO:0007275	multicellular organismal development	648	19	14
GO:0048519	negative regulation of biological process	98	2	1
GO:0043473	pigmentation	11	1	0
GO:0048518	positive regulation of biological process	89	5	3
GO:0050789	regulation of biological process	922	39	18
GO:0000003	reproduction	21	1	2
GO:0019953	sexual reproduction	14	1	2

* A master-target statistical test using eGOn software was performed with input gene lists of zebrafish UniGene identifiers. The master input lists contained all UniGene identifiers present on the microarray. The target lists contained the UniGene identifiers that were retrieved by the intersection analysis of the traf6-morpholino1 and 2 response signatures with an FDR adjusted P-value lower than 0.05. The table indicates the number of genes in each list that are associated with the indicated GO-terms. Numbers highlighted in grey are significantly enriched in the target list compared to the master whereas all numbers indicated in black demonstrated a significant underrepresentation in the target list compared to the master ($p < 0.05$).

Ontology and pathway analysis of general morpholino effects

We initially tested the control signature for enrichment of gene ontology groups using eGOn, a web-based data mining tool for transcriptome data (www.genetools.microarray.ntnu.no) (18). The analysis revealed several enriched GO terms in the down-regulated fraction, for instance "embryonic development", "pattern specification process" and "metabolic process" (Tab. I). Interestingly, we also found the GO term "immune response" to be significantly enriched in the control group, comprising genes of various TLRs such as *tlr3*, *tlr4a, tlr4b* and *tlr9*.

To analyse the general morpholino effect on the TLR-pathway in more detail we used the GenMapp software package (genmapp.org) (19). Analysis of the TLR-pathway revealed several more members to be regulated (Fig.5). Beside the Toll-like receptors we also found *toll-interleukin 1 receptor (TIR) domain containing adaptor protein* (*tirap*), one of the TLR adaptor proteins, as well as *nuclear factor of kappa light polypeptide gene enhancer in B-cells 1* (*nfkb1*) and several mitogen activated protein kinases (MAPK). Interestingly *traf6* was up-regulated in the control and *traf6*-morpholino treatments suggesting that *traf6* is induced by morpholino treatments


Expression Dataset
Color Sets:
MM LOW
MM MEDIUM
MM HIGH
SC LOW
SC MEDIUM
SC HIGH
Gene
pro - il1b
il8
il10
il12a
il12b
il15
il15l
il17a/f1
il17a/f2
il17c
il17d
il22
il26
il34
ifn
ifng1-2
ifng1-1
tnfa
tnfb
cox2a
cox2b
defb1
mmp9
cxcl-C1c
irak3
il1b
TRIAD3 like
SIGIRR like
tlr1
tlr2
tlr3
tlr4
tlr5
tlr5a
tlr5b
tlr7
tlr8a
tlr8b
tlr8
tlr18
tlr19
tlr20a
tlr20f
tlr21
tlr22
myD88
trap
caspa
socs1
pik3cg
tollip
irak1
irak4
irak3
ecsit
traf6
ube2nl
ube2v1
tak1
tab1
tab2
tab3
ikbkg
ikka
ikbkb
pik3ca
pik3r1
pik3r2
rac1a
rac1b
akt1
fadd
casp8
apoptosis
tpl2
map2k1
mapk3
mapk1
map2k4a
map2k4b
mapk8 (JNK)
dusp2*
map2k4
mapk14a (p38a)
mapk14b (p38b)
dusp1
fos
jun
atf3
maf
atf7b
atf7a
atf4
atf1
atf2l
atf5
atf6
AP1
MyD88 dependent pathway
traf4a
traf4b
arrb1
tnfaip3
socs3a
socs3b
nfkbiaa
nfkbiab
nfkbib
nfkbie
rel
rela
relb
nfkb1
nfkb2
NFkappaB
MyD88 independent pathway
trif
sarm1
ripk1l
traf1
traf3
nap1
tank
tbk1
ikbke
socs3a
socs3b
irf3
irf5
irf7
ep300a
ep300b
crebbpa
crebbpb
Nucleus

in general.

Ontology and pathway analysis of *traf6* knock-down signatures

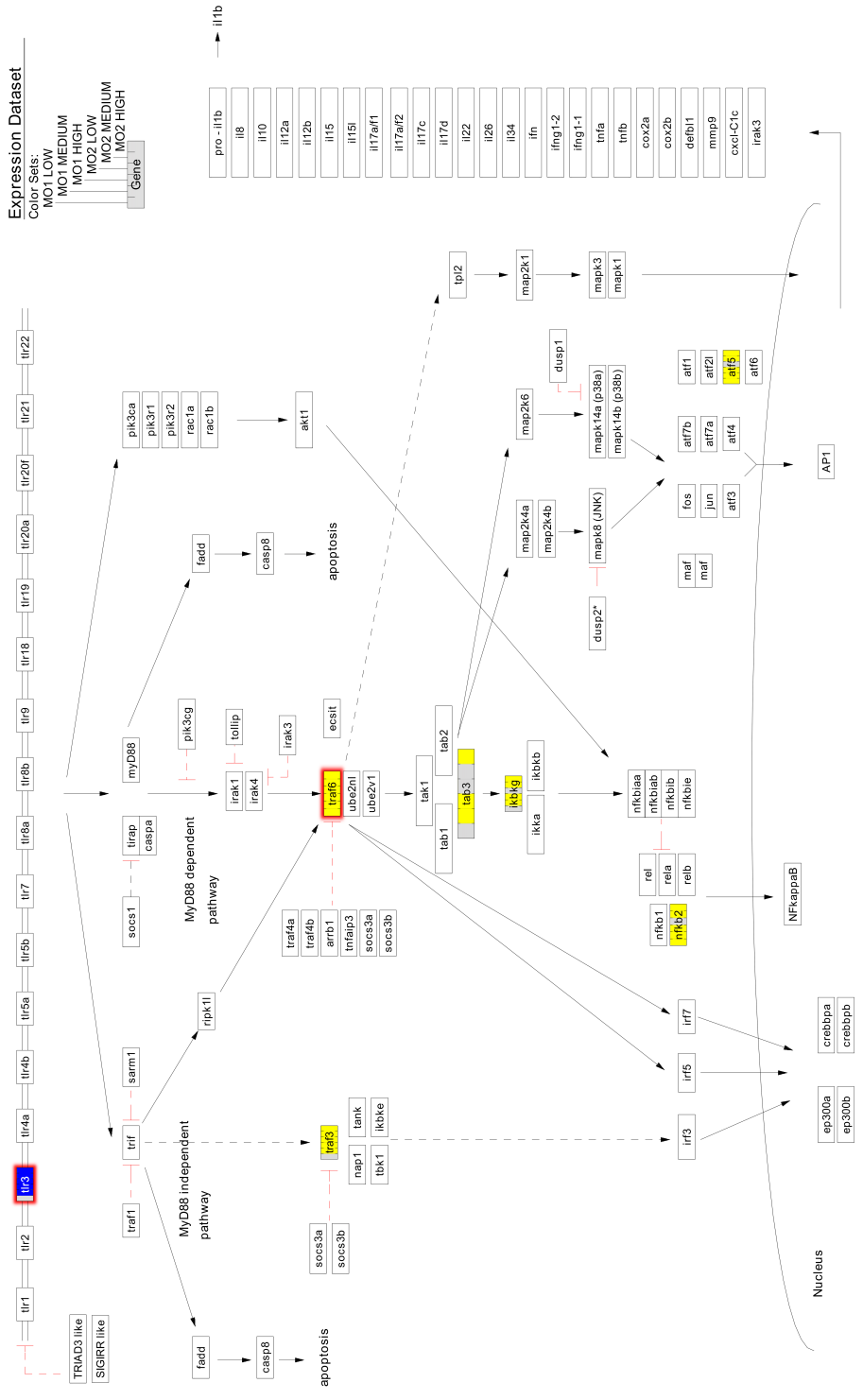
Analysis of the *traf6* knock-down signature with eGOn revealed the GO terms "death" and "catabolic process" to be significantly enriched in the up-regulated fraction (Tab. II). Under the "death" category we found such genes as the serine/threonine kinase *ripk2* and members of the BCL-2 protein family (*bad*, *bokb* and *bax*), all promoting programmed cell death. In agreement with this notion we also found genes that are counteracting programmed cell death down-regulated. For instance *baculoviral IAP repeat-containing 2* (*birc2*). Additionally we found GO-terms such as "gene expression" and "multicellular organismal development" showing significant underrepresentation in the up-regulated fraction.

Traf6 plays a pivotal role in the signal transduction of the TLR-pathway. We were therefore interested in the effect of *traf6* knock-down on members of this pathway. Projection of the *traf6* knock-down signature demonstrated an induction of *traf3* upon *traf6* knock-down (Fig. 6). Furthermore, the zebrafish homolog of TAB3, an interacting partner of TRAF6, was up-regulated. Likewise the regulatory subunit of the IKK-complex, *nemo* (*ikbkg*), was induced after *traf6* knock-down. NEMO was shown to be an ubiquitination target of TRAF6 in mice fibroblast cells and ubiquitination of NEMO by TRAF6 is involved in IL-1 mediated activation of NF-κB (21). Furthermore, the transcription factors *nuclear factor of kappa light polypeptide gene enhancer in B-cells 2* (*nfkb2*) and *activating transcription factor 5* (*aft5*) were induced upon *traf6* knock-down. We also performed pathway analysis of the TGF beta pathway. The results (not shown) showed only one gene in this pathway, namely *transforming growth factor, beta receptor II* (*tgfbr2*), to be up-regulated after *traf6* knock-down and not after control morpholino treatments.

Traf6 dependent genes in early embryogenesis and immunity

We previously indentified a set of genes that was dependent on Traf6 function in the context of a bacterial challenge (Chapter 4). To clarify whether there are genes that

FIGURE 5. Toll-like receptor (TLR) pathway analysis of the transcriptional effect that was elicited by morpholino treatment in general. Genes that were regulated due to the general morpholino effect were mapped on the TLR pathway. Gene boxes are colour coded from left to right with 0.5 mM (LOW), 1 mM (MEDIUM) and 2 mM (HIGH) expression data of the mm-morpholino (MM) and the standard control morpholino (SC). Up-regulation is indicated in yellow, down-regulation in blue. Genes that failed the fold-change cut off (>1.2 and <-1.2) were indicated in grey. White denotes genes that were not passing the significance cut-off value (FDR adjusted P-value <0.05) or were not represented on the array platform. The pathway is based on knowledge of TLR signalling in mammalian species and it should be noted that most interactions remain to be experimentally confirmed in zebrafish.


Expression Dataset
Color Sets:
MO1 LOW
MO1 MEDIUM
MO1 HIGH
MO2 LOW
MO2 MEDIUM
MO2 HIGH
Gene
pro - il1b
il8
il10
il12a
il12b
il15
il15l
il17af1
il17af2
il17c
il17d
il22
il26
il34
ifn
ifng1-2
ifng1-1
tnfa
tnfb
cox2a
cox2b
defb1
mmp9
cxcl-C1c
irak3
il1b
tlr1
tlr2
tlr3
tlr4a
tlr4b
tlr5a
tlr5b
tlr7
tlr8a
tlr8b
tlr9
tlr18
tlr19
tlr20a
tlr20f
tlr21
tlr22
TRIAD3 like
SIGIRR like
fadd
casp8
apoptosis
traf1
trif
sarm1
ripk1l
MyD88 independent pathway
socs3a
socs3b
traf3
nap1
tbk1
tank
ikbke
irf3
irf5
irf7
socs1
tirap
caspa
myD88
MyD88 dependent pathway
pik3cg
tollip
irak1
irak4
irak3
traf4a
traf4b
arrb1
tnfaip3
socs3a
socs3b
traf6
ube2ni
ube2v1
ecsit
tak1
tab1
tab2
tab3
ikbkg
ikka
ikbkb
nfkbiaa
nfkbiab
nfkbib
nfkbie
rel
rela
relb
nfkb1
nfkb2
NFkappaB
pik3ca
pik3r1
pik3r2
rac1a
rac1b
akt1
fadd
casp8
apoptosis
tpl2
map2k1
mapk3
mapk1
map2k6
dusp1
mapk14a (p38a)
mapk14b (p38b)
map2k4a
map2k4b
mapk8 (JNK)
dusp2*
maf
maf
fos
jun
atf3
atf7b
atf7a
atf4
atf1
atf2l
atf5
atf6
AP1
Nucleus
ep300a
ep300b
crebbpa
crebbpb

were dependent on Traf6 function during early embryogenesis and immune defence we compared the Traf6 dependent infection signature with the *traf6* knock-down signature of this study. Furthermore, we included a previously identified embryonic infection response signature in the analysis (Chapter 4). We identified 628 common regulated probes between the early embryonic *traf6* knock-down signature and the embryonic infection signature (Fig. 7, Supplemental Tab. IX). We classified the commonly shared probes into common up- and down-regulated and anti-correlated expressed probe sets and subsequently tested for enrichment of gene ontology groups using eGOn (www.genetools.microarray.ntnu.no). We found the GO terms "death" and "regulation of localization" to be significantly enriched in the common up-regulated group (Supplemental Tab. X.). In the shared down-regulated fraction we could identify GO terms linked to metabolic processes like "macromolecule metabolic process" and "catabolic processes" as significantly enriched. Probes that were up-regulated in the early embryonic knock-down signature and down-regulated in the embryonic infection signature were enriched for the GO terms "cell cycle" and "cell division".

In addition we found 15 probes (14 genes) to be regulated in all three signatures and 1 (*coproporphyrinogen oxidase*, *cpox*) to be common between the early embryonic *traf6* knock-down signature and the Traf6 dependent infection signature (Tab. III). The probes that were regulated in all three signatures in common contained genes such as *DNA-damage regulated autophagy modulator 1* (*dram1*), which was shown to be activated by p53 and promotes p53 induced autophagy as well as *rad17*, important for DNA-damage-induced cell cycle G2 arrest (22). Another gene of this group was *stx11a*, a homolog of the human *SYNTAXIN11* gene. SYNTAXIN11 was demonstrated to play a role in phagocytosis in human macrophages (23).

Discussion

As shown in chapter 4 the Traf6 protein is an important signal transduction protein in the innate immune system of vertebrates. In addition TRAF6 plays a role in various cellular developmental processes in mice (6, 7, 14). In this chapter it is shown for the first time that Traf6 is also involved in the regulation of a large gene set during early embryogenesis. In order to analyse the function of Traf6, transcriptome

FIGURE 6. Toll-like receptor (TLR) pathway analysis of the specific *traf6* knock-down effect. Traf6 knock-down specific expression profiles were mapped on the TLR pathway. Gene boxes are colour coded for 0.5 mM (LOW), 1 mM (MEDIUM) and 2 mM (HIGH) of the traf6-morpholino1 (M1) and traf6-morpholino2 (M2) expression data as described in figure 5. The pathway is based on knowledge of TLR signalling in mammalian species and it should be noted that most interactions remain to be experimentally confirmed in zebrafish.

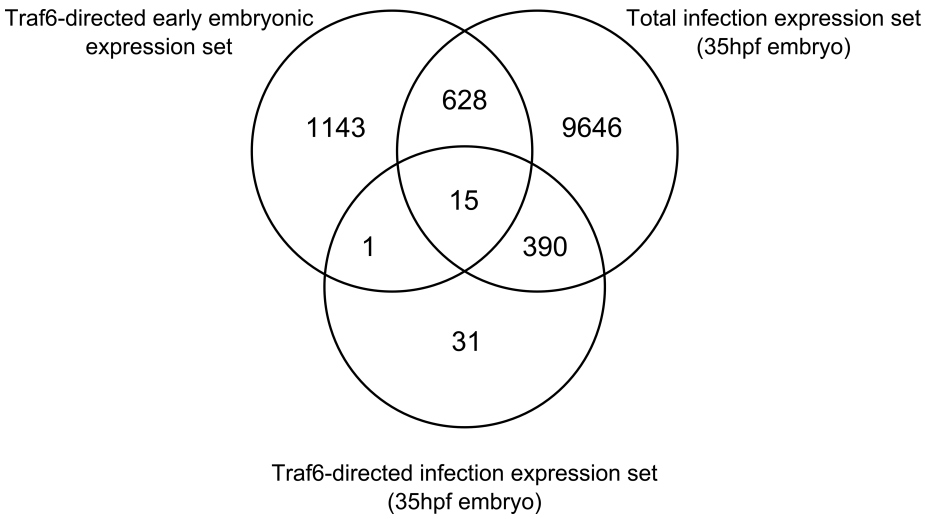


FIGURE 7. Traf6-controlled genes in early embryogenesis and embryonic immune response. Traf6-controlled probes in early embryogenesis were compared to a total infection expression set and to a Traf6-dependent infection expression set. Total and Traf6-controlled expression sets were retrieved from a previously performed Salmonella infection assay (Chapter4). In short, *traf6* knock-down and mm-morpholino treated embryos were infected with Salmonella at 27 hpf and the infection response was analysed after an incubation time of 8 hours. The Traf6-dependent infection expression set was retrieved by interaction term analysis.

analysis at 30% epiboly was performed using a morpholino based knock-down approach. This approach turned out to be very challenging since non-specific effects of control morpholinos also appeared to trigger many responses at the transcriptome level. However, using different morpholinos directed against *traf6* mRNA and by comparisons to two control morpholinos we were able to identify a large gene set that is specifically controlled by Traf6 during embryogenesis. Using GO and pathway analyses we were able to give new insights into the diverse functions of Traf6 in transcriptional control.

Knock-down of *traf6* leads to a strongly altered transcriptome profile with each of the tested morpholinos, even at concentrations as low as 0.5 mM. Apparently the response at the transcriptome level at 30% epiboly is far stronger than the observed morphological alterations at later stages would suggest (Fig. 1). For instance, injection of *traf6*-morpholino-1 at a concentration of 0.5 mM led to no detectable morphological changes at 1 dpf, whereas a significant change of expression of 2624 probes was observed at the 30% epiboly stage. Although the two morpholinos where very different in their dose response at the morphological level at 1 dpf, they showed strong similarity in the response at the transcriptome level at 30% epiboly. We could identify a stringent overlap set of the effects of the two morpholinos of 868 genes

Table III. Traf6 controlled genes in early embryogenesis and embryonic immune response*

Probe ID	UniGene ID	Symbol	Description	*traf6* k.d. early embryogenesis (fc)	Immune response (fc)	*traf6* k.d. immune response (fc)
LOLS08715	Dr.11530	zgc:152863	zgc:152863	1.5, 1.7, 1.8 ; 1.4, 2.1, 3.1	-1.4	n.s.
LOLS06846	Dr.13838	zgc:153057	zgc:153057	-1.2, -1.2, -1.2 ; -1.1, -1.2, -1.3	2.2	1.5
A_15_P115394	Dr.31220	rad17	RAD17 homolog (S. pombe)	1.3, 1.6, 1.6 ; 1.1, 1.2, 1.4	-1.4	-1.1
LOLS07060	Dr.75603	h3f3a	H3 histone, family 3A	-1.2, -1.5, -1.5 ; -1.5, -1.9, -3.1	-1.2	n.s.
A_15_P113277	Dr.7614	slc25a25	solute carrier family 25	1.3, 1.8, 1.6 ; 1.3, 1.7, 2.2	1.6	n.s.
A_15_P110827	Dr.77486	lass5	LAG1 homolog, ceramide synthase 5	1.0, 1.2, 1.3 ; 1.1, 1.2, 1.3	1.1	n.s.
A_15_P111539	Dr.77501	dram1	DNA-damage regulated autophagy modulator 1	-1.2, -2, -1.6 ; -1.4, -1.9, -2.9	2.2	n.s.
A_15_P103389	Dr.78554	cpox	coproporphyrinogen oxidase	1.2, 1.4, 1.5 ; 1.1, 1.3, 1.6	n.s.	-1.5
LOLS07574	Dr.79180	srpr	signal recognition particle receptor (docking protein)	-1.3, -1.3, -1.3 ; -1.2, -1.2, -1.1	1.5	n.s.
A_15_P114256	Dr.81309	psme1	proteasome activator subunit 1	-1.1, -1.4, -1.6 ; -1.2, -1.6, -2.2	5.1	2.1
LOLS00214	Dr.81309	psme1	proteasome activator subunit 1	-1.2, -1.5, -1.5 ; -1.2, -1.7, -2.3	3.9	1.8
LOLS01729	Dr.83170	stx11a	syntaxin 11a	1.3, 1.4, 1.3 ; 1.1, 1.4, 1.6	2.5	1.6
A_15_P101112	Dr.90156	f3b	coagulation factor IIIb	1.4, 1.6, 1.4 ; 1.2, 1.5, 2.0	2.8	1.7
A_15_P113317	n.a.	n.a.	n.a.	-1.2, -1.2, -1.3 ; -1.2, -1.2, -1.1	1.5	n.s.
LOLS09680	n.a.	n.a.	n.a.	-1.1, -1.3, -1.2 ; -1.2, -1.2, -1.3	1.4	n.s.
A_15_P113108	n.a.	n.a.	n.a.	1.2, 1.2, 1.2 ; 1.0, 1.2, 1.3	3.9	2.4

* For *traf6* knock-down during early embryogenesis the fold-changes (fc) are indicated for mo1 and mo2 with increasing concentrations (0.5mM - 2mM); probes that were not significantly changed are indicated as n.s. (p-value > 0.05)

after correction for general morpholino effects (Fig. 4). The ontology analyses of these genes, as shown in the results (Tab. I), indicate diverse functions ranging from catabolic processes (e.g. glycolysis) to gene regulation. Since the function of Traf6 in early embryogenesis in vertebrates has not yet been analysed, it is difficult to identify specific ontology classes that can be linked to functions of Traf6 previously described in the literature except for functions in apoptosis. Traf6 knock-down led to the induction of several genes involved in the regulation of programmed cell death. Genes such as *BCL2-antagonist of cell death* (*bad*) and *bcl2-associated X protein* (*bax*), known to promote apoptosis, were induced whereas genes promoting cell survival such as *birc2* showed decreased expression levels (24-26). Our results are in line with a recent publication of Yoon et al. were it was demonstrated that TRAF6 has an anti-apoptotic effect in mice cell lines (27). In these cell lines TNF stimulation caused sustained JNK activation through the accumulation of reactive oxygen species (ROS) eventually leading to cell death. It was shown by Yoon et al. that TRAF6 deficiency leads to the inactivation of GSK3β and in turn to impaired NF-κB dependent transcription.

The TLR signalling pathway has been shown to be crucial for embryogenesis in insects and nematodes and it might therefore be expected that Traf6 plays a role in early development of vertebrates as well. Considering the early stage of embryogenesis that we have studied we can expect that many of the genes affected by *traf6* knock-down are likely to play a role in development. We identified a large overlap in transcriptional gene response between the early embryonic *traf6* knock-down effect and embryonic infection responses, indicating that early development and infectious disease processes have many molecular mechanisms in common. However, it is notable that only a set of 14 annotated genes showed a Traf6 controlled response in early embryogenesis and in the context of an embryonic infection response at 35 hpf.

These genes include *DNA-damage regulated autophagy modulator1* (*dram1*), a target gene of p53 (28). This limited overlap shows that the functions of Traf6 in early embryogenesis differ from its functions in innate immunity at later stages of embryogenesis. This is remarkable considering the fact that many key partners of Traf6 play a role in both development and infectious disease. Further studies at a biochemical level might show how Traf6 function is modulated from a control factor of developmental genes to a control factor of genes involved in functions in infectious disease.

In addition to the analysis of the function of Traf6 we could identify a gene set whose transcription is controlled by morpholino injections in general. We could show that several genes previously linked to development or metabolism, are also triggered by morpholinos in general. By identifying these general effects of morpholinos at the transcriptome level we provide a reference set for morpholino off-target effects. Considering the general use of morpholinos in the studies of zebrafish development, immunity and metabolism this will be an important resource for the scientific community. Interestingly several of these genes are linked to the immune system. We could show that a group of four Toll-like receptors, namely *tlr3*, *tlr4a*, *tlr4b* and *tlr9* were down-regulated in response to morpholino treatments. In mammals, activation of the innate immune response by nucleic acids is known to be mediated via TLR3, TLR7 and TLR9 (29). However, it has not been yet reported that morpholinos can also activate these pathways. Furthermore, TLR4 is thus far not known as a receptor for DNA or RNA. From the *traf6* knock-down results we can conclude that the general response of *tlr3* to morpholino injections is not dependent on Traf6. In contrast the response of *tlr4a*, *tlr4b* and *tlr9* appears to be dependent on Traf6. It is very interesting that these pathways are activated in the early stages of embryogenesis and therefore we would like to further study the signal transduction pathways involved in the sensing of morpholinos. For instance it would be of interest to find out why these receptors were down-regulated. An explanation for the negative regulation of these receptors might be a negative feedback loop since the injection of morpholinos was approximately 5 hours prior to the analyses of the transcriptome response. The regulation of these Toll-like receptors in early embryogenesis indicates that also other players of this pathway are functionally present in the early embryo. This is consistent with previous results demonstrating that several TLR receptors and downstream signal transduction components are expressed at very early stages of embryogenesis (30). This includes *tlr3*, *tlr4a* and *tlr4b* as well as the adaptor proteins *tirap* and *trif*. However, there is nothing known on functional aspects of the innate immune system at the very early stages of embryogenesis and based on our results it would be of interest to test responses of early embryos to other immunogenic compounds and infectious agents at the very early stages of embryogenesis.

Materials and Methods

Zebrafish husbandry

Zebrafish were handled in compliance with the local animal welfare regulations and maintained according to standard protocols (http://ZFIN.org). All experiments were performed on mixed egg clutches from several pairs of AB strain zebrafish. Embryos were grown at 28,5 °C in egg water (60µg/ml Instant Ocean sea salts).

Morpholino knock-down experiments

For morpholino knockdown experiments, morpholino oligonucleotides (Gene Tools) were diluted to desired concentrations in 1x Danieu's buffer [58 mM NaCl, 0.7 mM KCl, 0.4 mM $MgSO_4$, 0.6 mM $Ca(NO_3)2$, 5.0 mM HEPES; pH 7.6] containing 1% Phenol red (Sigma). Translation of *traf6* was blocked by two non-overlapping morpholinos specifically targeting the 5' UTR region of *traf6* (*traf6*-morpholino-1, 5'GCCATATTGGCTCGGTACGGCCTC and *traf6*-morpholino-2, 5'GCCTATACTGCTGCTTCCTGTAAAG). To control for aspecific morpholino effects, a 5 bp mismatch morpholino (5'GCaATATTcGCTaGGTACaGCgTC) of *traf6*-morpholino-1 and a standard control morpholino (www.gene-tools.com) were injected. Embryos were injected at the one cell stage with 1 nl of either one of the above mentioned morpholinos with the following concentrations: 0.5, 1 or 2mM. In addition, 1x Danieu's buffer containing only Phenol red was injected to control for the injection effect per se. All injections were done in random order and the experiment was performed in quintuplicate.

RNA extraction

Pools of 20-30 embryos of each treatment group were collected at 30% epiboly for RNA isolation. Embryos were snap frozen in liquid nitrogen and subsequently stored at -80°C. Total RNA from each sample was extracted using TRIZOL followed by a cleanup procedure with Rneasy Mini kit (Qiagen, Valencia, CA, USA), and a DNase treatment with RNase-Free DNase Set (Qiagen Valencia, CA, USA). The RNA concentration was measured on a nanodrop ND-100 (NanoDrop Technologies Inc., Wilmington, DE,USA) and RNA quality was checked on an Agilent 2100 BioAnalyzer (Agilent Technologies, Palo Alto, CA, USA). Total RNA samples with an RNA integrity number (RIN) > 7 were used for further analysis. These assays were performed according to the manufacturer's protocols.

Microarray design and hybridization

A custom zebrafish 4 x 44 K microarray (Agilent) that was previously described was used (accession no. GPL7735 in the GEO database) (15). Technical handling of the microarrays was performed at the MicroArray Department (MAD) of the University of Amsterdam (Amsterdam, The Netherlands). In short, cyanine 3 and cyanine 5 labelled cRNA samples were prepared as described in the Amino allyl message AMP II

manual (Ambion) using 0.5 ug purified total RNA as template for the reaction. Test samples were labelled with Cy3 and the common reference was labelled with Cy5. The common reference was composed by combining 1 ug of cRNA from each sample and chemical coupling of this pool with Cy5. Hybridization of 825 ng of Cy3 labelled test sample and 825 ng of Cy5 labelled common reference was performed overnight according to Agilent protocols at 65° C. Images of the arrays were acquired using an Agilent DNA MicroArray Scanner (Agilent Technologies, Palo Alto, CA, USA).

Data extraction and statistical procedure

Spot intensities were quantified with Feature Extraction 9.5.1 (Agilent) as the foreground median signal intensity. Further processing of the data was performed using R (version 2.5.0), the Bioconductor MAANOVA package (version 1.6.0) (16).

All slides were subjected to a set of quality control checks, i.e. visual inspection of the scans, examining the consistency among the replicated samples by principal components analysis, testing against criteria for signal to noise ratios, testing for consistent performance of the labelling dyes, and visual inspection of pre- and post-normalized data with box plots and RI plots.

The data set concerned a two-factorial design, with the factors 'Treatment' (5 levels: 'Phenol Red', 'Standard Control', 'Mismatch', 'Morpholino 1' and 'Morpholino 2') and 'Dose' (3 levels: 'Low', 'Middle' and 'High'), with the factor 'Dose' being applicable only to the morpholino injections, not to the Phenol Red control.. After log2 transformation the data was normalized by quantile normalization. The data was analyzed using a two-stage mixed analysis of variance (ANOVA) model (17). First, array, dye, and array-by-dye effects were modelled globally. Next, the residuals from this first model were fed into a gene-by-gene model in which we took 'Group', 'Array', and 'Injection' as factors of which 'Array' and 'Injection' were modelled as random factors. 'Group' is defined by each unique treatment and dose combination. For hypothesis testing an Fs test was used and the significance of the differences between factor level means was tested using contrasts. To account for multiple testing, all P values were adjusted to represent a false discovery rate of 5%.

Gene Ontology, pathway and cluster analysis

Gene ontology (GO) analysis was performed using the GeneTools eGOn v2.0 web-based gene ontology analysis software (www.genetools.microarray.ntnu.no) (18). Master-target analysis was performed at the level of Unigene clusters (UniGene build #105). To test for enrichment or under representation at the level of GO criteria for Biological Process (BP) we compared the UniGene identifiers retrieved from our analysis (targets) to all identifiers present on the chip (master).

Pathway analysis was performed using the GenMapp software package (www.genmap.org) (19)116116116116. Analysis was done at the level of UniGene clusters (*D.rerio* UniGene build #114). Significance cut-off was set at >1.2 and <-1.2 fold change at an FDR adjusted P-value <0.05. Zebrafish homologs of the genes contributing to

the TLR and TGF-beta superfamily pathway were identified by either searching the ZFIN (http://zfin.org) database or the Gene and HomoloGene database of NCBI (http://www.ncbi.nlm.nih.gov).

Supplementary Data

Supplementary tables can be found online at: http://www.mediafire.com/?sharekey=686efof919604e919bf8d6369220dcab43aecfabc95fc71d759e682a8cd2154a

References

1. Xu, L. G., L. Y. Li, and H. B. Shu. 2004. TRAF7 potentiates MEKK3-induced AP1 and CHOP activation and induces apoptosis. *J Biol Chem* 279:17278-17282.
2. Chung, J. Y., Y. C. Park, H. Ye, and H. Wu. 2002. All TRAFs are not created equal: common and distinct molecular mechanisms of TRAF-mediated signal transduction. *J Cell Sci* 115:679-688.
3. Yamashita, M., K. Fatyol, C. Jin, X. Wang, Z. Liu, and Y. E. Zhang. 2008. TRAF6 mediates Smad-independent activation of JNK and p38 by TGF-beta. *Mol Cell* 31:918-924.
4. Kobayashi, T., M. C. Walsh, and Y. Choi. 2004. The role of TRAF6 in signal transduction and the immune response. *Microbes Infect* 6:1333-1338.
5. Lomaga, M. A., J. T. Henderson, A. J. Elia, J. Robertson, R. S. Noyce, W. C. Yeh, and T. W. Mak. 2000. Tumor necrosis factor receptor-associated factor 6 (TRAF6) deficiency results in exencephaly and is required for apoptosis within the developing CNS. *J Neurosci* 20:7384-7393.
6. Lomaga, M. A., W. C. Yeh, I. Sarosi, G. S. Duncan, C. Furlonger, A. Ho, S. Morony, C. Capparelli, G. Van, S. Kaufman, A. van der Heiden, A. Itie, A. Wakeham, W. Khoo, T. Sasaki, Z. Cao, J. M. Penninger, C. J. Paige, D. L. Lacey, C. R. Dunstan, W. J. Boyle, D. V. Goeddel, and T. W. Mak. 1999. TRAF6 deficiency results in osteopetrosis and defective interleukin-1, CD40, and LPS signaling. *Genes Dev* 13:1015-1024.
7. Naito, A., S. Azuma, S. Tanaka, T. Miyazaki, S. Takaki, K. Takatsu, K. Nakao, K. Nakamura, M. Katsuki, T. Yamamoto, and J. Inoue. 1999. Severe osteopetrosis, defective interleukin-1 signalling and lymph node organogenesis in TRAF6-deficient mice. *Genes Cells* 4:353-362.
8. Naito, A., H. Yoshida, E. Nishioka, M. Satoh, S. Azuma, T. Yamamoto, S. Nishikawa, and J. Inoue. 2002. TRAF6-deficient mice display hypohidrotic ectodermal dysplasia. *Proc Natl Acad Sci U S A* 99:8766-8771.
9. Mizukami, J., G. Takaesu, H. Akatsuka, H. Sakurai, J. Ninomiya-Tsuji, K. Matsumoto, and N. Sakurai. 2002. Receptor activator of NF-kappaB ligand (RANKL) activates TAK1 mitogen-activated protein kinase kinase kinase through a signaling complex containing RANK, TAB2, and TRAF6. *Mol Cell Biol* 22:992-1000.
10. Kobayashi, N., Y. Kadono, A. Naito, K. Matsumoto, T. Yamamoto, S. Tanaka, and J. Inoue. 2001. Segregation of TRAF6-mediated signaling pathways clarifies its role in osteoclastogenesis. *EMBO J* 20:1271-1280.
11. Boyle, W. J., W. S. Simonet, and D. L. Lacey. 2003. Osteoclast differentiation and activation. *Nature* 423:337-342.
12. Kopp, E., R. Medzhitov, J. Carothers, C. Xiao, I. Douglas, C. A. Janeway, and S. Ghosh. 1999. ECSIT is an evolutionarily conserved intermediate in the Toll/IL-1 signal transduction pathway. *Genes Dev* 13:2059-2071.
13. Xiao, C., J. H. Shim, M. Kluppel, S. S. Zhang, C. Dong, R. A. Flavell, X. Y. Fu, J. L. Wrana, B. L. Hogan, and S. Ghosh. 2003. Ecsit is required for Bmp signaling and mesoderm formation during mouse embryogenesis. *Genes Dev* 17:2933-2949.
14. Bai, S., J. Zha, H. Zhao, F. P. Ross, and S. L. Teitelbaum. 2008. Tumor necrosis factor receptor-associated factor 6 is an intranuclear transcriptional coactivator in osteoclasts. *J Biol Chem* 283:30861-30867.
15. Stockhammer, O. W., A. Zakrzewska, Z. Hegedus, H. P. Spaink, and A. H. Meijer. 2009. Transcriptome profiling and functional analyses of the zebrafish embryonic innate immune response to Salmonella infection. *J Immunol* 182:5641-5653.
16. Wu H, K. K., Cui X, Churchill GA: . 2003. *MAANOVA: A Sofware Package for the Analysis of Spotted cDNA Microarray Experiments.* Springer London.
17. Kerr, M. K., M. Martin, and G. A. Churchill. 2000. Analysis of variance for gene expression microarray data. *J Comput Biol* 7:819-837.
18. Beisvag, V., F. K. Junge, H. Bergum, L. Jolsum, S. Lydersen, C. C. Gunther, H. Ramampiaro, M. Langaas, A. K. Sandvik, and A. Laegreid. 2006. GeneTools--application for functional annotation and statistical hypothesis testing. *BMC Bioinformatics* 7:470.
19. Dahlquist, K. D., N. Salomonis, K. Vranizan, S. C. Lawlor, and B. R. Conklin. 2002. GenMAPP, a new tool for viewing and analyzing microarray data on biological pathways. *Nat Genet* 31:19-20.
20. Krens, S. F., M. Corredor-Adamez, S. He, B. E. Snaar-Jagalska, and H. P. Spaink. 2008. ERK1 and ERK2 MAPK are key regulators of distinct gene sets in zebrafish embryogenesis. *BMC Genomics* 9:196.
21. Walsh, M. C., G. K. Kim, P. L. Maurizio, E. E. Molnar, and Y. Choi. 2008. TRAF6 autoubiquitination-independent activation of the NFkappaB and MAPK pathways in response to IL-1 and RANKL. *PLoS One* 3:e4064.
22. Bao, S., R. S. Tibbetts, K. M. Brumbaugh, Y. Fang, D. A. Richardson, A. Ali, S. M. Chen, R. T. Abraham, and X. F. Wang. 2001. ATR/ATM-mediated phosphorylation of human Rad17 is required for genotoxic stress responses. *Nature* 411:969-974.
23. Zhang, S., D. Ma, X. Wang, T. Celkan, M. Nordenskjold, J. I. Henter, B. Fadeel, and C. Zheng. 2008. Syntaxin-11 is expressed in primary human monocytes/macrophages and acts as a negative regulator of macrophage engulfment of apoptotic cells and IgG-opsonized target cells. *Br J Haematol* 142:469-479.
24. Deveraux, Q. L., N. Roy, H. R. Stennicke, T. Van Arsdale, Q. Zhou, S. M. Srinivasula, E. S. Alnemri, G. S. Salvesen, and J. C. Reed. 1998. IAPs block apoptotic events induced by caspase-8 and cytochrome c by direct inhibition of distinct caspases. *EMBO J* 17:2215-2223.
25. Oltvai, Z. N., C. L. Milliman, and S. J. Korsmeyer. 1993. Bcl-2 heterodimerizes in vivo with a conserved homolog, Bax, that accelerates programmed cell death. *Cell* 74:609-619.

26. Yang, E., J. Zha, J. Jockel, L. H. Boise, C. B. Thompson, and S. J. Korsmeyer. 1995. Bad, a heterodimeric partner for Bcl-XL and Bcl-2, displaces Bax and promotes cell death. *Cell* 80:285-291.
27. Yoon, K., E. J. Jung, S. R. Lee, J. Kim, Y. Choi, and S. Y. Lee. 2008. TRAF6 deficiency promotes TNF-induced cell death through inactivation of GSK3beta. *Cell Death Differ* 15:730-738.
28. Crighton, D., S. Wilkinson, J. O'Prey, N. Syed, P. Smith, P. R. Harrison, M. Gasco, O. Garrone, T. Crook, and K. M. Ryan. 2006. DRAM, a p53-induced modulator of autophagy, is critical for apoptosis. *Cell* 126:121-134.
29. Kawai, T., and S. Akira. 2008. Toll-like receptor and RIG-I-like receptor signaling. *Ann N Y Acad Sci* 1143:1-20.
30. van der Sar, A. M., O. W. Stockhammer, C. van der Laan, H. P. Spaink, W. Bitter, and A. H. Meijer. 2006. MyD88 innate immune function in a zebrafish embryo infection model. *Infect Immun* 74:2436-2441.

6 Summary and Discussion

In order to combat infectious diseases, multicellular organisms have developed complex networks of cellular and humoral defence mechanisms allowing for the detection and destruction of pathogenic microorganisms. In vertebrates these complex mechanisms are traditionally categorized into the evolutionary ancient innate immune system (present in all multicellular organisms), and the relatively young adaptive (acquired) immune system that arose with the appearance of jawed fish.

In the last decade the study of the innate immune system has gained renewed scientific momentum as a result of the discovery of the essential receptor families that are required for pathogen recognition. It has been demonstrated that the innate immune system plays a pivotal role in the first line of defence against potentially pathogenic microorganisms, and is also required for activating subsequent adaptive responses. Many of the molecular mechanisms underlying the innate immune response have been elucidated. The recognition of invading pathogens is achieved by the innate immune system through various classes of receptors, commonly termed pattern recognition receptors (PRRs), such as the Toll-like receptor (TLR), NOD-like receptor (NLR) and RIG-I like (RLR) receptor families. These receptors are able to detect specific molecular structures of microorganisms termed pathogen-associated molecular patterns (PAMPs) or microbial-associated molecular patterns (MAMPs). Polymorphisms of these receptors and downstream signalling intermediates have been associated with increased susceptibility to infectious diseases and with several inflammatory disorders. Furthermore, both extracellular and intracellular pathogens have been shown to manipulate the signalling pathways of their hosts in order to evade detection or escape innate immune defences, underscoring the clinical relevance of studying the molecular basis of the innate immune system.

This thesis focuses on the use of the zebrafish as a model to study the vertebrate immune system to gain new insights into the mechanisms of innate immune defence against bacterial infections and TLR signalling. In zebrafish embryos, cells of the innate immune system develop prior to cells of the adaptive system, thus allowing specific analysis of innate immune functions in a genetically tractable vertebrate animal model. Furthermore, the transparency of zebrafish embryos enables real-time analysis of the response to infections.

At the onset of the project, little was known about TLR signalling function in the zebrafish embryo model. Previous studies had demonstrated the presence of TLRs and downstream signalling molecules in zebrafish, and bacterial and viral infections were found to induce expression of different zebrafish *TLR* genes. Furthermore, it was known that one-day-old zebrafish embryos already possessed leukocytes able to phagocytose bacteria. However, functional evidence to confirm the role of TLR signalling in zebrafish and the presence of an innate immune response in early embryos was lacking. Therefore, as described in **Chapter 2,** we initially aimed at a functional analysis of MyD88, an essential adaptor protein of vertebrate TLRs and of the interleukin-1 and -18 receptors that is activated through TLR signalling. Making use of morpholino-mediated knock-down in combination with a previously established

S. enterica serovar Typhimurium (*S. typhimurium*) infection system, we were able to demonstrate that loss of MyD88 led to a significantly impaired ability of zebrafish embryos to clear an otherwise non-pathogenic LPS O-antigen mutant of *S. typhimurium* (Ra strain). Thereby, we demonstrated for the first time that Myd88-dependent signalling events play a critical role in innate immune responses towards a bacterial infection in zebrafish embryos. These results were consistent with many infection studies in MyD88$^{-/-}$ adult mice, which showed increased susceptibility to a variety of pathogens. Our study therefore validated the zebrafish embryo as a useful model for analysis of vertebrate TLR signalling as well as the vertebrate innate immune system in general.

In **Chapter 3** we took advantage of the clear temporal separation of innate and adaptive immunity in the zebrafish embryo to specifically analyse vertebrate innate immune responses to a systemic bacterial infection using microarray technology. The host response of embryos infected with a pathogenic *S. typhimurium* wild-type strain was compared to the response of embryos infected with the attenuated LPS mutant strain (Ra) used in chapter 2. The time-resolved transcriptome analysis revealed distinct temporal expression profiles correlated to the symptoms of disease progression for both strains. The main difference between the strains was observed at 24 hours post infection (hpi). At that point the transient infection caused by the Ra mutant was nearly eliminated, whereas accumulation of wild type bacteria further increased, resulting in lethality around 30 hpi.

Subsequently, we compared the zebrafish transcriptome data to a meta-analysis of microarray data of various human cell lines challenged by different pathogens. The comparison revealed a considerable overlap between the zebrafish host response to *S. typhimurium* and those genes that were commonly induced in all cell lines upon pathogen challenge. The overlap included genes for well known immune responsive transcription factors, cell surface receptors, signal transduction intermediates, adhesion factors and proteins involved in tissue remodelling, as well as various interferons, chemokines, pro-inflammatory and anti-inflammatory cytokines (Fig.1). Our results therefore further underscore the predictive value of the zebrafish embryo model.

As we are particularly interested in TLR immune signalling, we analyzed our transcriptome data using GenMapp-based visualisation of the expression data on the TLR pathway. This pathway analysis showed that various signalling intermediates at different levels in the TLR pathway were induced upon *S. typhimurium* infection *in vivo*. Interestingly, the two isoforms of zebrafish Tlr5 were induced throughout the infection time course. In the mammalian system TLR5 signalling has previously been shown to be triggered by bacterial flagellin. We found that flagellin stimulation in zebrafish embryos was sufficient for strong induction of several of the genes that were also induced by *S. typhimurium* infection, including the inflammatory cytokine gene *il1b,* the chemokine genes *il8* and *cxcl-C1c,* the matrix metalloproteinase gene *mmp9*, and the putative negative regulator of TLR signalling, *irak3*. Using morpholinos directed against the two isoforms of Tlr5 followed by flagellin stimula-

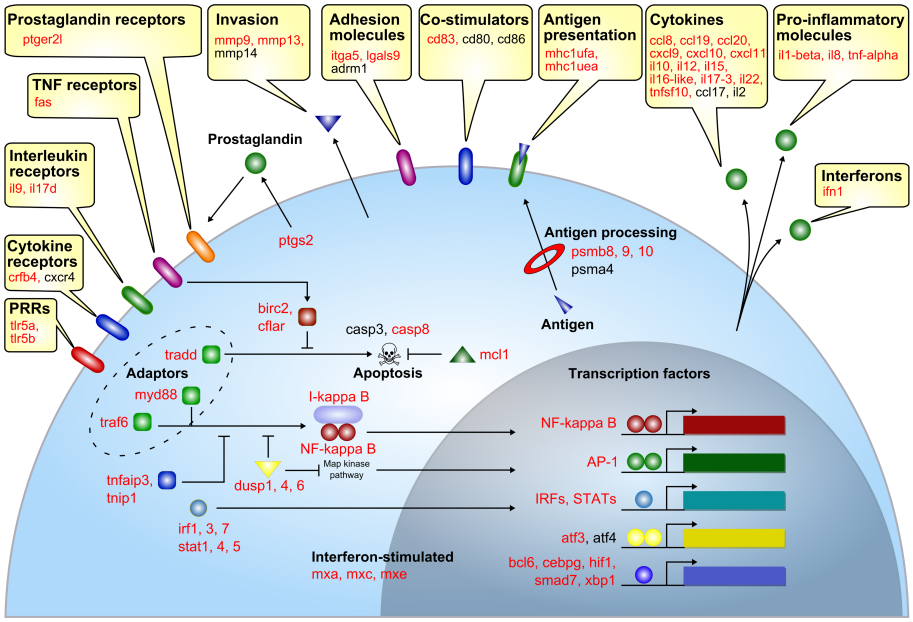


FIGURE 1. Schematic representation of the zebrafish embryonic host response (adapted from Jenner and Young, Nature Reviews Microbiology, 2005). Genes shown in red were up-regulated in zebrafish embryos after *S. typhimurium* infection. Genes shown in black were present on the microarray platform but not induced after infection.

tion, we attempted to assess Tlr5 signalling in zebrafish embryos. Our results clearly demonstrated Tlr5-dependent gene activation of *il1b*, *il8, cxcl-C1c, mmp9*, and *irak3* in the zebrafish embryo. Extending the work described in Chapter 2, we additionally assessed transcriptional effects of Myd88 on downstream target genes of innate immunity signalling. Our results demonstrated a clear dependency of *mmp9*, *il1b* and *irak3* on MyD88 for transcriptional activation upon *S. typhimurium* challenge. In contrast, *ifn1* and *il8* did not show changes in their induction levels upon bacterial challenge, demonstrating MyD88-independent activation of these genes. Taken together, these results are the first demonstration of a conserved TLR ligand specificity and of the presence of MyD88-dependent and MyD88-independent signalling pathways in the zebrafish embryo.

The detailed transcriptome analysis of the host response to *S. typhimurium* described in chapter 3 has linked a large set of zebrafish genes to the process of bacterial infection, providing a case study for future immunity research in the zebrafish embryo model. For many of these genes the specific function is still unknown, both in zebrafish and humans. Taking advantage of the rapid gene knock-down assays, the zebrafish embryo model will be of great use for the future functional characterization

of these genes, thereby supporting further annotation of the human genome.

Analysis of the function of Traf6 in the innate immune response of zebrafish embryos towards *S. typhimurium* infection is described in **Chapter 4**. TRAF6 functions downstream of MyD88 in the vertebrate TLR pathway and also transduces signals emanating from members of the TNF receptor superfamily that are involved in both the immune response and developmental processes. The fact that Traf6 is a key player at the cross-roads of development and immunity makes the analysis of its *in vivo* molecular function a great challenge. In mice, severe developmental defects and early lethality caused by *Traf6* deficiency have interfered with analyses of the immune response. In our approach, this problem was solved by titrating the effect of a Traf6 morpholino down to a level where developmental defects in zebrafish embryos were avoided. The morpholino-treated embryos were subsequently challenged by a *S. typhimurium* infection and the transcriptional response was assessed by microarray and RNA deep sequencing (RNAseq) analysis.

This approach allowed the identification of 146 genes (confirmed by RNAseq) that were dependent on Traf6 in the context of a bacterial infection. Among those were genes with well known functions in innate immunity, such as *il1b*, *mmp9, mmp13*, *hamp2, cxcl12* and *tnfb*. Using GenMapp analysis to focus on the TLR pathway, we could show that an infection by *S. typhimurium* was no longer able to trigger Tlr5 expression after Traf6 knock-down. In addition, several genes with no known Traf6 association were also identified, such as *gnrh2* (gonadotropin releasing hormone 2*)*, *stc1* (stanniocalcin 1), *dgat1b* (diacylglycerol O-acyltransferase homolog 1b) and *dram1* (DNA-damage regulated autophagy modulator 1). Expression trend analysis of the Traf6-dependent genes identified nine clusters with characteristic transcription response profiles, demonstrating the dynamic role of Traf6 as both a positive and negative regulator.

In our study we have also identified Traf6 targets of which no annotation could be derived either for zebrafish, mouse or human orthologs. Domain searches were equally unsuccessful in unearthing a possible function. Since the expression levels of some of these genes were strongly affected by *S. typhimurium* induction at early time points (2 hpi), as well as strongly dependent on Traf6 function, the further study of these genes in the vertebrate immune system will be of great interest. In addition, the data derived by RNAseq represent a wealth of disease-induced transcript information that will be of great value for future studies.

As discussed above, Traf6 does not exclusively mediate signalling processes of the immune system, but also has a function during development. In **Chapter 5** we therefore attempted to gain insight into the function of Traf6 during early zebrafish embryogenesis using a morpholino based knock-down approach. Transcriptome analysis was performed at the stage of 30% epiboly (4.7 hours post fertilization), which is the earliest phase of gastrulation where the outer cell layer of the blastula spreads to envelop the embryonic yolk sac. Using different morpholinos directed against *traf6* mRNA, and by comparison to two control morpholinos, we were able to

identify a large gene set of 868 genes that appear to be specifically controlled by Traf6 during embryogenesis. Gene Ontology analysis showed that a Traf6 knock-down led to the induction of several genes involved in the regulation of programmed cell death. Genes such as *bcl2-antagonist of cell death* (*bad*) and *bcl2-associated X protein* (*bax*), known to promote apoptosis, were induced, whereas genes promoting cell survival such as *birc2* showed decreased expression levels. Our results are in line with an anti-apoptotic effect of TRAF6 that has previously been demonstrated in mouse cell lines.

Comparison of the transcriptome data to the infection data from Chapter 4 showed only a limited overlap of 14 genes that were Traf6-dependent in early development and during infection, illustrating the diverse functions of Traf6 in development and immunity. As part of the analysis we also identified genes that showed altered expression even in response to the control morpholinos, and thus were regulated due to morpholino treatment in general. Interestingly, several of these genes could be linked to the immune system. The response of the immune system to morpholinos is consistent with the ability of the vertebrate innate immune system to sense microbial and viral DNA or RNA. However, a response to such treatments in early embryogenesis has never previously been shown. We could demonstrate that a group of four Toll-like receptors, namely *tlr3*, *tlr4a*, *tlr4b* and *tlr9*, were down-regulated in response to general morpholino treatments. From the *traf6* knock-down results we were able to conclude that the general response of *tlr3* to morpholino injections was not dependent on Traf6. In contrast, the response of *tlr4a*, *tlr4b* and *tlr9* appeared to be dependent on Traf6.

Taken together, we could show that Traf6 knock-down led to the alteration of a large set of genes during early zebrafish development, indicating a crucial role of Traf6 also in zebrafish development. However, the specific function of Traf6 in development seems to be distinct from its function in immunity, as only a small group of genes were differentially regulated due to Traf6 knock-down under both conditions. In addition, we revealed differential regulation of various TLR genes as a general response to morpholino treatments, suggesting that immune signaling pathways might already be functional in these early stages.

In conclusion, the studies described in this thesis have strongly contributed to the validation of the zebrafish embryo model for analysis of the vertebrate innate immune system. In addition to the characterization of the embryonic host transcriptome response to bacterial infection, we have demonstrated functions for key signalling molecules in the innate immune response, including Tlr5, MyD88 and Traf6. In recent years many zebrafish infection models for human pathogens have been published and their use has already led to new insights into host-pathogen interactions, most notably in the field of tuberculosis research. Our data will now enable in depth functional follow-up studies that will give unprecedented new insights into the mechanisms of innate immune defence systems. Such insights can subsequently be validated in mammalian systems. This, in combination with future applications of ze-

brafish embryo infection models in high-throughput compound screens, holds much promise for the discovery of novel anti-microbial and anti-inflammatory drugs.

Samenvatting

Het immuunsysteem is een complex netwerk van verdedigingsmechanismen, die ons in staat stellen om ziekteverwekkers, zoals bacteriën, virussen en parasieten, op een effectieve manier te bestrijden. Deze verdedigingsmechanismen omvatten een assortiment aan gespecialiseerde cellen, de witte bloedcellen, alsmede afweerstoffen die zich in het bloedplasma bevinden. Bij vertebraten (gewervelde dieren), waar ook de mens toe behoort, worden deze verdedigingsmechanismen traditioneel ingedeeld in het aangeboren of innate immuunsysteem en het verworven of adaptieve immuunsysteem. Het innate immuunsysteem is evolutionair gezien het oudste en is aanwezig in zowel ongewervelde als gewervelde dieren. Het adaptieve immuunsysteem maakte pas met het ontstaan van de kraakbeenvissen, bijna 450 miljoen jaar geleden, zijn entree.

In de afgelopen jaren heeft in het bijzonder de studie naar het innate immuunsysteem aan populariteit gewonnen. Dit was het gevolg van de ontdekking van een aantal receptorfamilies die essentieel zijn voor het herkennen van een breed spectrum van ziekteverwekkers door witte bloedcellen. Onderzoek heeft uitgewezen dat het innate immuunsysteem de primaire verdedigingslinie van het organisme tegen pathogene micro-organismen vormt en bovendien een belangrijke rol speelt bij het instrueren van het adaptieve immuunsysteem. Diverse moleculaire mechanismen die aan de functionele basis van het innate immuunsysteem staan, zijn inmiddels ontrafeld. Microbiële indringers worden in het organisme herkend door receptoren die bekend staan als patroon-herkennende receptoren (pattern recognition receptors). Tot deze groep van receptoren worden onder meer de families van Toll-receptoren (Toll-like receptors, TLRs), NOD-receptoren en RIG-receptoren gerekend. Deze receptoren zijn in staat om geconserveerde moleculaire structuren te herkennen die specifiek zijn voor micro-organismen. Kleinschalige mutaties in de genen, die coderen voor deze receptoren of de daarmee geassocieerde signaalmoleculen, leiden tot een verhoogde vatbaarheid voor infectieziekten of inflammatoire aandoeningen. Verder is aangetoond, dat zowel extracellulaire als ook intracellulaire ziekteverwekkers in staat zijn om de immuunreactie van de gastheer zodanig te manipuleren dat zij niet meer door de gastheer te detecteren zijn. Dit benadrukt tevens de klinische relevantie van fundamenteel onderzoek naar het innate immuunsysteem.

In het hier voorliggende proefschrift ligt de nadruk op het gebruik van het zebravisembryo als modelsysteem voor de studie van het immuunsysteem van vertebraten, met als doel nieuwe inzichten te verkrijgen in de mechanismen die ten grondslag liggen aan de innate immuunreacties bij bacteriële infecties. Met name is gekeken naar de functie van de Toll-receptor-signaaltransductieroute tijdens deze infectieprocessen. Het zebravisembryo is een uitermate geschikt model voor de studie van het innate immuunsysteem, omdat het in de eerste weken van de ontwikkeling geen functioneel adaptief immuunsysteem bezit en daarom geheel afhankelijk is van het innate immuunsysteem. Dit zorgt ervoor, dat men puur naar de effecten van

het innate immuunsysteem kan kijken, zonder invloed van het adaptieve immuunsysteem. Bovendien is de genetische code van de zebravis bekend en zijn manipulaties van het genoom mogelijk. Verder is het embryo doorzichtig, wat het volgen van immuuncellen in het lichaam van een levend embryo, alsmede het bestuderen van de interactie met pathogenen, mogelijk maakt.

Aan het begin van mijn onderzoeksproject was nauwelijks iets bekend over de functie van Toll-receptoren in het zebravisembryomodel. Voorafgaande studies hadden aangetoond, dat de genen voor zowel de Toll-receptoren als ook voor belangrijke TLR-adaptereiwitten in de zebravis aanwezig waren. Bacteriële infecties leidden tot een verhoogde expressie van deze genen, hetgeen een eerste indicatie voor een geconserveerde functie van de Toll-receptoren gaf. Bovendien was destijds al bekend, dat één-dag-oude embryo's leukocyten (immuuncellen) bezitten, die in staat zijn bacteriën te fagocyteren. Echter, er was nog geen functioneel bewijs dat de rol van TLRs tijdens een infectie, of het bestaan van een innate immuunreactie, kon onderbouwen.

Om die reden hebben wij, zoals in **Hoofdstuk 2** staat beschreven, in eerste instantie functioneel onderzoek gedaan naar de rol van MyD88, een essentieel adaptereiwit in de Toll-receptor-signaalroute, alsmede in de signaalroutes van de interleukin-1- en -18-receptoren. Het uitschakelen van Myd88 (knock-down) met behulp van morpholino's resulteerde in een sterk verhoogde vatbaarheid van het embryo voor infectie met een zwak pathogene stam van *Salmonella enterica* serovar Typhimurium (*S. typhimurium*). Hiermee hebben wij voor het eerst aangetoond, dat de signaaltransductieroutes die via Myd88 lopen een zeer belangrijke bijdrage leveren aan de immuunafweer van het zebravisembryo bij bacteriële infecties. In overeenstemming met onze resultaten, is ook voor MyD88-deficiënte ($MyD88^{-/-}$) muizen een significant verhoogde vatbaarheid voor verschillende infectieziekten beschreven. Deze resultaten ondersteunen dat het zebravisembryo een valide model is voor de studie van TLR-signaaltransductieprocessen in het innate immuunsysteem van vertebraten.

In **Hoofdstuk 3** hebben wij ernaar gestreefd, om de afweerreactie van het aangeboren immuunsysteem van het zebravisembryo op een systemische bacteriële infectie in kaart te brengen. Hiertoe hebben wij middels microarray-technologie gekeken naar de verschillen in het transcriptoom van met Salmonella geïnfecteerde zebravisembryo's ten opzichte van niet-geïnfecteerde embryo's. De zebravisembryo's werden geïnfecteerd met een sterk pathogene en een zwak pathogene (Ra) stam van Salmonella en de reactie van de embryo's op deze twee stammen werd gedurende 24 uur vergeleken. De transcriptoom-analyse bracht specifieke patronen van genexpressie over de duur van de infectie aan het licht, welke sterk gecorreleerd waren met de ziekteverschijnselen van de embryo's. Het grootste verschil in de immuunreactie op de twee stammen was 24 uur na infectie aantoonbaar. Op dat moment waren de embryo's er in geslaagd de infectie met de zwak pathogene (Ra) stam op te ruimen, terwijl de infectie met de pathogene stam aan intensiteit toenam en rond 30 uur na infectie tot 100% letaliteit leidde.

Vervolgens hebben wij onze resultaten vergeleken met data van infectiestudies in humane cellijnen. Een aanzienlijk gedeelte van de genen die gemeenschappelijk in alle humane cellijnen op infecties reageerden, kwam overeen met de genen die wij in de zebravisembryo's hebben ontdekt. Voorbeelden zijn interferonen, pro- en anti-inflammatoire cytokinen en chemokinen. Tevens was er overlap tussen zebravisembryo's en humane cellen in de expressie van verschillende transcriptiefactoren, receptoren en eiwitten die een rol spelen bij remodellering van het weefsel. Hiermee demonstreren onze resultaten de grote voorspellende waarde van het zebravis-infectiemodel.

In het verdere verloop van het onderzoek hebben wij onze aandacht gericht op de analyse van de TLR-signaaltransductieprocessen. Visualisatie van de transcriptoomdata met behulp van het GenMapp-programma liet zien dat verschillende elementen van de TLR- signaaltransductieroute door de infectie geïnduceerd waren. Onder de geïnduceerde genen waren ook de twee isovormen van de Tlr5-receptor van de zebravis. In zoogdieren is aangetoond dat TLR5 het bacteriële eiwit flagelline kan detecteren, wat vervolgens tot het activeren van verschillende immuunresponsgenen leidt. Wij hebben aangetoond dat, ook bij zebravisembryo's, stimulatie met flagelline resulteert in de inductie van een repertoire aan genen, die eveneens door infectie met *S. typhimurium* geïnduceerd waren. Voorbeelden zijn het cytokine *il1b*, de chemokines *il8* en *cxcl-C1c*, en het matrix-metalloproteinase *mmp9,* alsmede *irak3*, een mogelijke negatieve regulator van de TLR-signaaltransductieroute. Om de functie van Tlr5 in het signaalproces bij de immuunreactie op flagelline te kunnen onderzoeken, hebben wij vervolgens Tlr5 in zebravisembryo's uitgeschakeld en daarna de reactie op flagelline in deze embryo's geanalyseerd. Uit deze analyse bleek duidelijk dat de inductie van *il1b*, *il8*, *cxcl-C1c*, *mmp9* en *irak3* afhankelijk was van Tlr5. Daarnaast wilden wij weten welke van deze genen ook van Myd88 afhankelijk waren. Om deze reden hebben wij Myd88 in de zebravisembryo's uitgeschakeld en het effect van een Salmonella-infectie onderzocht. Van de geanalyseerde genen bleken *mmp9*, *il1b* en *irak3* afhankelijk van Myd88 te zijn. Daarentegen konden wij geen verschil in reactie van *ifn1* en *il8* vinden, wat aantoont dat deze genen op een Myd88-onafhankelijke manier geactiveerd worden. Concluderend hebben onze resultaten voor het eerst aangetoond dat de ligandspecificiteit van een lid van de Toll-receptorfamilie geconserveerd is tussen de zebravis en de mens. Bovendien heeft onze studie het bestaan van Myd88-afhankelijke en niet-afhankelijke signaaltransductieroutes in het zebravisembryo gedemonstreerd.

De in **Hoofdstuk 3** beschreven transcriptoomanalyse heeft de bacterieel-geïnduceerde immuunreactie van het zebravisembryo gedetailleerd in kaart gebracht en biedt daarmee een sterke basis voor toekomstig immuun-gerelateerd onderzoek in het zebravisembryomodel. Voor het merendeel van de gevonden genen is de functie zowel in de zebravis als in de mens nog steeds onduidelijk. Het zebravisembryomodel is bij uitstek geschikt voor functioneel onderzoek van deze genen, omdat gebruik kan worden gemaakt van de snelle en eenvoudige manier van knock-down van

genen met behulp van morpholino's. Gezien de grote mate van overeenkomst die wij gevonden hebben tussen de immuunrespons van zebravisembryo's en die van humane cellen, kan met deze knock-down-analyses ook de annotatie van het humane genoom worden verbeterd.

In **Hoofdstuk 4** wordt de functie van Traf6 tijdens de immuunreactie op een bacteriële infectie van zebravisembryo's uitgelicht. TRAF6 vormt een belangrijk onderdeel van ondermeer de TLR- en de TNF-receptor-signaalroutes in vertebraten, waardoor TRAF6 zowel een rol speelt in immuun- als ook in ontwikkelingsprocessen. Dit bemoeilijkt het onderzoek naar de immuunfunctie van TRAF6 in het levende organisme aanzienlijk. In muizen leidt het uitschakelen van *Traf6* bijvoorbeeld tot ernstige ontwikkelingsdefecten en vroegtijdige dood van pasgeboren muizen. In het hier beschreven onderzoek hebben wij handig gebruik gemaakt van de mogelijkheid om Traf6 in de zebravisembryo's met behulp van morpholino's gedeeltelijk uit te schakelen, waardoor het effect op de ontwikkeling van de embryo's nog maar een marginale rol speelde. Vervolgens hebben wij, evenals in het voorafgaande hoofdstuk, naar de transcriptionele effecten van een systemische *S. typhimurium*-infectie in deze embryo's gekeken. Hiervoor hebben wij deze keer naast microarray-technologie tevens gebruik gemaakt van de recent ontwikkelde technologie voor RNA-sequencing (RNAseq).

Met de combinatie van microarray- en RNAseq-analyse waren wij in staat om 146 genen te identificeren die afhankelijk waren van Traf6 in de context van de *S. typhimurium*-infectie. Van een deel van deze genen is bekend dat zij een rol spelen tijdens de immuunrespons van het organisme. Voorbeelden zijn *il1b*, *mmp9*, *mmp13*, *hamp2*, *cxcl12* en *tnfb*. Verder bracht de analyse van de TLR-signaalroute aan het licht dat na Traf6 knock-down, de Salmonella-infectie niet meer tot een verhoogde Tlr5-expressie leidde. Daarnaast konden wij verschillende genen identificeren die niet eerder in verband waren gebracht met de functie van TRAF6. Voorbeelden zijn *gnrh2* (*gonadotropin releasing hormone 2*), *stc1* (*stanniocalcin 1*), *dgat1b* (*diacylglycerol O-acyltransferase homolog 1b*) en *dram1* (*DNA-damage regulated autophagy modulator 1*). Trend-analyses van de expressiepatronen van de Traf6-afhankelijke genen lieten zien dat Traf6 een dynamische rol heeft tijdens de immuunrespons, zowel als positieve en negatieve regulator van specifieke gengroepen.

Tenslotte hebben wij in deze studie Traf6-afhankelijke genen gevonden, die op dit moment nog geen annotatie in de zebravis, muis of mens hebben. Ook was het niet mogelijk om een functie van deze genen te voorspellen op grond van geconserveerde eiwitdomeinen. Aangezien sommige van deze genen al twee uur na infectie een sterke inductie van het expressieniveau vertonen, zoals in hoofdstuk 3 staat beschreven, is toekomstig onderzoek naar deze genen van groot belang. Tevens bieden onze RNAseq-gegevens, de eerste transcriptoom-sequentiedata van een infectiestudie in vertebraten, een grote schat aan informatie die zeer waardevol is voor toekomstig onderzoek.

Zoals in Hoofdstuk 4 al staat beschreven, is Traf6 niet alleen belangrijk bij de sig-

naaltransductieprocessen tijdens infecties, maar ook bij de processen die gedurende de ontwikkeling van een organisme een rol spelen. In **Hoofdstuk 5** hebben wij om deze reden een poging ondernomen om de rol van Traf6 te ontrafelen in de context van de vroege embryogenese van de zebravis. Op dezelfde wijze als beschreven in de voorafgaande hoofdstukken, hebben wij Traf6 in embryo's met behulp van morpholino's uitgeschakeld en deze embryo's vervolgens op het transcriptoom-niveau vergeleken met controle-embryo's. De analyse vond plaats op het ontwikkelingsstadium van 30% epiboly (4.6 uur na fertilisatie), het moment waarop de gastrulatie van het zebravisembryo begint. Gebruikmakend van verschillende morpholino's gericht tegen *traf6* in combinatie met twee controle-morpholino's, waren wij in staat om een set van 868 genen te vinden, die tijdens vroege epiboly van Traf6 afhankelijk bleken te zijn.

Uit functionele classificatie van de geïdentificeerde set van genen bleek dat Traf6-knock-down tot een sterke inductie van genen leidde die een regulatieve functie bij apoptose hebben. Pro-apoptotische genen, zoals *bcl2-antagonist of cell death* (*bad*) en *bcl2-associated X protein* (*bax*) waren geïnduceerd, terwijl anti-apoptotische genen een verlaagd expressieniveau vertoonden. Deze resultaten zijn in overeenstemming met onderzoek uitgevoerd in celculturen van de muis, waaruit een anti-apoptotisch effect van TRAF6 bleek. Vergelijking van de transcriptoom-data uit hoofdstuk 4 met die van hoofdstuk 5 liet een beperkte overlap van 14 genen zien, die zowel in de vroege ontwikkeling als ook tijdens de immuunrespons van Traf6 afhankelijk waren. Deze slechts zeer beperkte overlap duidt erop dat Traf6 sterk verschillende functies tijdens de immuunrespons en de ontwikkeling heeft.

Bij de analyse van de transcriptoom-data in hoofdstuk 5 werd ook een set van genen gevonden die niet alleen door de Traf6-specifieke morpholino's, maar ook door de gebruikte controle-morpholino's gereguleerd werden. Verschillende van deze genen konden in samenhang gebracht worden met het immuunsysteem. Zo werd gevonden dat *tlr3*, *tlr4a*, *tlr4b* en *tlr9* een verlaagd expressieniveau vertoonden als respons op het morpholino-gebruik in het algemeen. Uit de *traf6* knock-down data konden wij concluderen dat de respons van *tlr3* op de morpholino's niet afhankelijk was van Traf6. Daarentegen bleek de respons van *tlr4a*, *tlr4b* en *tlr9* wel van Traf6 afhankelijk te zijn.

Concluderend konden wij laten zien dat na knock-down van Traf6 een groot aantal genen in expressieniveau veranderde, hetgeen op een cruciale rol van Traf6 tijdens de vroege zebravis-embryogenese duidt. De minimale overlap tussen de infectie-geïnduceerde Traf6-afhankelijke genen en de Traf6-afhankelijke genen tijdens de ontwikkeling, demonstreert de sterke context-afhankelijke rol van Traf6. Daarnaast konden wij laten zien, dat verschillende TLR-genen in het algemeen op morpholino-behandelingen reageren, onafhankelijk van de morpholino-sequentie. Dit zou erop kunnen duiden dat zelfs tijdens de vroege embryonale ontwikkeling signaaltransductieroutes van het immuunsysteem functioneel zijn.

De hier beschreven studies hebben in grote mate bijgedragen aan de validatie

van het zebravisembryomodel voor de analyse van het innate immuunsysteem van vertebraten. Naast de karakterisering van de embryonale transcriptoom-respons op een bacteriële infectie, hebben wij tevens de functie gedemonstreerd van signaaltransductiegenen, zoals *tlr5*, *myd88* en *traf6*, die een sleutelrol spelen in het innate immuunsysteem. In de afgelopen jaren zijn diverse zebravis-infectiemodellen voor humane pathogenen gepubliceerd. Het gebruik hiervan heeft al tot verschillende nieuwe inzichten in gastheer-pathogeen-interacties geleid, met name op het gebied van tuberculose-onderzoek. De hier gepresenteerde transcriptoom-data van de immuunrespons in zebravisembryo's leggen de basis voor functionele vervolgstudies, die nieuwe inzichten in signaaltransductieprocessen kunnen opleveren, welke vervolgens in zoogdiermodellen gevalideerd kunnen worden. De ontwikkeling van "high-throughput" screening-platforms, die gebaseerd zijn op zebravis-infectiemodellen is een veelbelovende strategie voor het vinden van nieuwe anti-microbiële en anti-inflammatoire stoffen.

List of publications

van der Zee, M., **O. W. Stockhammer**, C. von Levetzow, R. Nunes da Fonseca, S. Roth. 2006. Sog/Chordin is required for ventral-to-dorsal Dpp/BMP transport and head formation in a short germ insect. *Proc Natl Acad Sci U S A* 103:16307-12.

van der Sar, A. M., **O. W. Stockhammer**, C. van der Laan, H. P. Spaink, W. Bitter, and A. H. Meijer. 2006. MyD88 innate immune function in a zebrafish embryo infection model. *Infect Immun* 74:2436-2441.

Stockhammer, O. W., A. Zakrzewska, Z. Hegedus, H. P. Spaink, and A. H. Meijer. 2009. Transcriptome profiling and functional analyses of the zebrafish embryonic innate immune response to Salmonella infection. *J Immunol* 182:5641-5653.

Stockhammer, O.W., H. Rauwerda, F. R. Wittink, T. M. Breit, A. H. Meijer, H. P. Spaink. Transcriptome analysis of Traf6 function in the innate immune response of zebrafish embryos. Submitted to the Journal of Immunology

Zakrzewska, A., Cui C., **O. W. Stockhammer**, E. Benard, H. P. Spaink, A. H. Meijer. Macrophage-specific gene functions in Spi1-directed innate immunity. *Blood*, in press.

Stockhammer, O.W., H. Rauwerda, M. J. Jonker, F. R. Wittink, T. M. Breit, A. H. Meijer, H. P. Spaink. Transcriptome analysis of Traf6 function in early zebrafish embryogenesis. In preparation.

Curriculum vitae

Oliver Wilhelm Stockhammer werd geboren op 12 juli 1974 te Stuttgart, Duitsland. In 1994 behaalde hij zijn diploma (Abitur) aan het Gymnasium Rodenkirchen. Van 1994 tot 1996 heeft de auteur de zogenaamde Zivieldienst verricht, een sociale dienstverlening als alternatief voor dienst in het leger. In 1996 startte hij zijn studie biologie aan de Universiteit Keulen (Universität zu Köln), waar hij in 2003 afstudeerde. De auteur koos als hoofdvakken ontwikkelingsbiologie, biochemie en ecologie. Tijdens zijn studie heeft hij een onderzoeksstage van één jaar uitgevoerd in de groep van Prof. Dr. S. Roth aan het Instituut voor Ontwikkelingsbiologie. Gedurende deze stage werkte hij aan de ontwikkeling van de dorsoventrale as van *Tribolium castaneum*. Tevens schreef hij zijn afstudeerscriptie over dit onderzoek. In 2004 begon hij zijn promotieonderzoek aan het Instituut Biologie Leiden (IBL) van de Universiteit Leiden onder begeleiding van Dr. Annemarie H. Meijer en Prof. Dr. Herman P. Spaink. Tijdens zijn promotieonderzoek gebruikte hij het zebravisembryo als modelsysteem voor de studie van het aangeboren (innate) immuunsysteem van vertebraten. Het onderzoek was in het bijzonder gericht op de functie van de Toll-receptor-signaaltransductieroute en op de transcriptoomanalyse van de door deze route gereguleerde immuunrespons. Dit onderzoek heeft geresulteerd in een aantal publicaties en de totstandkoming van dit proefschrift. Van april 2009 tot april 2010 werkte de schrijver als Post Doctoral Scientist bij ZF-screens B.V. aan de implementatie van een high-throughput compound screening platform, gebaseerd op zebravis-infectiemodellen.